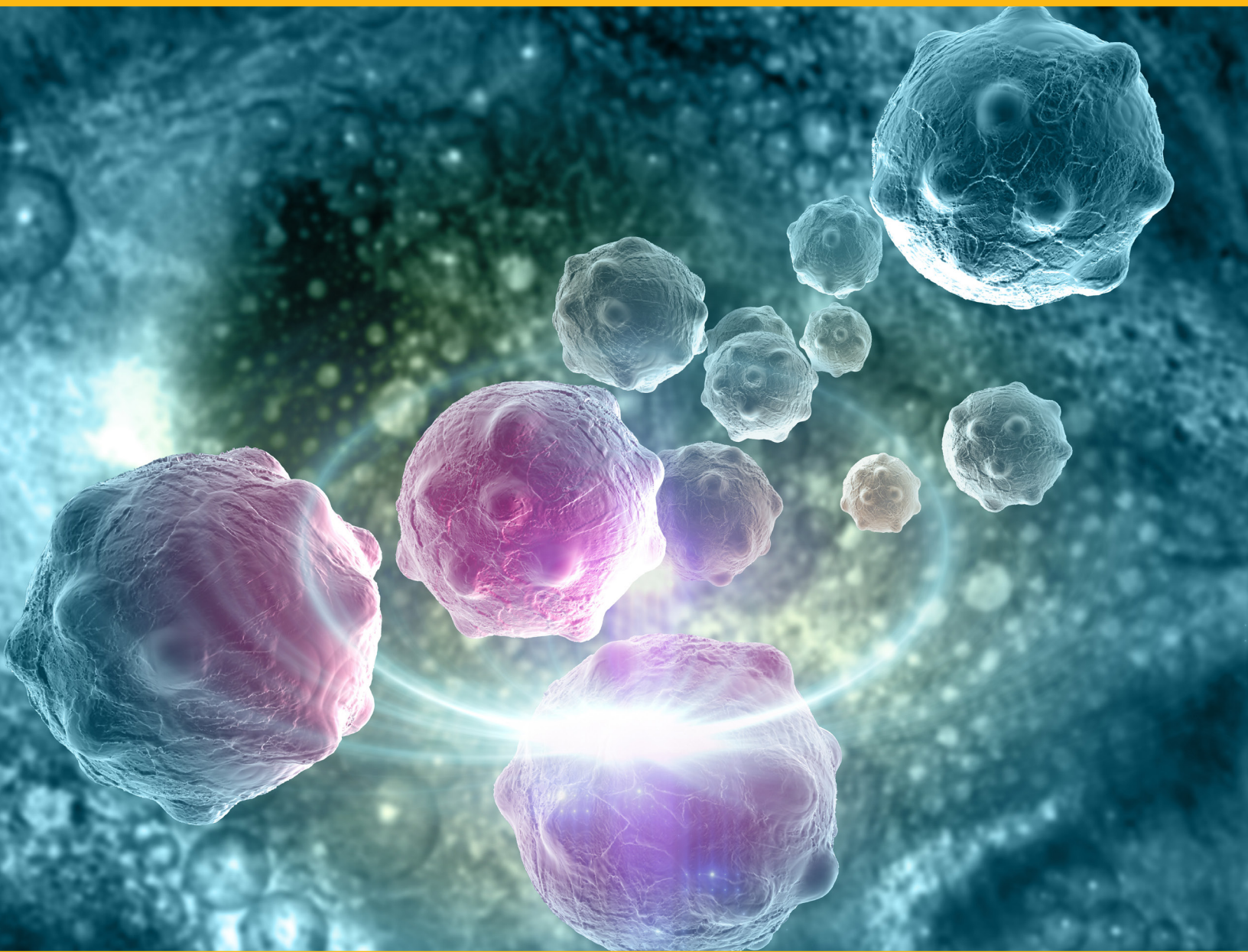


TOOLS TO MONITOR BIOLOGY IN 3D CULTURE



TOOLS TO MONITOR BIOLOGY IN 3D CULTURE

Contents

Introduction..... 1

1 Cell Health Changes in 3D..... 2

2 Metabolic Changes in 3D 21

3 Gene Expression Changes in 3D..... 33

4 Genome Analysis in 3D 45

5 Measuring Assays with a Plate Reader..... 56

Introduction

Cells in culture are used as in vitro models to represent what will happen in vivo. A variety of different culture models are used routinely during the drug discovery process to investigate signaling pathways or to predict cytotoxicity or safety of compounds in humans. Traditionally cells have been grown in suspension or as monolayers on a plastic surface to carry out those experiments.

In vitro models are constantly being improved to provide more physiologically relevant cell culture systems that more accurately represent human responsiveness. Although reported in the published literature for decades, one of the major improvements gaining in popularity is to culture cells as three dimensional (3D) clusters called “spheroids” that can mimic the cell-to-cell contacts that occur in vivo.

There is a spectrum of 3D culture models available. On one end of the spectrum are simple 3D spheroids (which will form in a matrix-free environment). Many tumor cell lines, as an example, will spontaneously self-aggregate to form spheroids when cultured using special conditions such as ultralow binding surfaces or the hanging drop method that prevent cell-to-plastic surface interaction necessary to form a monolayer. At the other end of the spectrum are more complex microphysiological systems. These multiple stem cell-derived organoids represent differentiated tissues (with multiple cell types) that are interconnected on chips containing microfluidic channels that mimic a functioning vasculature.

The choice of the model system involves a compromise between the number of samples to be tested (throughput) and the cost and complexity of the model system. High-throughput methods are available to generate and assay spheroids directly using homogeneous methods. However, most researchers use model systems of intermediate complexity. Examples of such systems include co-cultures of multiple cell types in hydrogels made of extracellular matrix components and culture systems that incorporate fluid flow to induce shearing forces that mimic natural movement.

When choosing a model system, it is important to consider exactly what you want to know at the end of the experiment. The culture model and assay system combination should be “fit-for-purpose”, meaning as simple as possible, but as complex as necessary to answer the experimental question. For example, you are studying whether a test compound (from an expansive library of small molecules) is directly cytotoxic, it is probably not necessary to use a complex model system composed of multiple interconnected organoids.

In addition to the culture model system, the choice of assay system also needs to be considered. Some assays may require a plate reader and a high throughput format to record the average signal from the entire sample well, while others may require microscopic confocal imaging to capture multiple fluorescent markers throughout the entire depth of the sample. (a) Additionally, not all commercially available cell-based assay systems will work with large (>350um) 3D culture models. Appropriate controls verifying cell lysis or reagent penetration are required for new model systems.

The following chapters address many of these issues and describe Promega assay systems that have been verified to work with 3D culture models.

(a) Riss, T. and Trask, O. J., Jr. (2021) Factors to consider when interrogating 3D culture models with plate readers or automated microscopes. *In Vitro Cellular & Developmental Biology – Animal*. **57**, 238.

Chapter 1

CELL HEALTH CHANGES IN 3D

Cell Viability Assays	3
CellTiter-Glo® 3D Cell Viability Assay	3
RealTime-Glo™ MT Cell Viability Assay	7
Cytotoxicity Assays	9
CellTox™ Green Cytotoxicity Assay	9
LDH-Glo™ Cytotoxicity Assay	11
Apoptosis Assays	13
Caspase-Glo® 3/7 3D Assay	13
RealTime-Glo™ Annexin V Apoptosis and Necrosis Assay.....	15
Autophagic Flux Assay	17
Autophagy LC3 HiBiT Reporter Assay	17
Modeling Hepatocyte Function.....	18
P450-Glo™ Assays	18

The most basic answer sought after cultured cells undergo treatment is whether the treatment resulted in cell death. This question is best answered with either a cell viability assay to measure the relative levels of live cells in a culture or a cytotoxicity assay to measure the relative levels of dead cells in the culture. Cell viability assays measure cells with intact plasma membranes. Cytotoxicity assays measure cells with compromised plasma membranes. The changes observed from a treatment are reflected by cell viability or cytotoxicity assays readings and are a function of compound dosage and length of exposure. Cell death can occur in a variety of ways, including necrosis and apoptosis. Apoptosis is a defined pathway of cell death whereas necrosis is not. Other cellular responses may also occur. Some cells, especially liver cells, may activate detoxifying pathways involving the cytochrome p450 enzymes. Cells may also respond to treatment by co-opting housekeeping pathways like autophagy to fulfill the energy and metabolite needs to survive.

This chapter presents assays for cell viability, cytotoxicity, apoptosis, autophagic flux and cytochrome p450 activity with verified performance with 3D cultured cells. Some assays require adjustments to the standard monolayer culture protocol.

Cell Viability Assays

ATP is a recognized biomarker of live cells and use of the firefly luciferase reaction is a sensitive means of measuring ATP. The basic firefly luciferase reaction requires the luciferase enzyme, ATP, luciferin, O_2 and Mg^{2+} to generate light. When luciferase and luciferin are in excess, light production becomes dependent on the ATP concentration. The CellTiter-Glo® Luminescent Cell Viability Assay is based on this principle. The “add-mix-measure” assay was designed to be added directly to cells in monolayer culture to lyse and stabilize the ATP while providing the luciferase and luciferin to generate light levels proportional to the amount of ATP released. Because native firefly luciferase from *Photinus pyralis* could not withstand these conditions so a new luciferase called Ultra-Glo™ Recombinant Luciferase was engineered to have greater tolerance for detergent, heat and pH (1).

CellTiter-Glo® 3D Cell Viability Assay

Based on the same principles and chemistry of the original CellTiter-Glo® Luminescent Cell Viability Assay assay, the **CellTiter-Glo® 3D Cell Viability Assay** was modified. The amount of detergent was increased to more effectively lyse cells cultured in 3D and

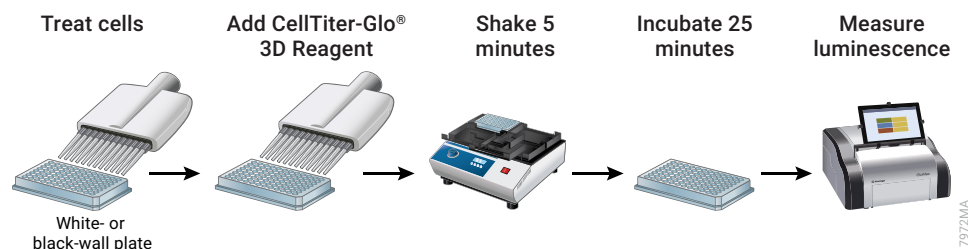


Figure 1. CellTiter-Glo® 3D Workflow.

OTHER RESOURCES

Learn More About 3D Viability & Toxicity Assays

Kijanzka, M. and Kelm, J. (2016) In vitro 3D spheroids and microtissues: ATP-based cell viability and toxicity assays. In: Assay Guidance Manual, Eli Lilly & Company and the National Center for Advancing Translational Sciences, Bethesda, MD. PMID: 26844332

Learn More About Cell Viability Assays

Riss, T.L. *et al.* (2016) Cell viability assays. In: Assay Guidance Manual, Eli Lilly & Company and the National Center for Advancing Translational Sciences, Bethesda, MD. PMID: 23805433

References

1. Hall, M.P. *et al.* (1998) Stabilization of firefly luciferase using directed evolution. In: *Bioluminescence and Chemiluminescence. Perspectives for the 21st Century*. Roda, A., Pazzagli, M., Kricka, L.J., and Staley, P.E., eds., John Wiley & Sons, New York, 392–395.

provide a more accurate determination of ATP (PC1). In addition to more detergent, the protocol was altered to optimize ATP release through a 5-minute shake and a 25-minute incubation (Figure 1). The stability of Ultra-Glo™ rLuciferase is key to this assay. Figure 2 demonstrates measurement of cell viability in spheroid cultures of HCT116 cells by the improved ATP release afforded by the additional detergent and optimized protocol in comparison to another ATP-dependent cell viability assay using the monolayer culture protocol supplied with the assay. CellTiter-Glo® 3D provides a greater window of measurement (Figure 2, Panel A) and inclusion of a DNA binding dye demonstrates greater

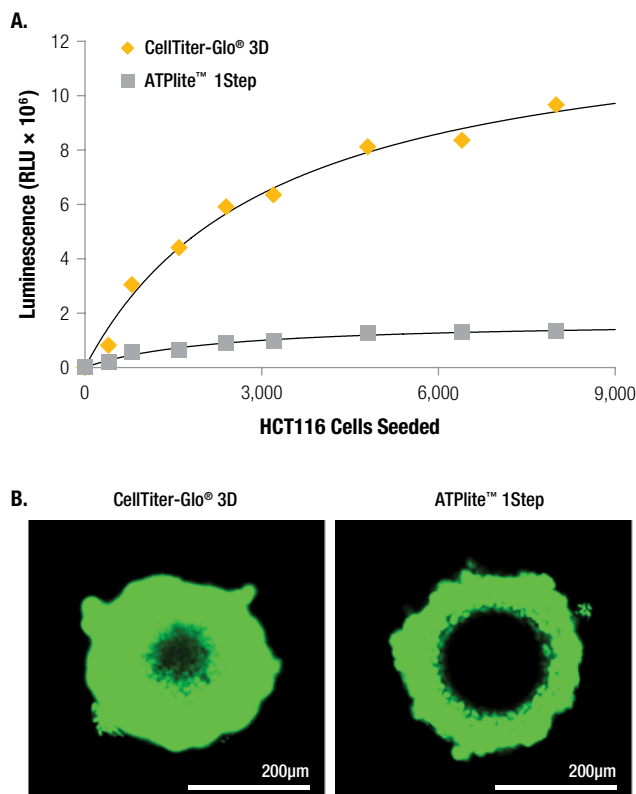


Figure 2. Improved 3D microtissue penetration and more accurate viability data. HCT116 colon cancer spheroids were generated by seeding cells in the InSphero GravityPLUS™ 96-well hanging-drop platform and grown for 4 days. **Panel A.** An equivalent volume of reagent was added to all samples, and, after 5 minutes of shaking, luminescence was recorded at 30 minutes. **Panel B.** A 2X concentration of CellTox™ Green Dye was added to CellTiter-Glo® 3D Reagent (left) or ATPlite™ 1Step Reagent (right) prior to sample addition as an indicator of cell lysis and images were acquired at 30 minutes. The spheroids in Panel B are ~300µm in diameter, and the bars in each image represent a distance of 200µm.

penetration of the spheroid (Figure 2, Panel B). A more dramatic difference is obtained in comparison to colorimetric and fluorometric assays intended for monolayer cultures (Figure 3). CellTiter-Glo® 3D yields a far greater signal-to-background ratio than the other assays with HCT116 cells and human liver microtissue spheroids. The data in Figures 2 and 3 report information from 3D spheroid cultures generated through the hanging drop method. Figure 4 demonstrates compatibility with cells cultured on a hydrogel scaffold (e.g., Matrigel® Matrix) and ULA plates.

OTHER RESOURCES

PC1

Valley, Michael P. et al. (2014)
CellTiter-Glo(R) 3D: A Sensitive,
Accurate Viability Assay for 3D
Cell Cultures.

Can I use the classic CellTiter-Glo® or the more stable CellTiter-Glo® 2.0 assays with my 3D cultures?

The answer is a qualified “yes”. There are many citations on the use of the classic CellTiter-Glo® Assay with 3D cultures, and the assay still produces a signal proportional to microtissue diameter. However, in our hands the CellTiter-Glo® 3D gives a larger window of measurement than the classic CellTiter-Glo® Assay because it is able to release ATP more completely from the cultured microtissues (PC1). CellTiter-Glo® 3D has also been shown to work with many different 3D culture systems, which is likely due to the additional detergent. Regardless of which assay you use with your 3D cultures, be sure to follow the protocol changes outlined for the the CellTiter-Glo® 3D Assay.

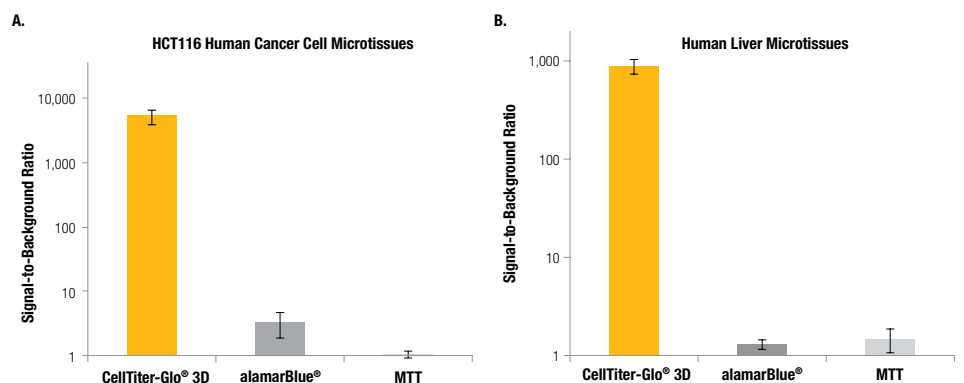


Figure 3. Performance of the CellTiter-Glo® 3D Assay compared to other viability assays. Signal-to-background ratios for the luminescent CellTiter-Glo® 3D Assay compared to fluorescence (alamarBlue®) and absorbance (MTT) assays. **Panel A.** HCT116 colon cancer cells (~340µm) grown for 4 days in the InSphero GravityPLUS™ 96-well hanging-drop platform. **Panel B.** InSphero human liver microtissues (~250µm). All microtissues were assayed according to the assay manufacturers' protocols. Total assay times for the CellTiter-Glo® 3D, alamarBlue® and MTT assays were 30 minutes, 3 hours and 8 hours, respectively.

3D Method	Made by	Cells	Citation
ULA	Corning	MCF-7 and SKBR-3	Novohradsky, V. <i>et al.</i> (2019) <i>Sci. Rep.</i> 9 , 13327. PMID: 31527683
ULA	Corning	1° Hepato-cellular carcinoma tumoroids	Gavini, J. <i>et al.</i> (2019) <i>Cell Death Dis.</i> 10 , 749. PMID: 31582741
ULA	Sumitomo Bakelite	1° human ovary & endometrial cells	Yoshimura, C. <i>et al.</i> (2019) <i>Mol. Cancer Ther.</i> 18 , 1205–1216. PMID: 31092565
ULA	Sumitomo Bakelite	A549	Akizuki, R. <i>et al.</i> (2018) <i>Biochim. Biophys. Acta-Mol. Cell Res.</i> 1865 , 769–780. PMID: 29524521
ULA	Greiner Bio-One	COV434, KGN	Gogola, J., Hoffmann, M., and Ptak, A. (2019) <i>Chemosphere</i> 217 , 100–110. PMID: 30414542
ULA	Greiner Bio-One	1° pediatric high-grade gliomas	Metselaar, D.S. <i>et al.</i> (2019) <i>EBioMedicine</i> 50 , 81–92. PMID: 31735550
Hydrogel	Corning (Matrigel®)	1° human and mouse intestinal epithelial cells	VanDussen, K.L., Sonnek, N.M. and Stappenbeck, T.S. (2019) <i>Stem Cell Res.</i> 37 , 101430. PMID: 30933720
Hydrogel	Corning (Matrigel®)	Human rectal cancer organoids	Yao, Y. <i>et al.</i> (2020) <i>Cell Stem Cell</i> 26 , 17–26. PMID: 31761724
Hydrogel	Thermo Fisher (Cultrex®)	Human and Mouse Bladder Organoids	Mullenders, J. <i>et al.</i> (2019) <i>PNAS</i> 116 , 4567–4574. PMID: 30787188
Hydrogel	Thermo Fisher (Cultrex®)	SW620	Abraham, A.D. <i>et al.</i> (2019) <i>J. Med. Chem.</i> 62 , 10182–10203. PMID: 31675229
Hydrogel	Lab-made gel from heart and liver ECMs	iCell® Cardiomyocytes & Hepatocytes	Yu, C. <i>et al.</i> (2019) <i>Biomaterials</i> 194 , 1–13. PMID: 30562651
Hydrogel	Lab-made peptide-modified hyaluronic acid-based gel	Neuralized H9 human embryonic stem cells	Seidlits, S.K. <i>et al.</i> (2019) <i>J. Biomed. Mater. Res. A</i> 107 , 704–718. PMID: 30615255
Hydrogel	Lab-made alginate, collagen, gelatin & methacrylated gelatin gels	Human mesenchymal stem cells	Bedell, M.L. <i>et al.</i> (2020) <i>Bioprinting</i> 17 , e00068. DOI: 10.1016/j.bprint.2019.e00068
Hydrogel	Lab-made crosslinked plasma protein gel	Human dermal fibroblasts	Barreda, L. <i>et al.</i> (2019) <i>J. Mech. Behav. Biomed. Mater.</i> 89 , 107–113. PMID: 30267992

Table 1. Example citations of CellTiter-Glo® 3D Cell Viability Assay with 3D cultures on ultra-low attachment plates (ULA) or hydrogel scaffolds. ECM = extracellular matrix; 1° = primary

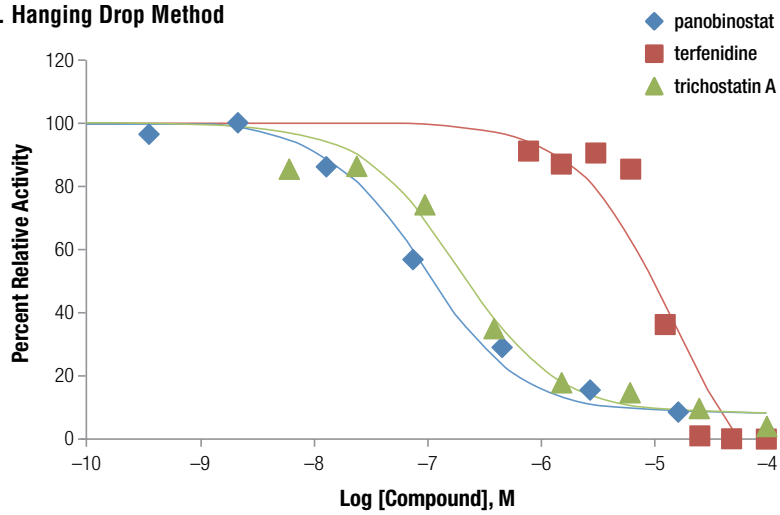
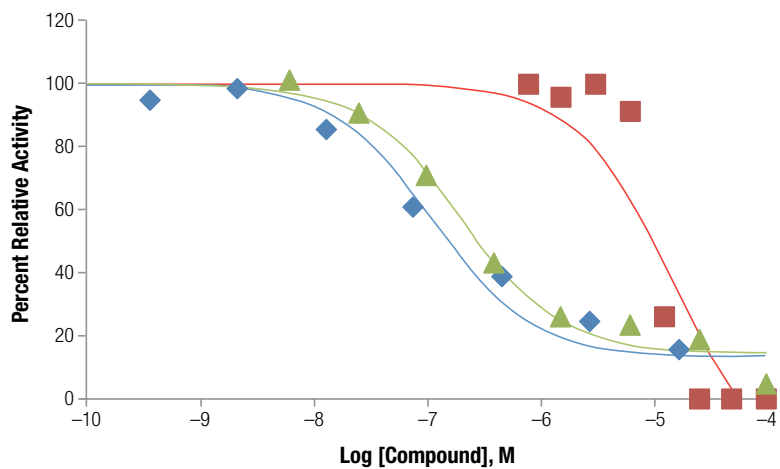
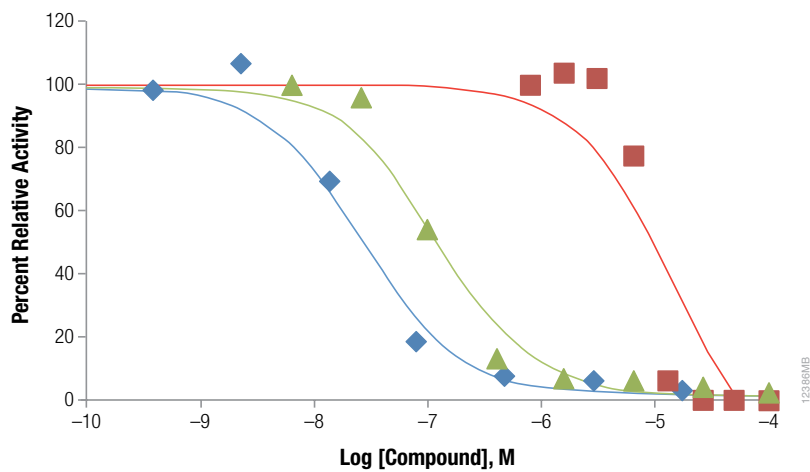
A. Hanging Drop Method**B. ULA****C. Matrigel®**

Figure 4. CellTiter-Glo® 3D Assay is compatible with a variety of 3D culture methods. HCT116 colon cancer cells were seeded as follows: 400 cells in hanging-drop (**Panel A**); 1,000 cells in ULA or Matrigel® (**Panels B and C**). Microtissues were grown for 4 days, treated with compounds for 48 hours, then assayed with the CellTiter-Glo® 3D Reagent.

RealTime-Glo™ MT Cell Viability Assay

One of the challenges with using an endpoint assay like CellTiter-Glo® 3D is deciding when to perform the assay. Typically, this challenge is solved by performing a time course experiment. Replicate plates are set up with compounds and assayed at various time points (e.g., 6 hours, 12 hours, 24 hours, etc.) to discover the window of time when a compound exhibits toxicity. Once you determine this window, subsequent experiments are performed within this window. Time course experiments can consume a large number of cells and reagents but are critical to find the ideal window of time for an experiment.

A live-cell kinetic assay of cell viability would be the ideal solution to this challenge. Imagine setting up one plate and reading it at multiple time points to obtain the same time course data. This method could identify the window of toxicity and you could continue to use the live-cell kinetic assay for subsequent experiments or switch to an endpoint assay. This was the design concept behind the non-lytic **RealTime-Glo™ MT Cell Viability Assay (PC2)**.

The non-lytic RealTime-Glo™ MT Cell Viability Assay has two components: purified NanoLuc® Luciferase (NLuc) and the MT (i.e. metabolic) Cell Viability Substrate, together referred to as the RealTime-Glo™ Reagent. The NLuc protein and MT Cell Viability Substrate are added to the culture media of live cells. NLuc cannot use the MT Substrate to generate light. The MT Substrate enters live cells and reducing equivalents within the cell reduce the MT Substrate to an NLuc substrate which passes out of the cell and reacts with NLuc in the medium, generating light. A dead cell rapidly loses the ability to reduce the MT Substrate to the NLuc substrate and the NLuc signal ceases (**PC2**, Figure 5).

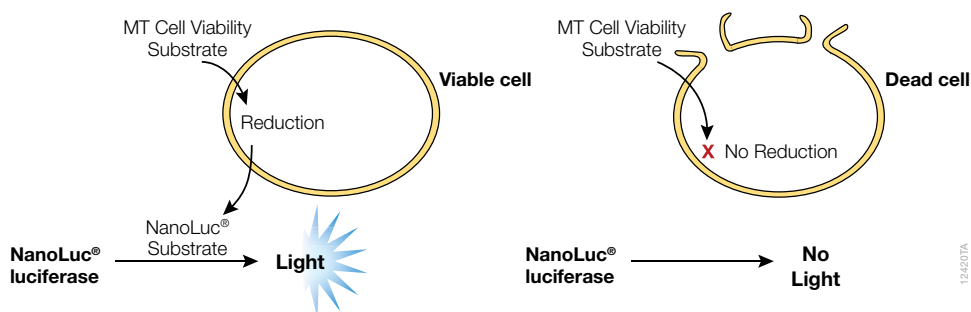


Figure 5. RealTime-Glo™ MT Cell Viability Assay overview. The assay involves adding NanoLuc® luciferase and a cell-permeable prosubstrate, the MT Cell Viability Substrate, to cells in culture. The MT Cell Viability Substrate is reduced to a NanoLuc® substrate by metabolically active cells. The NanoLuc® substrate diffuses from cells into the surrounding culture medium and is rapidly used by NanoLuc® Enzyme to produce a luminescent signal. The signal correlates with the number of viable cells. Dead cells do not reduce the substrate and produce no signal.

Owing to the stability of the NLuc enzyme and MT substrate, the assay can be performed for an extended period up to 72 hours. Measurements of the NLuc signal can be taken at any time during the incubation. You can add the RealTime-Glo™ Reagent at the time of plating, dosing or even wait until the end of the assay and use it as an endpoint assay (Figure 6).

OTHER RESOURCES

PC2

Duellman, Sarah J. et al. (2015) Bioluminescent, Nonlytic, Real-Time Cell Viability Assay and Use in Inhibitor Screening. *Assay and Drug Development Technologies* 456-465.

What is NanoLuc® Luciferase?

NanoLuc® Luciferase is an extremely bright 19kDa luciferase engineered from the luciferase of a deep-sea shrimp, *Oplophorus gracilirostris*. The engineered protein is extremely stable with a half-life exceeding 4 days in culture media at 37°C. With its ideal substrate furimazine, NanoLuc® Luciferase is 100-fold brighter than either firefly or *Renilla* luciferases. Get the whole story of the creation of NanoLuc® Luciferase and furimazine in Hall et al. (**PC3**).

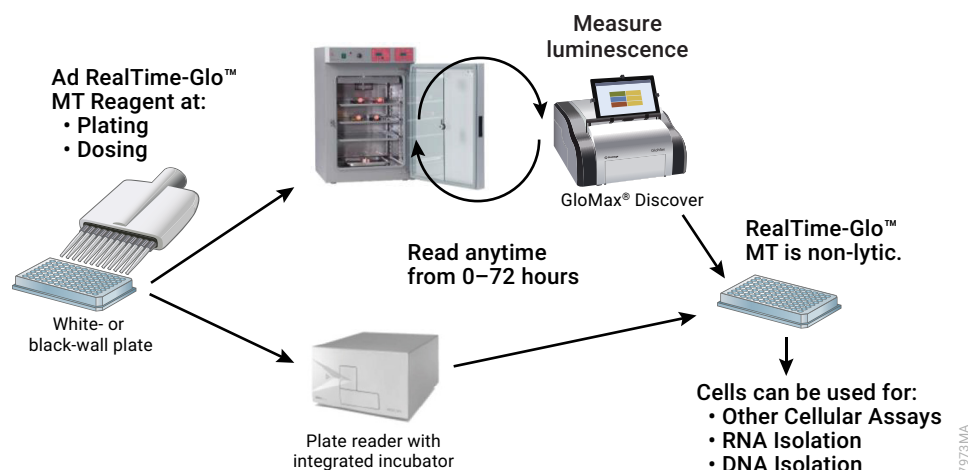


Figure 6. The adaptable workflow of the RealTime-Glo™ MT Cell Viability Assay. Assay reagent can be added at plating or dosing, and viability monitored over 72 hours. An endpoint method is available but not shown. The assay is non-lytic so assayed cells can be used for other assays. More information about reading live-cell, kinetic assays on a standard plate reader can be found in Chapter 5.

The RealTime-Glo™ MT Cell Viability Assay was developed on monolayer cultures but the reagent has been tested with 3D cultures (TM431). The assay methods are identical for monolayer and 3D cultures, and both require that you determine how many cells can be used to maintain a linear response of the reagent over the course of the experiment. Figure 7 demonstrates the response of HCT116 spheroids to doxorubicin treatment. Codrich *et al.* (2) monitored responses of patient-derived colorectal cancer organoid cultures on the hydrogel scaffold Matrigel® with RealTime-Glo™ MT. Krainer *et al.* (PC4) demonstrated the utility of using the RealTime-Glo™ MT Assay for optimizing the culture conditions needed for patient-derived colorectal cancer organoids. Ferreira *et al.* (3) used

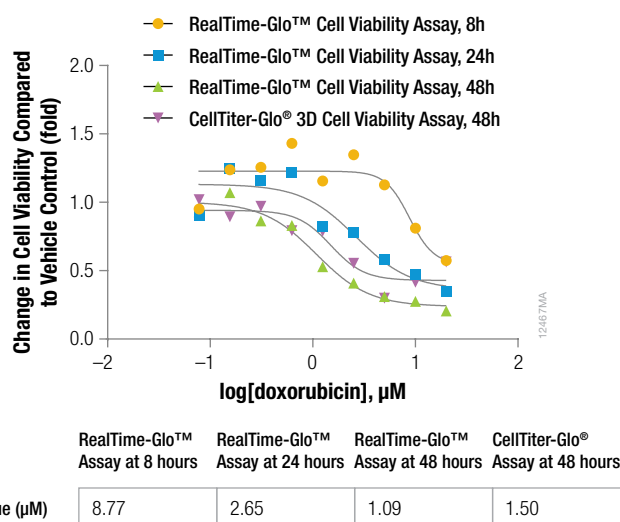


Figure 7. Analysis of doxorubicin-treated HCT116 spheroids with the RealTime-Glo™ MT Cell Viability Assay and the CellTiter-Glo® 3D Assay. HCT116 spheroids (~520μm) were treated with various concentrations of doxorubicin over the course of 48 hours. A subset of cells was assayed with RealTime-Glo™ MT Reagent and read at 8, 24 and 48 hours. The other subset of cells was assayed with CellTiter-Glo® 3D Reagent at 48 hours. Luminescence was measured with a GloMax® Discover Microplate Reader.

OTHER RESOURCES

AN308

Assaying Cell Health in 3D Cell Culture with the GloMax® Discover System.

TM431

RealTime-Glo™ MT Cell Viability Assay Technical Manual.

PC4

Krainer, Iris M. *et al.* (2019) Determining the Optimal Culturing Conditions of Patient-Derived Colorectal Cancer Organoids using the RealTime-Glo(TM) Cell Viability Assay.

References

- Codrich, M. *et al.* (2019) Inhibition of APE1-endonuclease activity affects cell metabolism in colon cancer cells via a p53-dependent pathway. *DNA Repair* **82**, 102675. PMID: 31450087
- Ferreira, S.A. *et al.* (2018) Neighboring cells override 3D hydrogel matrix cues to drive human MSC quiescence. *Biomaterials* **176**, 13–23. PMID: 29852376

How do you know the RealTime-Glo® Reagent is penetrating to the center of the culture?

The short answer is that we do not know. We know that the assay has a signal proportional to the size of the microtissue (AN308). We know that with spheroid cultures, the RealTime-Glo™ MT signal parallels the signal from CellTiter-Glo® 3D Assay. Small molecules like the pro-substrate likely penetrate the depths of the microtissue, but whether NanoLuc® Luciferase does is unknown.

the assay to monitor human mesenchymal stem cells on lab-made thiolated hyaluronidate hydrogels. Orbach *et al.* (4) used the assay to monitor human and rat liver organotypic sandwich cultures between collagen and fibronectin/collagen hydrogels.

Microfluidic flow devices containing multiple tissue organoids or tissue spheroids offer a more complex “body-on-a-chip” model. These models can provide a more realistic view of how an organism would respond to a treatment versus how individual cell types respond to treatment. Media is shared among cells in these devices, allowing the metabolites or secretion from one cell type to potentially affect responses in other cells. Methods for analyzing these models are likely to be non-lytic, using either cells engineered with biosensors or methods based on analysis of the culture media. The RealTime-Glo™ MT Assay is non-lytic and has been used to monitor overall cell viability in such systems. Candini *et al.* (5) designed a microfluidic device, called VITVO, to more accurately reproduce the tumor microenvironment. The device has two chambers separated by a 3D fibrous matrix with oxygen-permeable, optically transparent windows next to each chamber. Media flows from one chamber to the other through cells in the matrix. The RealTime-Glo™ MT Assay was used to monitor growth of cells cultured for up to 96 hours on the matrix and reductions in cell number upon treatment. The device was used with tumor cell lines engineered to express fluorescent proteins as well as primary human lung cancer cells. Fluorescent and luminescent signals were monitored with a GloMax® Discover Microplate Reader.

Cytotoxicity Assays

Cell death, or loss of membrane integrity, can be measured non-radioactively in two ways: active enzymatic methods or passive dye-based methods. Enzymatic methods rely on the assay of normally cytoplasmic enzymes (e.g., lactate dehydrogenase or LDH) in conditioned cell culture medium and, by necessity, are non-lytic. The substrates used to assay the enzyme are bulky and do not freely cross an intact cell membrane. Dye-based methods typically rely on access to cellular proteins or double-stranded DNA in cells with damaged membranes.

Cytotoxicity assays are a true measure of cell death because the assays rely on rupture of the cell membrane. The assays are built on measuring the presences of an enzyme or other molecule in the conditioned cell culture medium, rather than those safely hidden behind an intact cellular membrane. Proteases—those already in the culture medium and those released upon rupture of the cell membrane—are present, causing released enzymes to have a finite half-life outside of the cell. Assays must be properly timed to catch active enzymes. Although enzymatic assays are subject to timing issues, they do provide the greatest signal-to-background ratios due to enzymatic amplification of the signal.

CellTox™ Green Cytotoxicity Assay

Passive dyes, like those that bind double-stranded DNA, alleviate this timing issue. Once the cell membrane is compromised, the dyes can bind to DNA in the cell or DNA released from the cells (PC5). Passive dyes do not offer the amplification of signal obtained from enzymatic assays, so the signal change caused by cell death will occur in a smaller window. Passive dyes can be a useful tool to learn the timing of a cytotoxic event for a

OTHER RESOURCES

Learn More About Cytotoxicity Assays

Riss, T. *et al.* (2019) Cytotoxicity Assays: In vitro methods to measure dead cells. In: *Assay Guidance Manual*. Eli Lilly & Company and the National Center for Advancing Translational Sciences, Bethesda, MD. PMID: 31070879

PC5

CellTox™ Green Cytotoxicity Assay Technical Manual. Promega Corporation.

References

- Orbach, S.M., Ehrich, M.F. and Rajagopalan, P. (2018) High-throughput toxicity testing of chemicals and mixtures in organotypic multi-cellular cultures of primary human hepatic cells. *Toxicol. In Vitro* **51**, 83–94. PMID: 29751030
- Candini, O. *et al.* (2019) A novel 3D in vitro platform for pre-clinical investigations in drug testing, gene therapy, and immuno-oncology. *Sci. Rep.* **9**, 7154. PMID: 31073193

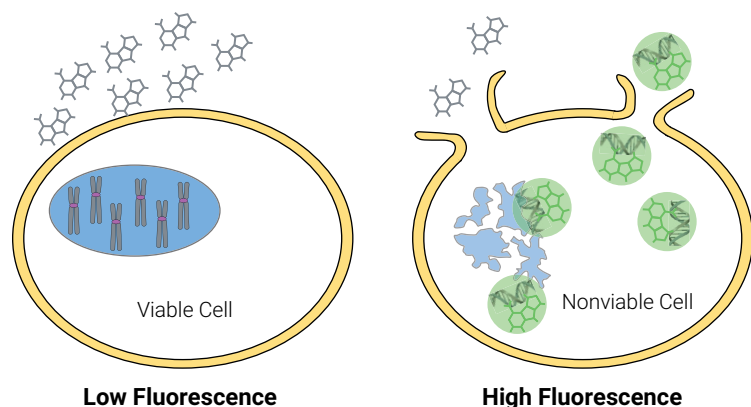


Figure 8. CellTox™ Green Dye binds DNA of cells with impaired membrane integrity.

more sensitive enzymatic assay or perform other assays that are dependent on timing of cytotoxicity, like caspase assays (PC6).

The **CellTox™ Green Cytotoxicity Assay** provides an easy, fast and accurate method to determine toxic effects during or after long-term exposure of cells in culture. CellTox™ Green Cytotoxicity Assay is a non-toxic dye that can be added upon plating of the cells or with dosing of test compounds and assayed at anytime up to 72 hours, much like the RealTime-Glo™ MT Assay (Figure 6). The CellTox™ Green dye binds to DNA in cells with compromised membranes and is not subject to the limitations of enzymatic assays. CellTox™ Green can allow kinetic studies of cytotoxicity to pinpoint when to perform other assays.

CellTox™ Green was used by Obinu *et al.* (6) to examine the effects of nanoparticles on HepG2 and A498 cells grown as spheroids. Romagnoli *et al.* (7) examined cytotoxicity of a conditional knockout of a protein in mouse mammospheres grown on ULA plates. Merriman and Fu (8) monitored cytotoxicity over a 48 hour period of a β cell line grown on a Matrigel®/fibronectin matrix following treatment. At the end of the experiment, all cells were lysed with detergent and a reading for total cells was measured from the CellTox™ Green. The total cell data were used to normalize the cytotoxicity data.

CellTox™ Green is often cited for use upstream of a CellTiter-Glo® Viability Assay. Relying on cell viability measurements alone for cytotoxicity can lead to misinterpretation if the compounds under study actually cause cytostasis and not cytotoxicity. A truly cytotoxic event will demonstrate a drop in the signal from the cell viability assay with a concurrent rise in the signal from the cytotoxicity assay (Figure 9). Depping *et al.* (9) used CellTox™ Green followed by CellTiter-Glo® 3D to examine drug effects of MCF-7 cell spheroids. Pahk *et al.* (10) used CellTox™ Green and the classic CellTiter-Glo® Assay to examine the ability of a focused ultrasound beam to disrupt MDA-MB-231 cells in a hydrogel. Neirinckx *et al.* (11) looked at the response of patient-derived organoids to treatments using CellTox™ Green followed by CellTiter-Glo® 2.0.

CellTox™ Green lends itself easily to fluorescent imaging. An example image is in Figure 2B where CellTox™ Green was used as a tool to demonstrate how effectively CellTiter-Glo® 3D lyses spheroids. Fluorescence microscopy offers a secondary means of confirming

References

- Obinu, A. *et al.* (2019) Poly (ethyl 2-cyanoacrylate) nanoparticles (PECA-NPs) as possible agents in tumor treatment. *Colloids Surf. B Biointerfaces* **177**, 520–528. PMID: 30822627
- Romagnoli, M. *et al.* (2019) Deciphering the mammary stem cell niche: A role for laminin-binding integrins. *Stem Cell Rep.* **12**, 831–844. PMID: 30905738
- Merriman, C. and Fu, D. (2019) Down-regulation of the islet-specific zinc transporter-8 (ZnT8) protects human insulinoma cells against inflammatory stress. *J. Biol. Chem.* **294**, 16992–17006. PMID: 31591269
- Depping, R. *et al.* (2019) The nuclear export inhibitor selinexor inhibits hypoxia signaling pathway and 3D spheroid growth of cancer cells. *Oncotargets Ther.* **12**, 8387–8399. PMID: 31632086
- Pahk, K.J. *et al.* (2019) Boiling histotrophy-induced partial mechanical ablation modulates tumour microenvironment by promoting immunogenic cell death of cancers. *Sci. Rep.* **9**, 9050. PMID: 31227775
- Neirinckx, V. *et al.* (2019) The soluble form of pan-RTK inhibitor and tumor suppressor LRIG1 mediates downregulation of AXL through direct protein-protein interaction in glioblastoma. *Neuro-Oncology Adv.* **1**, vdz024. PMID: 32642659



Naturally-derived hydrogels can give high background signals.

Naturally-derived matrices may contain exogenous DNA. For example, the Matrigel® Matrix is formed by the Engelbreth-Holm-Swann (EHS) mouse sarcoma. Being a product of cultured cells, the matrix can contain remnants of cell death, like EHS DNA. Exogenous DNA in the well can complicate the use of the CellTox™ Green Cytotoxicity Assay to the point that the contaminating DNA can make the assay unsuitable for use. The more Matrigel® Matrix used, the greater the background signal.

OTHER RESOURCES

PC6

Vidugiriene, J. et al. (2014). Bioluminescent Cell-Based NAD(P)/NAD(P)H Assays for Rapid Dinucleotide Measurement and Inhibitor Screening. *Assay and Drug Development Technologies*.

PC7

Leippe, D. et al. (2016). Bioluminescent Assays for Glucose and Glutamine Metabolism: High-Throughput Screening for Changes in Extracellular and Intracellular Metabolites. *Society for Laboratory Automation and Screening*.

PC8

Dixon, A.S. et al. (2016). NanoLuc Complementation Reporter Optimized for Accurate Measurement of Protein Interactions in Cells. *ACS Chem. Biol.*

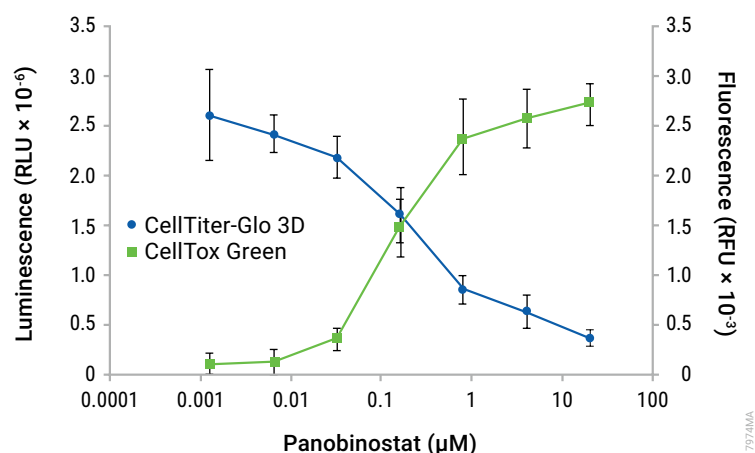


Figure 9. Multiplexing viability and cytotoxicity assays using 3D spheroids. HCT116 spheroids (~350μm) were treated with CellTox™ Green and panobinostat for 47 hours. After recording CellTox™ Green fluorescence, an equal volume of CellTiter-Glo® 3D was added to measure viable cells.

cytotoxicity results. Obinu *et al.* (6) captured images of cells on an imaging plate reader. Some of the images show spheroids with glowing centers, supporting the concept that large spheroids likely have a necrotic center due to poor penetration of nutrients and oxygen to the center.

LDH-Glo™ Cytotoxicity Assay

As mentioned previously, active enzymatic assays are the most sensitive cytotoxicity assays due to signal amplification through catalysis. A widely used biomarker for cytotoxicity is the release of lactate dehydrogenase (LDH) into the culture media, and LDH levels are typically measured with colorimetric or fluorescent readouts. The **LDH-Glo™ Cytotoxicity Assay** borrows heavily from the technology developed for the NAD(P)H-Glo™ Assay (PC7), and is adapted for measuring energy metabolites like lactate (PC8). In the assay, released LDH oxidizes lactate to pyruvate and reduces NAD⁺ to NADH. NADH is used by a reductase to convert proluciferin to luciferin, which is used in a luciferase reaction that generates light (Figure 10).

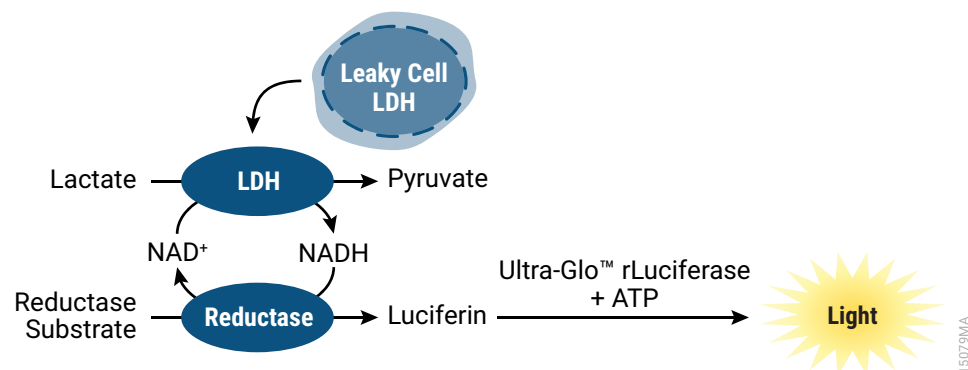


Figure 10. LDH-Glo™ Cytotoxicity Assay principle. Lactate Dehydrogenase (LDH) catalyzes the oxidation of lactate with concomitant reduction of NAD⁺ to NADH. Reductase uses NADH and reductase substrate to generate luciferin, which is converted to a bioluminescent signal by Ultra-Glo™ rLuciferase. The light signal generated is proportional to the amount of LDH present.

The LDH-Glo™ Assay is performed on culture media and requires no manipulation of the cells, so the assay protocol is identical for monolayer and 3D cultures. This bioluminescent assay is much more sensitive than colorimetric or fluorescent assays and only 2–5 µl of the culture medium is required for the assay. Multiple culture medium samples can be withdrawn from a well and either assayed immediately or stored for assaying at the end of the time course (Figure 11), making this a live-cell semi-kinetic assay. Normally, sampling and storage of samples for later assays would present problems as the enzyme has a finite half-life outside the cell. To counter this problem, an LDH storage buffer was developed to stabilize LDH even when frozen and thawed.

OTHER RESOURCES

TM548

LDH-Glo™ Cytotoxicity Assay
Technical Manual

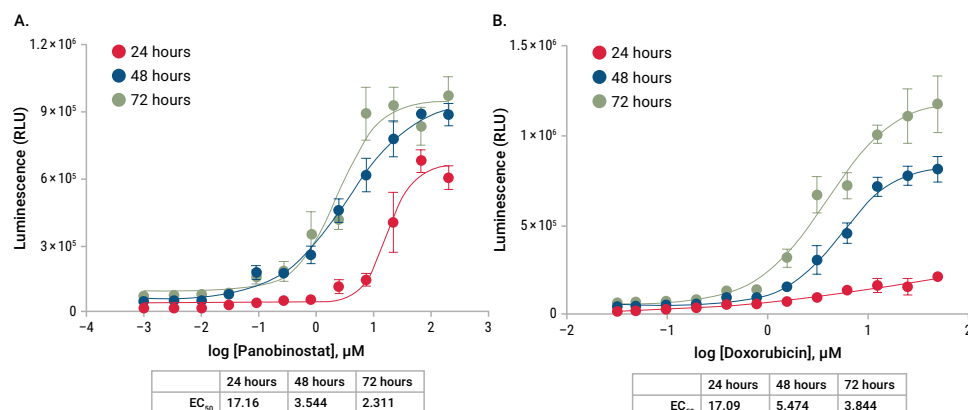


Figure 11. Measuring time-dependent cytotoxicity from the same sample well. HCT116 cells were grown as spheroids in 384-well ULA plates (Corning) and treated with either panobinostat (**Panel A**) or doxorubicin (**Panel B**). Culture medium samples (2.5 µL) were removed at the indicated time points and frozen in LDH Storage Buffer at a 1:10 dilution. Samples were thawed and further diluted 2.5-fold before measuring with the LDH-Glo™ Assay.

Since the LDH-Glo™ Assay uses cell culture media for measurement, the remaining cells can be used for further experiments. The CellTiter-Glo® 3D Cell Viability Assay is a common choice. In Figure 12, culture media was removed for LDH measurement and the remaining viable cells were measured with CellTiter-Glo® 3D. As mentioned previously for multiplexing CellTox™ Green and CellTiter-Glo® 3D, monitoring cytotoxicity with only a viability assay can lead to erroneous results if the experimental compounds induce cytostasis instead of cytotoxicity. Confirming a loss of membrane integrity with a cytotoxicity assay confirms the cytotoxic effects.

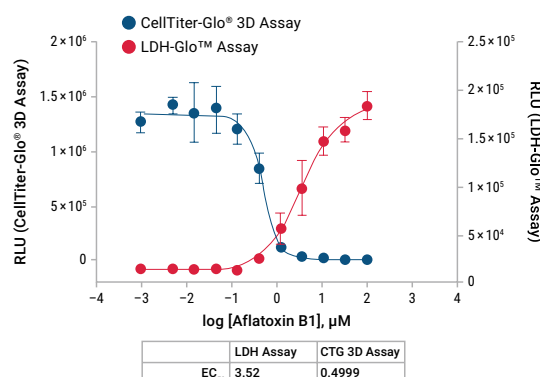


Figure 12. Multiplexing the LDH-Glo™ Assay and the CellTiter-Glo® 3D Assay. Human liver microtissues were treated with aflatoxin B1 for 48 hours. Media samples were collected and diluted in PBS. A portion was assayed with the LDH-Glo™ Assay. The remaining cells were assayed for viability with the CellTiter-Glo® 3D Assay. Experimental details available in TM548.

Apoptosis Assays

A treatment resulting in cell death can occur in a variety of ways. One of the most common is through apoptosis, or programmed cell death. Necrosis, by contrast, is typically rapid and does not activate the apoptotic pathways. A series of events like mitochondrial damage or DNA damage can activate apoptosis, ultimately leading to the activation of the key apoptosis executioner, caspase-3. Cells with activated caspase-3 are committed to apoptotic cell death. Interestingly, caspase-3 activation occurs in cells with intact membranes. With cells in monolayer or 3D culture, the apoptotic cells undergo secondary necrosis, losing membrane integrity.

Caspase-Glo® 3/7 3D Assay

Bioluminescent, fluorescent and colorimetric options exist to measure the activity of the caspase-3 enzyme. Most use some form of cleavage of the amino acid sequence Aspartate-Glutamate-Valine-Aspartate (DEVD) from the reporter molecule. The caspase-3 enzyme cleaves the c-terminal to the DEVD peptide. The **Caspase-Glo® 3/7 3D Assay** has been recognized as the most sensitive means of measuring caspase-3 activity since its introduction about two decades ago. The assay relies on lysis of the cells under study so that the active caspase-3 can react with the proluciferin DEVD-aminoluciferin conjugate substrate (12). Cleavage of the DEVD peptide releases luciferase substrate, aminoluciferin. The amount of light produced is directly related to the amount of active caspase-3 or caspase-7 in the sample.

OTHER RESOURCES

**Learn More
About Cytotoxicity
Assays**

Riss, T. et al. (2019) Cytotoxicity Assays: In vitro methods to measure dead cells. In: *Assay Guidance Manual*. Eli Lilly & Company and the National Center for Advancing Translational Sciences, Bethesda, MD. PMID: 31070879

References

12. Niles, A.L., Moravec, R.A. and Riss, T.L. (2008) Caspase activity assays. *Methods Mol. Biol.* **414**, 137–150. PMID: [18175817](#)

Why is it called the Caspase-Glo® 3/7 Assay?

Cysteine-aspartate proteases (caspases) can be somewhat promiscuous regarding cleavage specificity. Both caspase-3 and caspase-7 can cleave the DEVD peptide so you cannot truly say that you're measuring either caspase exclusively in a cellular extract. Caspase-3 is far more abundant than caspase-7 so measured DEVDase activity most likely originates from caspase-3.

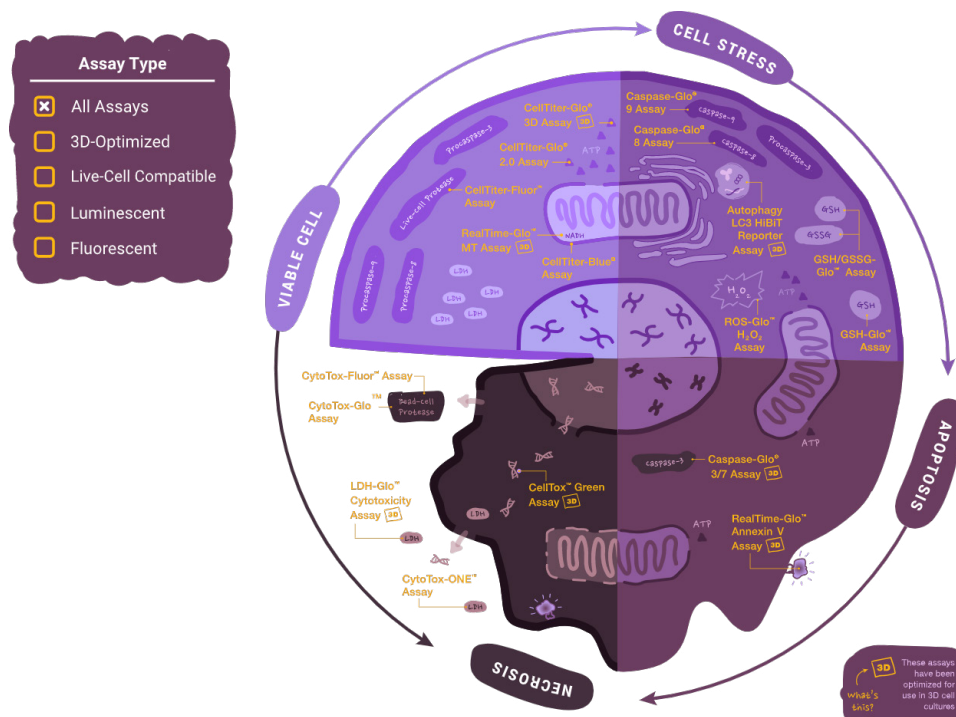


Figure 13. Illustration of the Caspase-Glo® 3/7 3D Assay.

The Caspase-Glo® 3/7 3D Assay is adapted to 3D culture with a simple modification to the protocol. After addition of the reagent to the cells in culture, the plate is shaken for 5 minutes followed by a 25-minute incubation at room temperature prior to measurement of the bioluminescent signal (Figure 14).

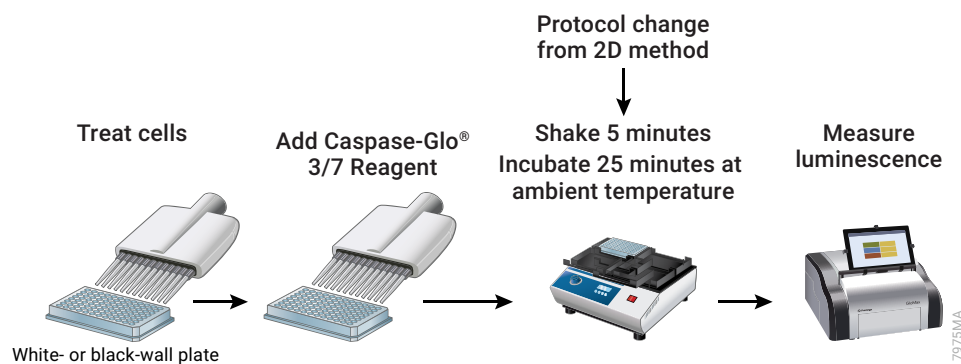


Figure 14. Caspase-Glo® 3/7 3D Assay with protocol modifications for 3D culture assay.

References

13. Tan, M. *et al.* (2019) The FZD7-TWIST1 axis is responsible for anoikis resistance and tumorigenesis in ovarian carcinoma. *Mol. Oncol.* **13**, 757–780. PMID: [30548372](#)
14. Kermanizadeh, A. *et al.* (2019) The importance of inter-individual Kupffer cell variability in the governance of hepatic toxicity in a 3D primary human liver microtissue model. *Sci. Rep.* **9**, 7295. PMID: [31086251](#)
15. Palazzolo, S. *et al.* (2019) An effective multi-stage liposomal DNA origami nanosystem for in vivo cancer therapy. *Cancers* **11**, 1997. PMID: [31842277](#)
16. Gačanić, J. *et al.* (2019) Autonomous ultrafast self-healing hydrogels by pH-responsive function nanofiber gelators as cell matrices. *Adv. Mater.* **31**, 1805044. PMID: [30411838](#)
17. Sharifnia, T. *et al.* (2019) Small-molecule targeting of brachyury transcription factor addition in chordoma. *Nat. Med.* **25**, 292–300. PMID: [30664779](#)

Figure 15 demonstrates the multiplex measurement of cytotoxicity with CellTox™ Green followed by Caspase-Glo® 3/7 measurement of HCT116 spheroids treated with panobinostat, a histone deacetylase inhibitor. The Caspase-Glo® 3/7 Assay has been cited for working with 3D cultures grown on ULA plates (13), hanging drop spheroids (14), organoids (15) and hydrogels (16, 17).

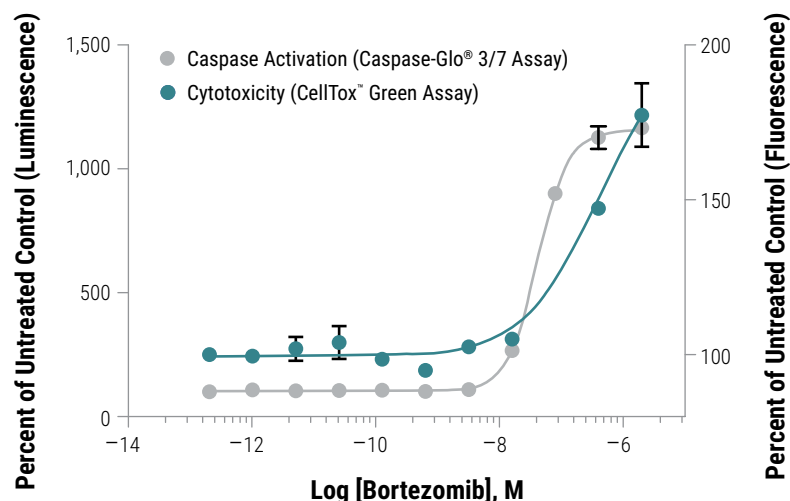


Figure 15. Same-well multiplexing of the CellTox™ Green Cytotoxicity Assay and the Caspase-Glo® 3/7 3D Assay on HCT116 spheroids after 72-hour exposure to panobinostat. Instructions for use of the Caspase-Glo® 3/7 3D Assay are in TM627.

RealTime-Glo™ Annexin V Apoptosis and Necrosis Assay

An early event following caspase-3 activation in cells undergoing apoptosis is the translocation of phosphatidylserine (PS) from the inner leaflet of the plasma membrane to the outer leaflet. The appearance of PS on the outside of the plasma membrane and measurement with fluorophore, Ca^{2+} -dependent, PS-binding annexin V (AnV) has been used to reliably measure apoptosis (18). Fluorophore-labeled AnV molecules are typically used for apoptosis analysis using either fluorescent microscopy or flow cytometry.

While investigating methods to monitor apoptosis in a plate-based, live-cell kinetic format, attention was drawn to AnV after discovering that it can form a lattice-like structure on membranes (19). This structure suggested that a protein:protein interaction (PPI) technology could be applied to measure the kinetics of apoptosis.

The NanoBiT® Protein:Protein Interaction Assay is based on the formation of a NanoBiT™ Luciferase by the SmBiT (11aa) and LgBiT subunits (156aa) (PC9). The SmBiT and LgBiT subunits were engineered to have low affinity for one another. Thus, the interaction of the two subunits is dependent upon other interactions bringing the two into proximity for interaction (Figure 16).

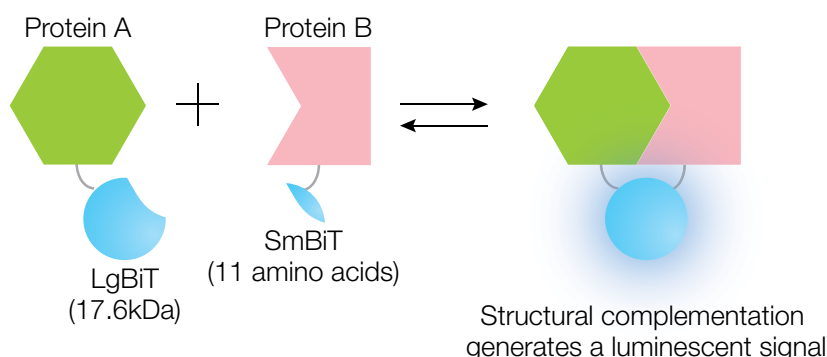


Figure 16. The NanoBiT® Protein:Protein Interaction (PPI) System concept. For a PPI of interest, proteins A and B are fused to LgBiT and SmBiT and expressed in cells. Interaction of fusion partners leads to structural complementation of LgBiT with SmBiT, generating a functional enzyme with a bright, luminescent signal after furimazine substrate addition.

The **RealTime-Glo™ Annexin V Apoptosis Assay** is composed of AnV-SmBiT and AnV-LgBiT plus a NanoLuc® Substrate (PC10). The reagents are added to the culture media and the appearance of PS on the outer leaflet is monitored through the formation of a NanoBiT® Luciferase when the AnV subunits bind proximal PS molecules (Figure 17). A version of this assay is also available with a Necrosis Detection Dye to monitor the appearance of secondary necrosis and loss of membrane integrity, which allows AnV access to inner leaflet PS. Cells can be monitored with this non-lytic assay for up to 48 hours. Figure 18 demonstrates the appearance of the AnV signal prior to the Necrosis Dye signal, which is consistent with apoptosis preceding secondary necrosis. Other lytic bioluminescent cell assays can be performed after taking the last reading of the

OTHER RESOURCES

PC9

Kupcho, K. et al. (2019). A real-time, bioluminescent annexin V assay for the assessment of apoptosis. Springer Open Choice.

PC10

Lazar, D. F. et al. Assessing Autophagic Flux in 2D and 3D Cell Culture Models with a Novel Plate-Based Assay. Promega Corporation.

References

18. Martin, S. et al. (1995) Early redistribution of plasma membrane phosphatidylserine is a general feature of apoptosis regardless of the initiating stimulus: inhibition by overexpression of Bcl-2 and Abl. *J. Exp. Med.* **182**, 1545–1556. PMID: 7595224
19. Bouter, A. et al. (2011) Annexin-A5 assembled into two-dimensional arrays promotes cell membrane repair. *Nat. Comm.* **2**, 270 PMID: 21468022

RealTime-Glo™ Annexin V Apoptosis and Necrosis Assay signal. The lytic nature of assays like Caspase-Glo® 3/7 Assay or the CellTiter-Glo® 3D Assay will disrupt the SmBiT:LgBiT interaction and stop NanoBiT™ Luciferase light production.

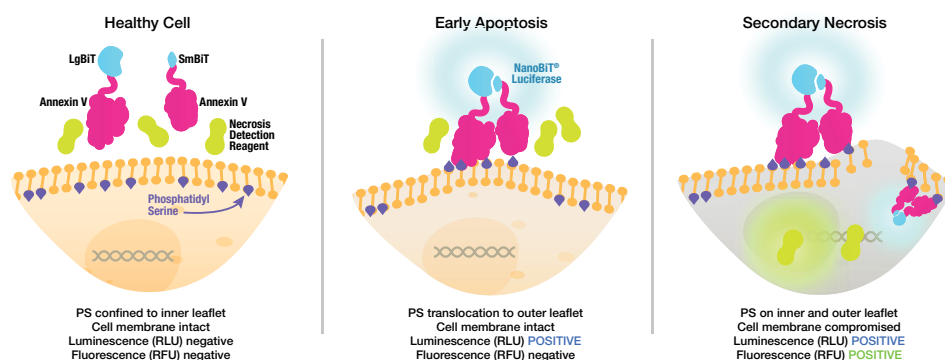


Figure 17. Real-time bioluminescence detection of PS exposure on apoptotic cells. In the RealTime-Glo™ Annexin V Apoptosis and Necrosis Assay, time-dependent increases in luminescence that occur before increases in fluorescence (due to loss of membrane integrity) reflect the apoptotic process. Increases in both luminescent and fluorescent signals are consistent with secondary necrosis following apoptosis or other nonapoptotic mechanisms.

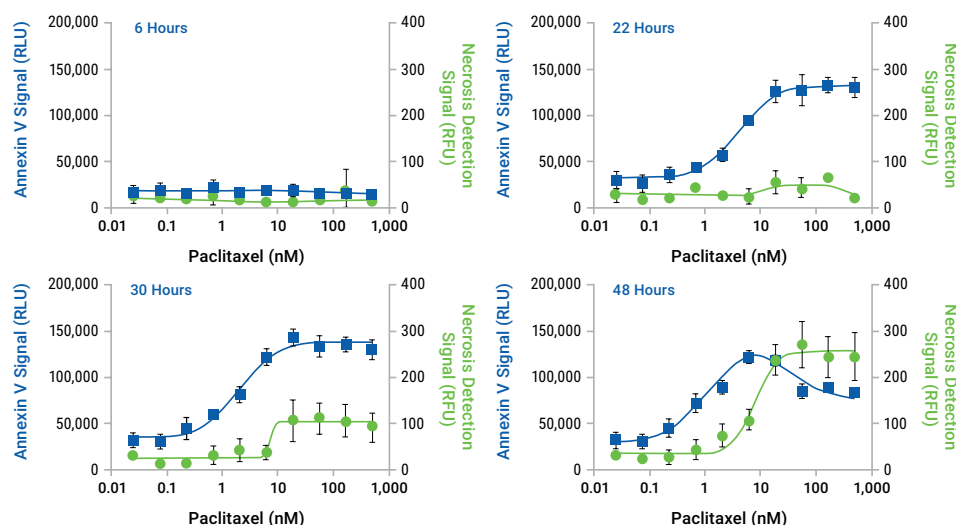


Figure 18. Annexin V binding precedes secondary necrosis in a 3D model system. HepG2 cell spheroids (~450µm) were grown in ULA plates and transferred to white plates prior to challenge with paclitaxel for 48 hours in the presence of the RealTime-Glo™ Annexin V Apoptosis and Necrosis Assay Reagent. Plates were removed from the incubator at various times and measured for luminescence (i.e., Annexin V Signal) and fluorescence (i.e., Necrosis Detection Signal) using a GloMax® Discover Instrument. The t=0 measurement (data not shown) was indistinguishable from the 6-hour time point.

Kota *et al.* (20) screened for differences in response between the BxPC-3 pancreatic ductal adenocarcinoma cell line overexpressing wild-type and mutant KRAS grown in monolayer or 3D culture (spheroids) versus a compound library in 384-well plates. They found that apoptosis was induced more rapidly in 3D cultured versus 2D cultured cells. Herring *et al.* (21) employed a 3D model of human pancreatic neuroendocrine tumors cultured in a

OTHER RESOURCES

References

- Kota, S. *et al.* (2018) A novel three-dimensional high-throughput screening approach identifies inducers of a mutant KRAS selective lethal phenotype. *Oncogene* **37**, 4372–4384. PMID: [29743592](#)
- Herring, B. *et al.* (2020) A growth model of neuroendocrine tumor surrogates and the efficacy of a novel somatostatin-receptor-guided antibody-drug conjugate: perspectives on clinical response? *Surgery* **167**, 197–203. PMID: [31543319](#)

collagen/Matrigel® matrix within a peristaltic micropump perfusion chamber. Response of this tumor model to an antibody-drug conjugate was monitored with the RealTime-Glo™ Annexin V Apoptosis and Necrosis Assay. The signals from the assay were recorded with an in vivo imaging system (IVIS) system commonly used for whole animal imaging.

References

22. Mizushima, N. *et al.* (2010) Methods in mammalian autophagy research. *Cell* 140, 313–326. PMID: 20144757

Autophagic Flux Assay

Autophagy is a normal process where cells recycle building blocks from damaged or unnecessary organelles. When the cell is under stress and lacking sufficient building blocks to respond to that stress, autophagy can increase. Autophagy is critical for maintaining cell health under normal or stress-inducing conditions. Since cancer cells are in constant and increasing need of nutrients to maintain a proliferative phenotype, research is ongoing to modulate autophagy as a means of controlling cancer cell proliferation.

Autophagy LC3 HiBiT Reporter Assay

Most methods to monitor autophagy make use of the normally cytosolic protein LC3-I. Attachment of a PS converts LC3-I to LC3-II. LC3-II is tethered to the interior and exterior lipid bilayers of the phagophore as it encapsulates damaged or redundant organelles, eventually forming an autophagosome. The autophagosome fuses with a lysosome and the interior is reduced to smaller building blocks for reuse. The LC3-II proteins in the interior are degraded along with the organelles. Overall, there is a constant level of LC3-II degradation. Stress due to autophagy increases the flow (or flux) of LC3-II, resulting in a decrease in LC3-II levels compared to normal. Inhibition of autophagy will result in an increase in LC3-II levels. Therefore, changes in the total level of LC3 protein can be used to monitor changes in autophagic flux (22).

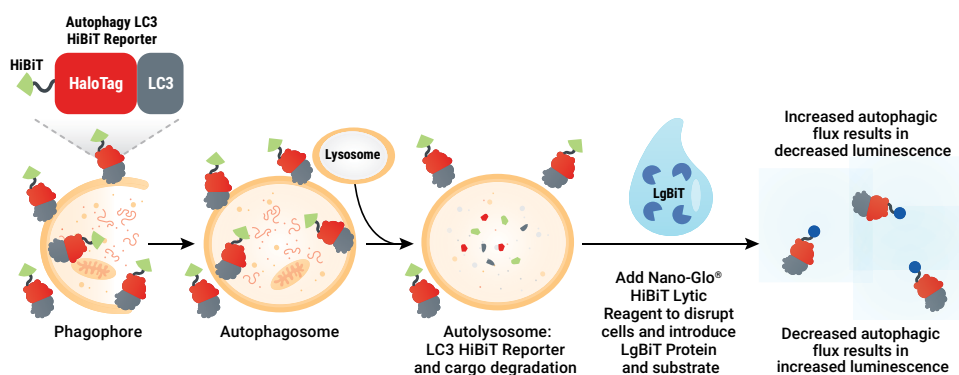


Figure 19. Principle of the Autophagy LC3 HiBiT Reporter Assay. Like endogenous LC3 protein, the Autophagy LC3 HiBiT Reporter expressed in cells becomes targeted to phagophores upon autophagy induction. The reporter molecules captured within the lumen of autophagosomes are subsequently degraded upon autolysosome formation. After cell treatment, the level of intact Autophagy LC3 HiBiT Reporter is indicated by luminescent signal following application of the NanoGlo® HiBiT Lytic Detection System.

Use of fluorescent proteins fused to LC3 is a common method for monitoring autophagic flux, and typically requires fluorescent microscopy or flow cytometry. The **Autophagy LC3 HiBiT Reporter** offers an alternative means of monitoring autophagic flux with plate-based monitoring of LC3 levels (**PC11**). In this system, LC3-I is stably expressed as a fusion with HaloTag® (Figure 19) and the HiBiT peptide. Transient expression is not recommended as transfection is a cellular stressor that induces autophagy. The LC3-I-HaloTag-HiBiT is converted by the cell into LC3-II-HaloTag-HiBiT and is incorporated into phagophores and, ultimately, into autophagosomes. Cells are treated with stressors or inhibitors and levels of LC3-II-HaloTag-HiBiT are monitored with addition of the Nano-Glo® Lytic HiBiT Detection System (Figure 19).

The assay was developed on monolayer cultures but is easily adapted to 3D cultures by increasing the incubation time with the Nano-Glo® Lytic HiBiT Detection Reagent from 2 minutes to 30 minutes. Similar results were seen with HEK293 cells grown in monolayer and spheroid cultures (Figure 20). Other reporter assays can be adapted for use in 3D cultures in a similar manner.

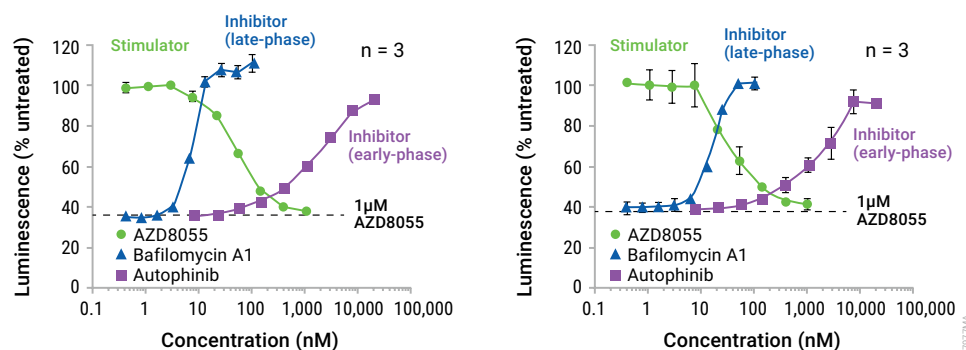


Figure 20. Assessing autophagic flux in monolayer and 3D culture with the Autophagy LC3 HiBiT Reporter. HEK293 Autophagy LC3 HiBiT Reporter Cells were grown in both 2D and 3D conditions. For 2D cultures, 20,000 cells were plated in standard white-walled 96-well culture plates and cultured overnight. For 3D culture, 500 cells were plated into 96-well ULA round bottom, black walled plates and cultured for 4 days prior to assay. (**PC12**)

Modeling Hepatocyte Function

Most small molecule drugs are metabolized by cytochrome P450 (CYP450) enzymes. CYP450-mediated metabolism influences clearance rates of drugs, their toxicity and their interactions with co-administered drugs. Drug discovery researchers need to determine how new drug entities are metabolized by CYP450s and to what extent they may alter CYP450 activity. 3D models are increasingly used to predict the action of drugs or toxins on liver function.

P450-Glo™ Assays

Determining whether a drug candidate induces or inhibits a specific P450 is an important step in the drug development pipeline. To monitor P450 activity at the cellular or biochemical level, modified proluciferin substrate offers a sensitive assay. Generation of luciferin through the action of the cytochrome P450 provides substrate for a luciferase

OTHER RESOURCES

TM548

LDH-Glo™ Cytotoxicity Assay
Technical Manual

PC11

Lazar, D. et al. HiBiT-Halo Tag-LC3 Tandem Reporter Enables Multiple Autophagy Assay Modalities. Promega Corporation.

PC12

Lazar, D. et al. Assessing Autophagic Flux in 2D and 3D Cell Culture Models with a Novel Plate-Based Assay. Promega Corporation.

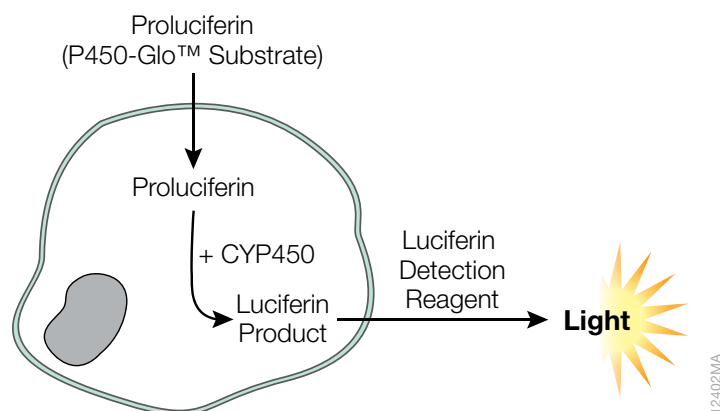


Figure 21. Overview of a cellular P450-Glo™ Assay.

reaction. The proluciferin (P450-Glo™ Substrate) is cell permeable and the generated product will diffuse out of the cell into the culture media. The culture media may be assayed for the presence of the luciferin (Figure 21).

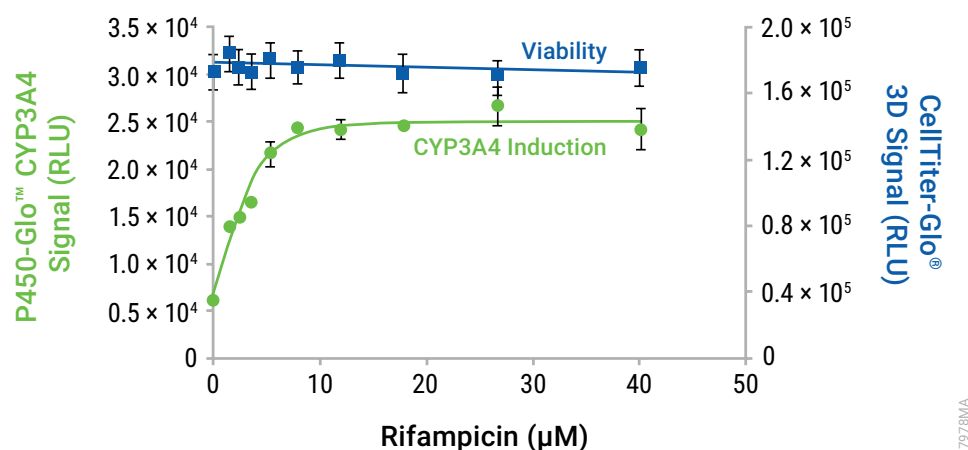


Figure 22. Monitoring human liver microtissue spheroids, cytochrome P450 3A4 activity and viability in response to rifampicin. Liver microtissue spheroids ($\sim 250\mu\text{m}$) were obtained from InSphero. CYP3A4 activity was measured using the non-lytic P450-Glo™ 3A4 Assay with Luciferin-IPA followed by same-well measurement of viability with the CellTiter-Glo® 3D Assay. Measured with a GloMax® Discover Instrument.

Researchers studying hepatocyte-derived 3D cultures often choose to use the P450-Glo™ Assay in the non-lytic, media sampling mode. A portion of the culture media is removed and processed for the P450-Glo™ Assay. The remaining cells are often assayed with the CellTiter-Glo® 3D Assay to check for toxicity (Figure 22) or to normalize CYP450 activity to ATP levels.

Ahn *et al.* (23) examined different methods of generating hepatocyte spheroids on agarose-coated wells or tubes. The response of the spheroids to rifampicin was monitored with the P450-Glo™ CYP3A4 Assay with Luciferin-IPA and activity normalized to ATP with the CellTiter-Glo® 3D Assay. Ryu *et al.* (24) used Matrigel® matrix to culture

References

23. Ahn, J. *et al.* (2019) Developing scalable cultivation systems of hepatic spheroids for drug metabolism via genomic and functional analyses. *Biotechnol. Bioengin.* **116**, 1496–1508. PMID: 30737956
24. Ryu, J.-S. *et al.* (2019) Targeting CYP4A attenuates hepatic steatosis in a novel multicellular organotypic liver model. *J. Biol. Eng.* **13**, 69. PMID: 31406506
25. Eilenberger, C. *et al.* (2019) Effect of spheroidal age of sorafenib diffusivity and toxicity in a 3D HepG2 spheroid model. *Sci. Rep.* **9**, 4863. PMID: 30890741

HepaRG, HUVEC and cord blood mesenchymal stem cells in 3D. CYP3A4 activity was compared from monolayer and 3D cultured cells using the P450-Glo™ CYP3A4 Assay with the Luciferin-IPA substrate. Data was normalized to ATP levels determined with the CellTiter-Glo® 3D Assay. Eilenberger *et al.* (25) generated HepG2 spheroids using plates coated with a bacterial protein (SbpA, isolated from *Lysinibacillus sphearicus*) due to its cell-repulsive properties. CYP3A4 levels were examined from culture day 1 to culture day 18 using the P450-Glo™ CYP3A4 Assay with Luciferin-IPA. Data was normalized to ATP levels with the CellTiter-Glo® 3D Assay. Khanal *et al.* (26) examined CYP1A1 activity from alginate-encapsulated HepG2 cells with the P450-Glo™ CYP1A1 Assay.

References

26. Khanal, S. *et al.* (2019) Nano-fibre integrated microcapsules: A nano-in-micro platform for 3D cell culture. *Sci. Rep.* 9, 13951. PMID: 31562351

Product	Cat. #	Assay Type	Assay Method	Cell Engineering?	DNA/RNA Isolation
CellTiter-Glo® 3D Cell Viability Assay	G9682	EP	Lytic	No	Parallel
RealTime-Glo® MT Cell Viability Assay	G9711	LCK	Non-Lytic	No	Same
CellTox™ Green Cytotoxicity Assay	G8741	LCK	Non-Lytic	No	Same
LDH-Glo™ Cytotoxicity Assay	J3280	MSK	Non-Lytic	No	Same
RealTime-Glo® Annexin V Apoptosis and Necrosis Assay	JA1011	LCK	Non-Lytic	No	Same
Caspase-Glo® 3/7 3D Assay	G8981	EP	Lytic	No	Parallel
Autophagy LC3 HiBiT Reporter Assay Systems	GA2550	EP	Lytic	Yes	Parallel
P450-Glo™ Assays	Various	MS/EP	Non-Lytic/Lytic	No	Same/Parallel

Table 2. Summary of cell health assays in this chapter. The P450-Glo™ Assays can be performed in either a media-sampling or endpoint assay. Cell Engineering refers to whether plasmid transfection is needed. DNA/RNA Isolation refers to whether nucleic acids can be extracted from the same well or require a parallel plate incubated under the same conditions. EP = Endpoint; LCK = Live-Cell Kinetic; MS = Media Sampling; MSK = Media-Sampling Kinetic

Advanced 3D Cell Culture Models

Organoid models have emerged as powerful tools in cell biology research, enabling scientists to study cell behavior and tissue development in a more physiologically relevant context. Organoids are three-dimensional structures derived from stem cells or tissue-specific progenitor cells that self-organize and mimic the structural and functional complexity of real organs. They exhibit cell types, cell-cell interactions and tissue organization – similar to those found in vivo. By recapitulating the in vivo architecture, organoids provide a unique opportunity to study the development, function and pathology of specific organs or tissues in a controlled laboratory setting.

Organoids can be generated through different methods, including directed differentiation, reaggregation or tissue explant culture. Typically, pluripotent stem cells or tissue-specific progenitor cells are cultured under specific conditions that mimic the microenvironment of the target organ. As the cells proliferate and differentiate, they self-organize into complex structures, resembling the architecture of an organ of interest. These structures can be maintained for extended periods, allowing researchers to study them at various stages of development or under different experimental conditions.

Organoids differ from spheroids in a variety of ways: 1) Organoids typically include added extracellular matrix, 2) have heterogenous morphology and size and 3) take three to four weeks to culture. These differences, especially heterogeneity, should be considered when analyzing experiments using organoids.

HOW ARE THEY DIFFERENT?		
SPHEROID		vs. ORGANOID
Can be any cell type (e.g., primary cells, iPSCs or cell lines).	What cell types do they come from?	Stem cells or progenitor cells.
Can be a single cell type or co-culture of multiple cell types.	Are they co-cultures?	Differentiation of the original stem cells generates a co-culture of multiple organ-specific cell types.
No, some cells generate their own endogenous ECM during spheroid.	Do you need to provide extracellular matrix (ECM)?	Yes, hydrogels containing ECM components are typically used to form organoids.
Yes, the shape is usually spherical and uniform, depending on the culture method.	Is the morphology consistent?	No, usually not; long-term culture periods can result in heterogeneous sizes.
Yes, spheroids can be formed and screened in same ultra-low binding plate.	Good for high-throughput screening (HTS)?	No, multi-step protocols over long-term culture periods that include size selection make it expensive to generate adequate numbers of organoids for HTS.
Typically 50–500µm	What is their size?	Can be up to 2–3mm
2–3 days	How many days do they need to form?	21–28 days

Biological Applications

Disease Modeling: Organoids serve as a valuable platform to investigate disease mechanisms such as cancer, genetic disorders and neurodegenerative diseases, enabling researchers to study disease progression, assess drug efficacy and tailor treatment approaches.

- **Drug Screening and Development:** Organoids offer a more accurate representation of human tissues compared to traditional cell culture models, which allows pharmaceutical companies to screen potential drug candidates, evaluate drug toxicity and optimize treatment strategies.
- **Developmental Biology:** Organoids provide insights into the complex processes of organogenesis and tissue development, allowing researchers to manipulate specific signaling pathways or genetic factors to study the molecular mechanisms underlying tissue formation and maturation.
- **Regenerative Medicine:** Organoids can serve as a source of functional tissues for transplantation or be used to study tissue regeneration and repair mechanisms. In the future, organoids derived from patient cells could even be used to develop personalized therapies.

Assays that have been optimized and validated with other 3D cell culture models can easily be applied to organoid analysis. Because of the precious nature of organoid samples, live-cell real-time assays such as RealTime-Glo™ MT Cell Viability Assay may be preferred over CellTiter-Glo® 3D Cell Viability Assay (a lytic assay). Changes in metabolic pathways can also easily be measured by sampling cell culture medium for metabolite assay measurements, such as Lactate-Glo™.

Chapter 2

METABOLIC CHANGES IN 3D

Nicotinamide Adenine Dinucleotide Assays.....	22
NAD/NADH-Glo™ Assay	23
NADP/NADPH-Glo™ Assay	24
Energy Metabolite Assays	25
Lipid Metabolism Assays	27
Oxidative Stress Assays	28
ROS-Glo™ H ₂ O ₂ Assay	29
GSH/GSSG-Glo™ Assay.....	30

Cultured cells must maintain a balance of energy levels, new material biosynthesis and control of reactive oxygen species (ROS, a byproduct of energy generation). Cells cultured in 3D experience gradients in oxygen, nutrients and waste products far different than monolayer cultures where oxygen and nutrients are plentiful and available to all cells. The nature and importance of metabolic restriction in cancer has often been masked owing to the use of monolayer cultures, where both oxygen and nutrients are always in excess (1). Spheroid cultures, in contrast, typically have cells experiencing proliferation, quiescence or even necrosis depending upon the availability of oxygen and nutrients.

This chapter introduces tools to investigate metabolism in 3D culture.

The NAD/NADH-Glo™ and NADP/NADPH-Glo™ Assays monitor these abundant cofactors, which undergo reversible oxidation and reduction in major metabolic pathways. The Glucose-Glo™ and Lactate-Glo™ Assays allow monitoring of glycolytic pathways while the Glutamate-Glo™ and Glutamine/Glutamate-Glo™ Assays allow investigation of glutaminolysis. Assays to monitor lipogenesis and lipolysis are also important for metabolic research. ROS are a natural consequence of energy generation. ROS levels can be monitored with the ROS-Glo™ H₂O₂ Assay. Glutathione plays a major role in combating ROS. The levels of free glutathione (GSH) and oxidized glutathione (GSSG) can be monitored with the GSH/GSSG-Glo™ Assay.

References

1. Cairns, R.A., Harris, I.S. and Mak, T. W. (2011) Regulation of cancer cell metabolism. *Nat. Rev. Cancer* 11, 85–95. PMID: 21258394

Nicotinamide Adenine Dinucleotide Assays

Nicotinamide adenine dinucleotides (NAD) are abundant soluble cofactors that undergo reversible oxidation and reduction in major metabolic pathways. The cofactors have become a focus in cancer research because, as metabolites, they can tie metabolic pathways to transcriptional control, epigenetics and cell signaling as cells switch from a normal metabolism to a cancer cell (proliferative) metabolism. In cells, they are present in unphosphorylated (NAD and NADH) and phosphorylated (NADP and NADPH) forms. These dinucleotides work in pairs, and each pair has distinct functions.

Classic methods to detect NAD, like absorbance changes and redox-coupled colorimetric or fluorescent assays, lack sensitivity and reproducibility. They also require extensive sample manipulation and large numbers of cells for cell-based applications. A redox-coupled bioluminescent assay (Figure 1) allows sensitive detection with much smaller numbers of cells and is more compatible with high-throughput applications (PC1).

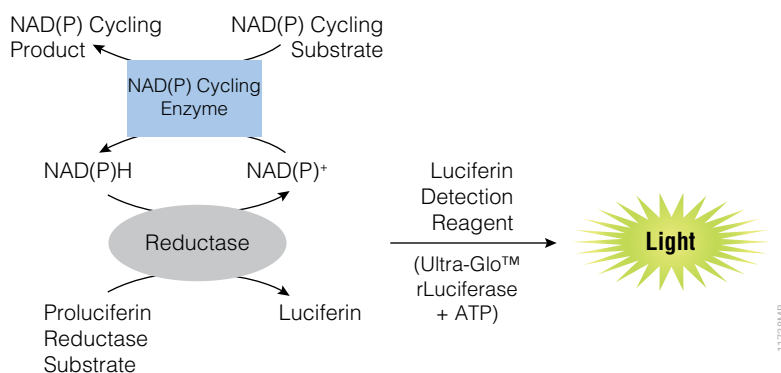


Figure 1. Overview of the bioluminescent reactions behind NAD/NADH-Glo™ and NADP/NADPH-Glo™ Assays.

NAD/NADH-Glo™ Assay

NAD is most often associated with catabolic pathways (glycolysis and oxidative phosphorylation). However, its role in the cell involves more than energy metabolism. NAD is an important substrate in several signaling pathways and is involved in the epigenetic control of gene expression. NAD is the substrate used for ADP ribosylation and has roles in DNA repair, and signaling regulation. The ratio of NAD to NADH influences the activity of many enzymes, especially the glycolytic enzymes (PC2).

The NAD/NADH-Glo™ Assay was designed for use with monolayer cell cultures. To assay spheroid cultures, the protocol was modified to double the amount of detergent in the lysis step and prolong the incubation in the lysis buffer (Figure 2). After lysis, the

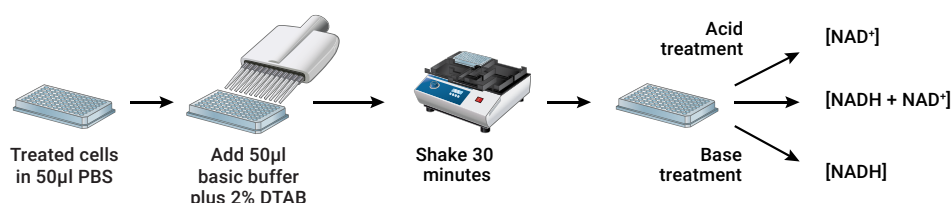


Figure 2. Overview of NAD⁺ and NADH measurement with the NAD/NADH-Glo™ Assay. Changes to the standard protocol for monolayer cultures are to the cell lysis step (see TM399) indicated in orange. Processing after lysate production are exactly the same to measure either [NAD⁺], [NADH] or total [NADH + NAD⁺] (PC3).

sample is split in two and one half treated with acid to eliminate the NADH and measure NAD⁺ only. The other half is treated with base to eliminate NAD⁺ and measure NADH only. The relative light unit values may be compared to derive the NAD to NADH ratio, or standard curves may be used to quantitate the concentration of NAD⁺ and NADH on the same plates. Valley et al. (PC3) plated different quantities of HCT116 cells to generate spheroids of various sizes. One set of spheroids was processed as in to determine NAD⁺ and NADH (Figure 3). Another set was assayed with the CellTiter-Glo® 3D Cell Viability Assay. As noted in Figure 3, both the NAD⁺ and NADH levels correlated with increasing spheroid diameter (i.e., CellTiter-Glo® 3D Cell Viability Assay response). The NAD⁺ levels were slightly higher than NADH levels. In a study of oxidative phosphorylation, Bell et al. (2) used the NAD/NADH-Glo™ Assay to monitor changes in NAD⁺ levels in mouse myoblasts grown in a Matrigel® Matrix and treated with various compounds.

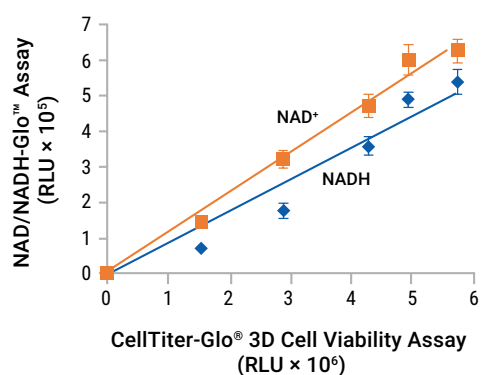


Figure 3. NAD⁺ and NADH signals from NAD/NADH-Glo™ Assay correlate with increasing 3D spheroid diameter.

Various numbers of HCT116 cells were grown as hanging drop cultures for 4 days then one set of cells were processed for NAD⁺ and NADH levels. A duplicate set of cells were processed with CellTiter-Glo® 3D Assay. Details can be found in PC3.

OTHER RESOURCES

TM399

NAD/NADH-Glo™ Assay
Technical Manual.

PC3

Valley, M. P. et al. Cell-Titer-Glo® 3D: Luminescent Cell Health Assays for Tumor Spheroid Evaluation. Promega Corporation.

References

2. Bell, E.L. et al. (2019) PPAR δ modulation rescues mitochondrial fatty acid oxidation defects in the mdx model of muscular dystrophy. *Mitochondrion* **46**, 51–58. PMID: 29458111

NADP/NADPH-Glo™ Assay

NADP/NADPH is the least abundant of the nicotinamide adenine dinucleotide pairs. NADPH is associated with biosynthesis of macromolecules, providing the reducing power necessary for those synthetic reactions. Increased biosynthesis is characteristic of rapidly proliferating cells, such as cancer cells. Because of this, NADPH is considered a key molecule produced as a result of cancer metabolism. It also has a role in responding to the buildup of ROS (PC2).

Like the NAD/NADH-Glo™ Assay, the NADP/NADPH-Glo™ Assay was developed on monolayer cultures and the same modifications can be used to assay cells in 3D cultures (Figure 2). In the same study as described above, Valley et al. (PC3), examined the levels of NADP and NADPH in relation to microspheroid diameter (Figure 4). The levels of NADPH were higher in general than the NADP levels. Wang et al. (3) examined the differences in ratios of NADP to NADPH in of HCT15 and HCT116 cells grown under monolayer and spheroid conditions. Chan et al. (4) examined the changes in NADP/NADPH ratios of human-derived organoids and mouse-derived organoids following various treatments.

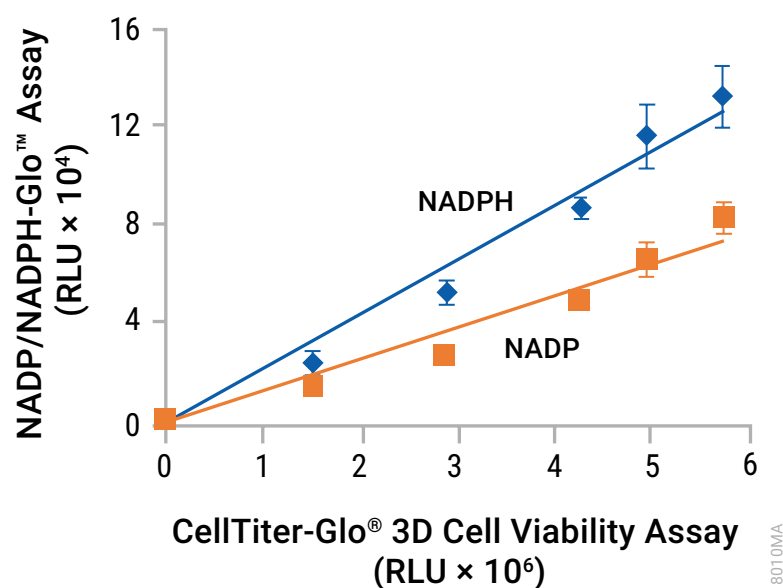


Figure 4. NADP⁺ and NADPH signals from NAD/NADH-Glo™ Assay correlate with increasing 3D spheroid diameter. Various quantities of HCT116 cells were grown as hanging drop cultures for 4 days, then one set of cells were processed for NADP and NADPH levels. A duplicate set of cells were processed with CellTiter-Glo® 3D Cell Viability Assay. Details can be found in PC3.

References

- Wang, Y.-N. et al. (2018) CPT1A-mediated fatty acid oxidation promotes colorectal cancer cell metastasis by inhibiting anoikis. *Oncogene* **37**, 6025–6040. PMID: 29995871
- Chan, K. et al. (2019) eIF4A supports an oncogenic translation program in pancreatic ductal adenocarcinoma. *Nat. Commun.* **10**, 5151. PMID: 31723131

Energy Metabolite Assays

Energy uptake and utilization in cells is a dynamic process regulated by interacting metabolic networks. Interrogation of this complex network would benefit from rapid, simple and sensitive techniques to measure key metabolites. Promega has developed bioluminescent assays for robust detection of glucose, lactate, glutamate and glutamine in a plate-based format. The assays are versatile and amenable to higher-throughput formats and are compatible with many sample types.

Regarding 3D cultures, monitoring metabolites in cell culture medium can provide information about changes that occur in cellular metabolic pathways. Glucose consumption and lactate secretion can serve as indicators of glycolysis, while glutamine uptake and glutamate secretion can provide information about glutaminolysis. Changes can be monitored over time or after treatments, such as exposure to hypoxic conditions, by assaying small amounts of diluted medium.

The reactions involved for the energy metabolite assays (PC4) follow the core reactions used in the NAD/NADH-Glo™ and NADP/NADPH-Glo™ Assays. The specificity of the reaction is defined by the dehydrogenase used to feed the reductase reaction (Figure 5). Assays can be performed on culture media, cell lysates, cells plus media and tissue lysates. The culture media method is particularly useful for 3D cultures as it is a non-lytic assay, allowing further experiments with the cells in culture. The method also requires very little media (2-5µl) so multiple samples can be obtained and analyzed from the same well over time, providing a kinetic view of metabolite uptake or secretion. The four assays for glucose, lactate, glutamate and glutamine use common sample preparation procedures so one medium sample

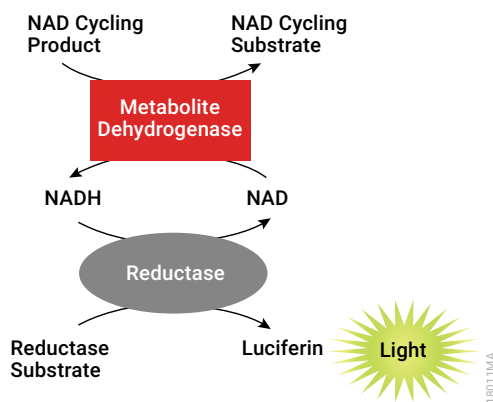


Figure 5. Overview of the core reaction used by the energy metabolite assays.

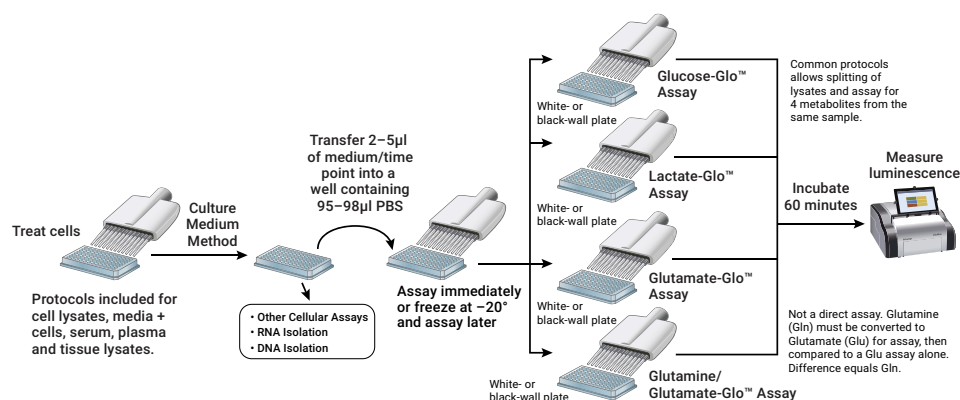


Figure 6. Overview of the "real-time" workflow for measuring glucose, lactate, glutamate and glutamine from a sample of culture medium.

can be split to measure all four metabolites (Figure 6). Unlike colorimetric or fluorescent methods, deproteination of the medium sample is not needed due to the small sample size and subsequent dilution. An example of culture media and cell lysate assay of glucose is shown in Figure 7. Spheroids generated from iCell® Hepatocytes were cultured in a glucose-free media to promote gluconeogenesis and, thus, secretion of glucose. The cells were treated with insulin and the dose-dependent decrease in glucose secretion was monitored. The data demonstrates that the culture media method is suitable for such determinations.

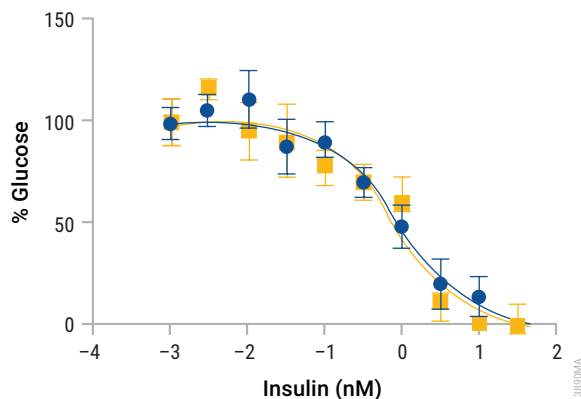


Figure 7. Insulin-mediated inhibition of gluconeogenesis in iPSC-derived human liver spheroids. iCell® Hepatocytes 2.0 (Cellular Dynamics, Inc.), grown as spheroids, were cultured for 1.5 hours in a glucose-free gluconeogenesis medium to promote hepatic glucose production. The cells were washed, and medium replaced with 50µl of gluconeogenesis medium containing various concentrations of insulin and incubated for 6 hours. Glucose secretion was monitored with the Glucose-Glo™ Assay. The culture medium appears here in blue, and the cell lysates in orange. Details can be found in TM494.

OTHER RESOURCES

TM494

Glucose-Glo™ Assay Technical Manual.

References

5. Deshmukh, A., Arfuso, F., Newsholme, P., and Dharmarajan, A. (2018) Regulation of cancer stem cell metabolism by secreted Frizzled-Related Protein 4 (sFRP4). *Cancers* 10, 40. PMID: 29385093

Glucose-Glo™ Assay

This assay uses glucose dehydrogenase to confer specificity to glucose (Figure 5). Glucose in the media can be monitored over the course of hours or days in culture.

Lactate-Glo™ Assay

This assay uses lactate dehydrogenase to confer specificity to lactate (Figure 5). Lactate in the media can be monitored over the course of hours to days in culture.

Glutamate-Glo™ Assay

This assay uses glutamate dehydrogenase to confer specificity to glutamate (Figure 5). Glutamate in the media can be monitored over the course of hours to days in culture.

Glutamine/Glutamate-Glo™ Assay

Unfortunately, the enzyme glutamine dehydrogenase does not exist, but glutamine is easily converted to glutamate by the enzyme glutaminase. To measure glutamine, the sample is split in two. One sample is directly assayed for glutamate (i.e., the Glutamate-Glo™ Assay method) and the other sample is treated with glutaminase, then assayed for glutamate (i.e., the Glutamate-Glo™ Assay method). The difference between the untreated and glutaminase-treated samples yields the amount of glutamine in the sample.

Deshmukh et al. (5) examined changes in glutamine and glutamate in 2µl samples of culture media from breast and prostate cancer stem cell spheroid cultures exposed to a constant level of glutamine and variable glucose concentrations, both with and without growth factor treatment.

Lipid Metabolism Assays

Lipids play several vital roles in an organism such as sending signaling functions, forming biological membranes and creating energy storage vesicles. Alteration of lipid metabolism results in a variety of disorders. Steatosis refers to the aberrant accumulation of lipids in tissues. Steatosis and the measurement of abnormal lipid levels in tissues is relevant to metabolic disorder research, including diabetes, obesity and liver disorders. Non-alcoholic fatty liver disease (NAFLD) and non-alcoholic steatohepatitis (NASH), two liver disorders drastically increasing in global prevalence, are key targets of many drug discovery programs. Lipid metabolism assays are useful tools in the study of these disorders, and can be used to measure and understand changes in lipid levels in cell culture samples, cultured 3D cell structures, tissues and plasma or serum samples. Promega offers assays to detect levels of glycerol, triglyceride, cholesterol and cholesterol ester in 3D cell culture samples.

The **Triglyceride-Glo™ Assay (PC5)** is designed to examine the result of lipogenesis in cultured cells, serum or tissue, but uses detergent release rather than organic extraction to assay triglycerides. The sample is treated with a lipase to remove fatty acids from the core glycerol molecule and the released glycerol is quantitated in a redox-coupled reaction with a bioluminescent readout (Figure 8).

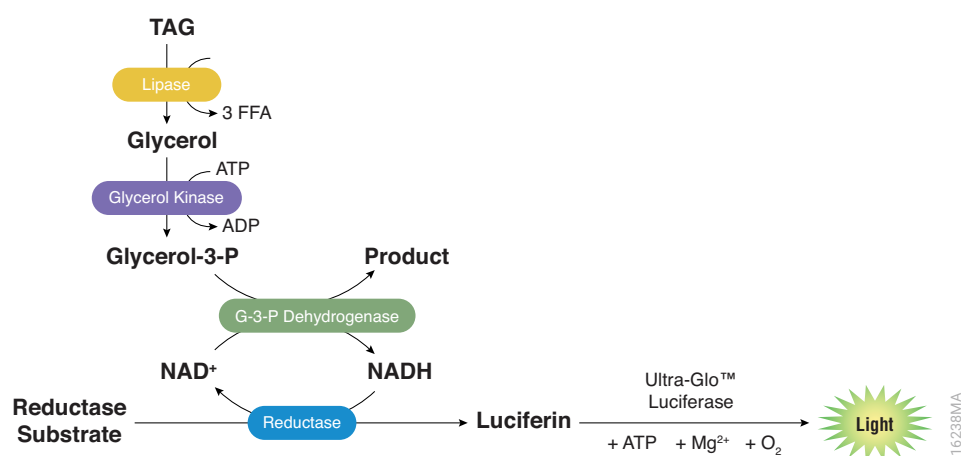


Figure 8. Schematic diagram of the Triglyceride-Glo™ Assay. Lipase converts triglyceride (TAG) to glycerol. Glycerol kinase and glycerol-3-phosphate dehydrogenase are used to generate NADH. In the presence of NADH, reductase enzymatically reduces a pro-luciferin Reductase Substrate to luciferin. Luciferin is detected in a luciferase reaction using Ultra-Glo™ rLuciferase and ATP, and the amount of light produced is proportional to the amount of glycerol in the sample.

Quantifying triglyceride levels in liver cells is used in research on liver disorders like non-alcoholic fatty liver disease (NAFLD) and non-alcoholic steatohepatitis (NASH). Figure 9 demonstrates triglyceride levels of human liver microtissue spheroids cultured under different conditions. Cells cultured with physiologically low or high low-density lipoproteins (LDL) accumulate more triglycerides than other conditions. The protocol for Triglyceride-Glo™ Assay includes instructions for working with 3D cultured cells (TM600).

The [Glycerol-Glo™](#) (TM599) and the [Cholesterol/Cholesterol Ester-Glo™](#) Assays (TM601) also include instruction for working with 3D cultured cells.

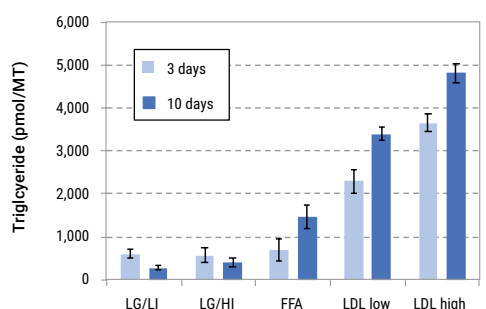


Figure 9. Triglyceride levels in human liver microtissues cultured under different conditions. Human liver microtissues (3D InSight™, InSphero) were incubated for indicated days in serum-free media containing either physiological (LG/LI) or supraphysiological (LG/HI) levels of glucose and insulin, and supplemented with either free fatty acids bound to BSA (FFA) or low-density lipoprotein plasma fraction (LDL). The triglyceride levels were measured with the Triglyceride-Glo™ Assay. Details can be found in TM600. Data courtesy InSphero, A.G., Zurich, Switzerland.

OTHER RESOURCES

TM599

Glycerol-Glo™ Assay Technical Manual.

TM600

Triglyceride-Glo™ Assay Technical Manual.

TM601

Cholesterol/Cholesterol Ester-Glo™ Assay Technical Manual.

References

- Alfadda, A.A. and Sallam, R.M. (2012) Reactive oxygen species in health and disease. *J. Biomed. Biotechnol.* **2012**, 936486. PMID: 22927725
- Wittman, C. et al. (2012) Hydrogen peroxide in inflammation: messenger, guide, and assassin. *Adv. Hematol.* **2012**, 541471. PMID: 22737171
- Newsholme, P. et al. (2012) Reactive oxygen and nitrogen species generation, antioxidant defenses and β -cell function: A critical role for amino acids. *J. Endocrin.* **214**, 11–20. PMID: 22547566
- Sies, H. (1999) Glutathione and its role in cellular functions. *Free Radic. Biol. Med.* **27**, 916–921. PMID: 10569624
- Griffith, O.W. (1999) Biologic and pharmacologic regulation of mammalian glutathione synthesis. *Free Radic. Biol. Med.* **27**, 922–935. PMID: 10569625
- Pompella, A. et al. (2003) The changing faces of glutathione, a cellular protagonist. *Biochem. Pharmacol.* **66**, 1499–1503. PMID: 14555227
- Ballatori, N. et al. (2009) Glutathione dysregulation and the etiology and progression of human diseases. *Biol. Chem.* **390**, 191–214. PMID: 19166318
- Rebrin, I. and Sohal, R.S. (2008) Pro-oxidant shift in glutathione redox state during aging. *Adv. Drug Deliv. Rev.* **60**, 1545–1552. PMID: 18652861
- Ghezzi, P. (2005) Regulation of protein function by glutathionylation. *Free Radic. Res.* **39**, 573–580. PMID: 16036334

Oxidative Stress Assays

Reactive oxygen species (ROS) are chemically reactive molecules that contain oxygen (e.g., superoxide, singlet oxygen, H_2O_2). ROS are beneficial to the cell, with roles in cell signaling, and are a natural byproduct of normal metabolism (6). However, ROS can also lead to cellular damage, or oxidative stress, as a result of environmental factors (e.g., radiation) or aberrant metabolism (6,7). Most ROS have short half lives in solution, and both enzymatic and non-enzymatic reactions result in conversion of ROS species to hydrogen peroxide (H_2O_2) in cells (8). For example, superoxide dismutase rapidly converts superoxide to H_2O_2 . Unlike other ROS, H_2O_2 has a relatively long half-life in solution and can diffuse out of the cell, which makes it a good marker of oxidative stress.

Cells counter ROS with glutathione. Glutathione, a three-amino-acid peptide (γ -glutamyl-cysteinylglycine), is an abundant antioxidant found in eukaryotic cells (9–11). Most physiological glutathione exists in reduced form (GSH) in which the sulfhydryl group of the cysteine is not linked in a disulfide linkage to a second glutathione. A small percentage of the glutathione is oxidized and present as a dimer of two of the peptide elements connected by a disulfide bond. Oxidized glutathione (GSSG) is an indicator of cell health and oxidative stress. Certain chemicals react with GSH to form adducts or to increase the GSSG levels, decreasing the ratio of reduced to oxidized glutathione (GSH/GSSG). Measurements of both GSH and GSSG are useful in experimental systems because changes in the ratio of GSH to GSSG are associated with human disease, aging and cell signaling events (12–14).

ROS-Glo™ H₂O₂ Assay

Since various ROS are converted to H₂O₂ in the cell, and H₂O₂ is the longest-lived ROS, an increase in H₂O₂ can reflect a general increase in the ROS level. The ROS-Glo™ H₂O₂ Assay (PC6) uses a derivatized luciferin to directly react with H₂O₂ to generate a proluciferin molecule (Figure 10). The H₂O₂ Substrate is added directly to cells in culture. A portion of the culture media may be removed for further assay or the cells and media may be lysed for measurement. Addition of the ROS-Glo™ Detection Reagent to either the culture media sample or cellular lysate converts the proluciferin to luciferin, which reacts with the ATP and Ultra-Glo™ rLuciferase in the reagent to generate light proportional to the amount of H₂O₂ in the sample (Figure 10). When using the non-lytic culture media protocol, the remaining cells may be used for further assay.

Menadione disrupts the mitochondrial electron transport chain, producing an increase in ROS. Treatment of variously sized spheroid cultures with menadione produces a dose-dependent increase in ROS production (Figure 11).

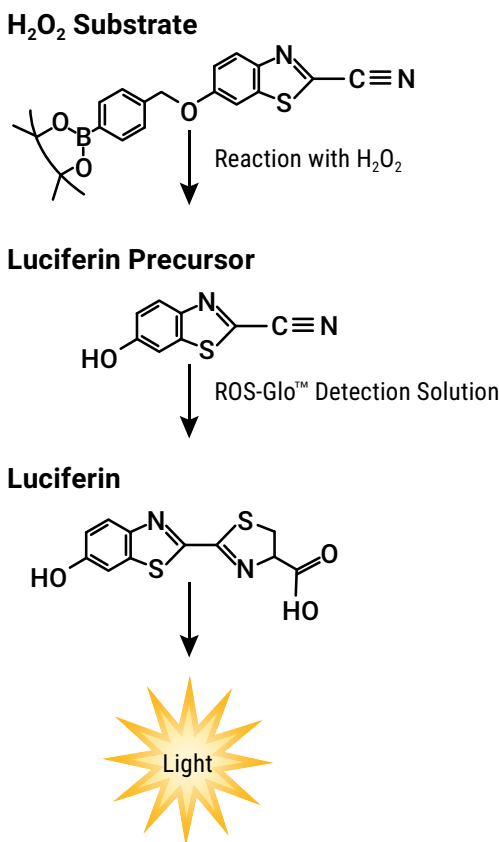


Figure 10. ROS-Glo™ H₂O₂ Assay chemistry. H₂O₂ Substrate is added to samples containing H₂O₂, which converts it to a luciferin precursor. Upon addition of a second reagent containing Ultra-Glo™ rLuciferase, ATP and D-cysteine, the precursor is converted to luciferin and, in the presence of Ultra-Glo™ rLuciferase, produces light.

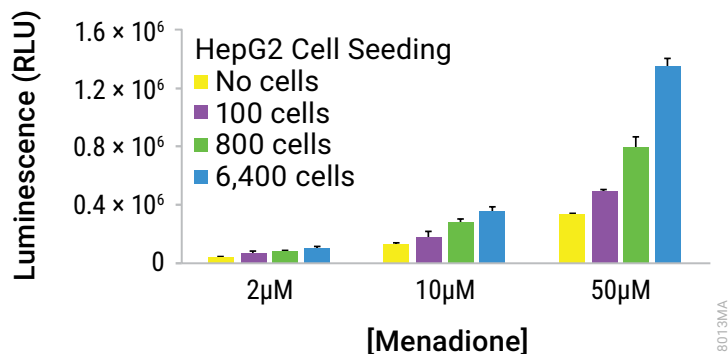


Figure 11. ROS-Glo™ H₂O₂ Assay signals from HepG2 spheroid cultures treated with ROS-inducing menadione. HepG2 cells were seeded in ULA plates at 100, 800 and 6,400 cells/well and grown for 4 days. Microtissues were transferred to a white-walled assay plate in 25μl of media and treated with menadione plus the H₂O₂ Substrate. The cells were exposed to menadione for 2 hours before addition of the ROS-Glo™ Detection Reagent (n=3).

OTHER RESOURCES

PC6

Duellman, S. et al. A New Luminescent Assay for Detection of Reactive Oxygen Species. Promega Corporation.

Controls are extremely important when measuring H_2O_2 . Cells have a tremendous capacity to neutralize ROS (e.g., glutathione) and serum-supplemented culture media can neutralize ROS as well. Some compounds spontaneously produce H_2O_2 when added to an aqueous solution and can falsely indicate that the compound induces ROS production originating from the cells.

Chang *et al.* (15) examined the effect of a bioactivatable compound on cancer spheroids co-cultured with cancer-associated fibroblasts. Changes in viability were monitored with the CellTiter-Glo® 3D Cell Viability Assay and changes in ROS levels were monitored with the ROS-Glo™ H_2O_2 Assay. In a study of embryonic development, Guo *et al.* (16) studied the effects of nicotine on the viability and ROS levels of embryoid body spheroids. Viability was monitored with the CellTiter-Glo® 2.0 Cell Viability Assay and ROS levels were monitored with the ROS-Glo™ H_2O_2 Assay. Tomlinson *et al.* (17) generated mixed spheroids with a 4:2:1 ratio of human iPSC cardiomyocytes, cardiac fibroblasts and cardiac endothelial cells. The effect of doxorubicin on the spheroids was examined through ROS generation and changes in viability using the ROS-Glo™ H_2O_2 and CellTiter-Glo® Cell Viability Assays.

GSH/GSSG-Glo™ Assay

Changes in the GSH/GSSG ratio can indicate if a cell is experiencing oxidative stress. The **GSH/GSSG-Glo™ Assay** is designed to measure the amount of GSH and GSSG through a bioluminescent assay with the aid of glutathione-S-transferase (GST) and a modified luciferin. The assay requires duplicate cells, one set for measuring total glutathione (GSH + GSSG) and one set for GSSG alone. The difference between these values yields the amount of GSH (Figure 12). The reaction for total glutathione reduces GSSG to two molecules of GSH prior to measurement in the GST reaction. The reaction with GSSG alone relies on addition of a free sulfhydryl-reactive compound, N-ethylmaleimide, to the lysis buffer to eliminate free GSH. The remaining GSSG is reduced to GSH for measurement in the GST reaction. The amount of light produced is directly related to how much luciferin was generated in the GST reaction (PC7). The 3D protocol requires a longer shaking step compared to the monolayer method (Figure 13).

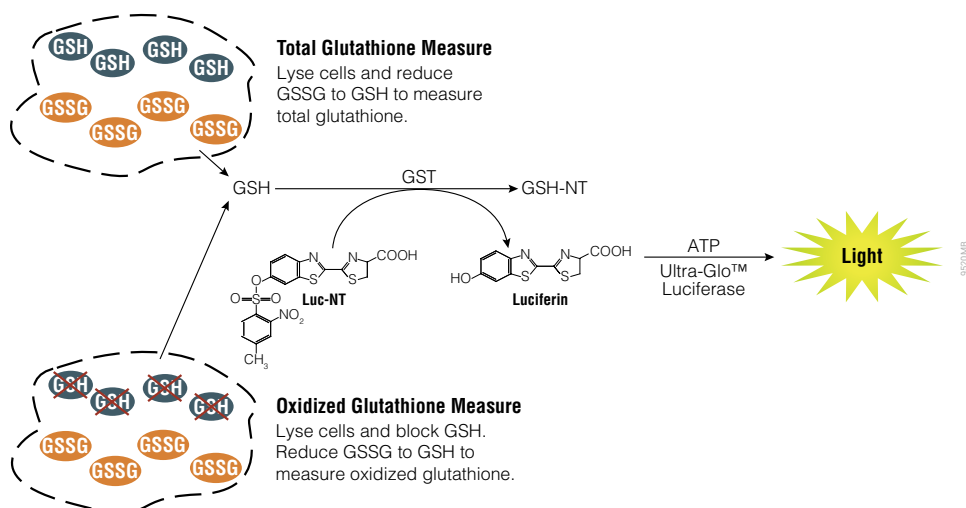


Figure 12. Overview of the GSH/GSSG-Glo™ Assay. GSH-dependent conversion of GSH probe Luciferin-NT to luciferin by glutathione S-transferase is coupled to a firefly luciferase reaction.

OTHER RESOURCES

PC7

Chaffant, M & Bernd, K. Detecting Ozone-Induced Changes in Cellular Redox Balance via GSH/GSSG-Glo™ Assay. Promega Corporation.

References

- Chang, A.-Y. *et al.* (2019) Evaluation of tumor cell-tumor microenvironment component interactions as potential predictors of patient response to napabucasin. *Mol. Cancer Res.* **17**, 1429–1434. PMID: 31043490
- Guo, H. *et al.* (2019) Single-cell RNA sequencing of human embryonic stem cell differentiation delineates adverse effects of nicotine on embryonic development. *Stem Cell Rep.* **12**, 772–786. PMID: 30827876
- Tomlinson, L. *et al.* (2019) Attenuation of doxorubicin-induced cardiotoxicity in a human in vitro cardiac model by the induction of the NRF-2 pathway. *Biomed. Pharmacother.* **112**, 108637. PMID: 30798127

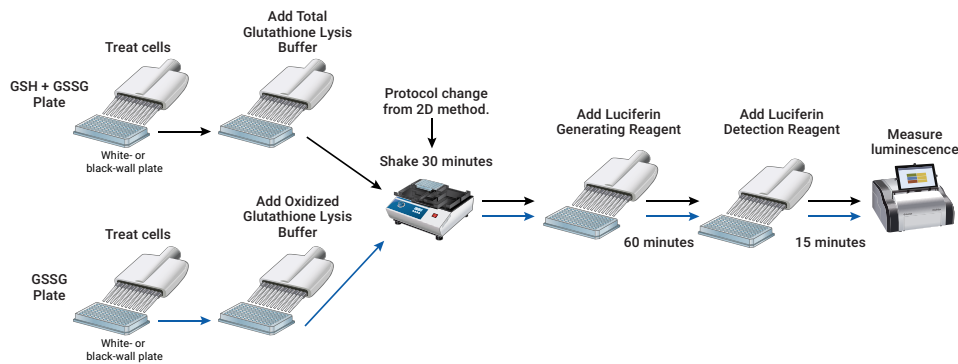


Figure 13. Protocol steps for the GSH/GSSG-Glo™ Assay. To modify the standard 2D monolayer culture to 3D culture, simply increase the lysis stage to 30 minutes on a plate shaker.

HCT116 spheroids were treated with buthionine sulfoximine, a GSH synthetase inhibitor, and levels of glutathione were measured with the total glutathione method illustrated in Figure 13. The 48-hour treatment significantly decreased the amount of GSH in the cells without much effect on viability (Figure 14). Tangtrongsup and Kisiday (18) used the GSH/GSSG-Glo™ Assay to monitor the levels of total glutathione and the GSH/GSSG ratio when agarose hydrogel-grown equine mesenchymal stem cells were exposed to chondrogenic media. The GSH/GSSG ratio improved with the addition of FBS to the media, indicating less oxidative stress. Park et al. (19) analyzed cells treated with siRNA to knockdown SIRT1 and compared GSH/GSSG ratios of MD cells grown as adherent (monolayer) or adapted to suspension culture in ULA plates using the GSH/GSSG-Glo™ Assay. The suspension cells demonstrated higher GSH/GSSG ratios, indicating low oxidative stress. Ohata et al. (20) found that inhibition of the ROCK kinase did not affect levels the GSH/GSSG ratio of colon cancer organoids as measured with the GSH/GSSG-Glo™ Assay, nor did inhibition affect mRNA levels of the enzymes responsible for making GSH.

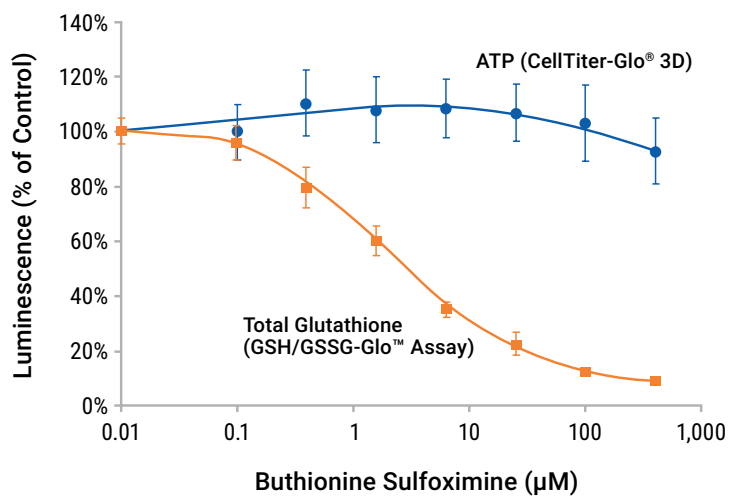


Figure 14. Monitoring total glutathione levels and cell viability in HCT116 spheroids treated with GSH synthetase inhibitor buthionine sulfoximine. Duplicate sets of spheroids (~350μm) were treated with various amounts of buthionine sulfoximine. One set was assessed for viability with the CellTiter-Glo® 3D Cell Viability Assay and the other set assessed for total glutathione levels with the GSH/GSSG-Glo® Assay. Details can be found in the poster (PC3).

References

18. Tangtrongsup, S. and Kisiday, J.D. (2018) Modulating the oxidative environment during mesenchymal stem cells chondrogenesis with serum increases collagen accumulation in agarose culture. *J. Ortho. Res.* **36**, 506–514. PMID: 28548680
19. Park, J.Y. et al. (2019) Silent mating-type information regulation 2 homolog 1 overexpression is an important strategy for the survival of adapted suspension tumor cells. *Cancer Sci.* **110**, 2773–2782. PMID: 31348594
20. Ohata, H. et al. (2019) NOX1-dependent mTORC1 activation via S100A9 oxidation in cancer stem-like cells leads to colon cancer progression. *Cell Rep.* **28**, 1282–1295. PMID: 31365870

Product	Cat.#	Assay Type	Assay Method	Cell Engineering	DNA/RNA Isolation
NAD/NADH-Glo™ Assay	G9071	EP	Lytic	No	Parallel
NADP/NADPH-Glo™ Assay	G9081	EP	Lytic	No	Parallel
Lactate-Glo™ Assay	J5021	MSK/EP	Non-Lytic/Lytic	No	Same/Parallel
Glucose-Glo™ Assay	J6021	MSK/EP	Non-Lytic/Lytic	No	Same/Parallel
Glutamate-Glo™ Assay	J7021	MSK/EP	Non-Lytic/Lytic	No	Same/Parallel
Glutamine/Glutamine-Glo™ Assay	J8021	MSK/EP	Non-Lytic/Lytic	No	Same/Parallel
Glycerol-Glo™ Assay	J3150	MSK/EP	Non-Lytic/Lytic	No	Same/Parallel
Triglyceride-Glo™ Assay	J3160	EP	Lytic	No	Parallel
Cholesterol/ Cholesterol-Glo™ Assay	J3190	EP	Lytic	No	Parallel
ROS-Glo™ H ₂ O ₂ Assay	G8820	MS/EP	Non-Lytic/Lytic	No	Same/Parallel
GSH/GSSG-Glo™ Assay	V6611	EP	Lytic	No	Parallel

Table 1. Summary of assays for monitoring metabolic changes in 3D cultured cells. EP = Endpoint; MS = Media Sampling; MSK = Media-Sampling Kinetic. Cell Engineering refers to whether plasmid transfection is needed. DNA/RNA isolation refers to whether nucleic acids can be extracted from the same well or requires a parallel plate incubated under the same conditions.

Chapter 3

GENE EXPRESSION CHANGES IN 3D

RNA Extraction 34

 ReliaPrep™ RNA Miniprep Systems 34

 Maxwell® RSC Instrument and simplyRNA Kits 36

 Merging Gene Expression Analysis with Cell Health and Metabolism Assays 37

Downstream RNA Analysis..... 39

 RNase Protection..... 39

 Conversion to cDNA..... 40

 RT-qPCR Analysis 41

 Transcriptional Reporter Assays 43

Cells grown in 3D culture can have differences in gene expression when compared to monolayer cultures. The significant changes in cell-to-cell contacts, cell-to-matrix contacts and the gradient of oxygen and nutrients within the culture will influence gene expression. To analyze differences in gene expression, RNA must be isolated and quantified. Then, specific genes are analyzed by Reverse Transcription Quantitative Polymerase Chain Reaction (RT-qPCR) or cellular changes are monitored through techniques like RNA-seq.

This chapter will illustrate tools to monitor changes in gene expression. Application of the manual ReliaPrep™ RNA Miniprep Systems and the automated Maxwell® RSC Systems to spheroid and hydrogel cultures will be presented. All other assays discussed use purified RNA and will not vary with different culture types. The QuantiFluor® RNA system provides accurate RNA quantitation, which is key for downstream analyses. RT-qPCR systems like BRYT Green® Dye-based GoTaq® qPCR and the probe-based GoTaq® Probe qPCR enable analysis of individual transcripts. The GoScript™ Reverse Transcription System is used for conversion of RNA to cDNA. This chapter will also briefly address monitoring transcriptional changes with reporter gene assays.

OTHER RESOURCES

PC1

Hook B. & Bratz M. RNA Isolation from 3D Microtissue Cultures: A Comparison of Manual and Automated Methods. Promega Corporation.

RNA Extraction

RNA isolated from cultured cells must have sufficient purity and integrity for use in downstream applications like RT-qPCR, microarray analysis and sequencing. As the use of amplification as a research tool has grown, the need for methods to rapidly isolate high-quality RNA that is substantially free of genomic DNA contamination from small amounts of starting material (i.e., cultured cells) has also increased.

ReliaPrep™ RNA Miniprep Systems

ReliaPrep™ RNA Miniprep Systems are manual, spin-column preps designed for low-throughput applications. Options are available for extracting total RNA from cells ([ReliaPrep™ RNA Cell Miniprep System](#)) or tissues ([ReliaPrep™ RNA Tissue Miniprep System](#)) and isolating miRNA from either cells or tissues ([ReliaPrep™ miRNA Cell and Tissue Miniprep Systems](#)) ([PC1](#), [AN296](#)). The ReliaPrep™ RNA Systems share a common processing method (Figure 1), and only vary in reagent components.

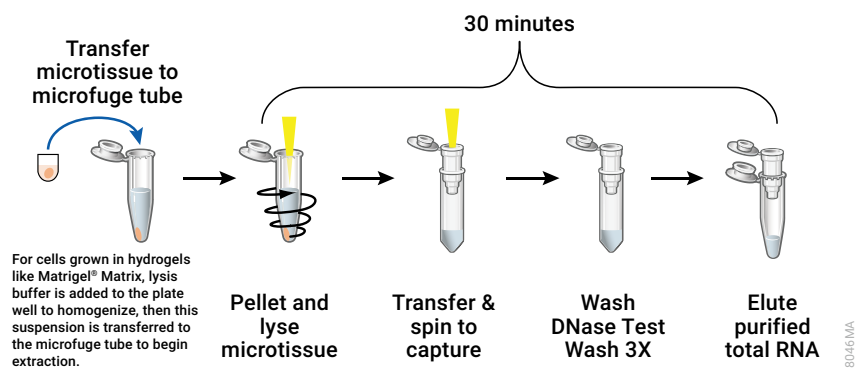


Figure 1. Overview of ReliaPrep™ RNA Miniprep System protocols.

To demonstrate the compatibility of the ReliaPrep™ RNA Tissue Miniprep System with spheroid cultures, RNA was extracted from various numbers of InSphero™ human liver microtissues and analyzed for yield and quality prior to RT-qPCR analysis (Figure 2). The yield increased in relation to the number of individual microtissues per extraction and all produced high-quality RNA as judged by RNA Integrity number (RIN) (PC2, 1). Equal volumes of the extracted RNA were analyzed with the GoTaq® 1-Step RT-qPCR System for HPRT expression. C_q values were consistent with yields as higher concentration samples gave lower C_q values.

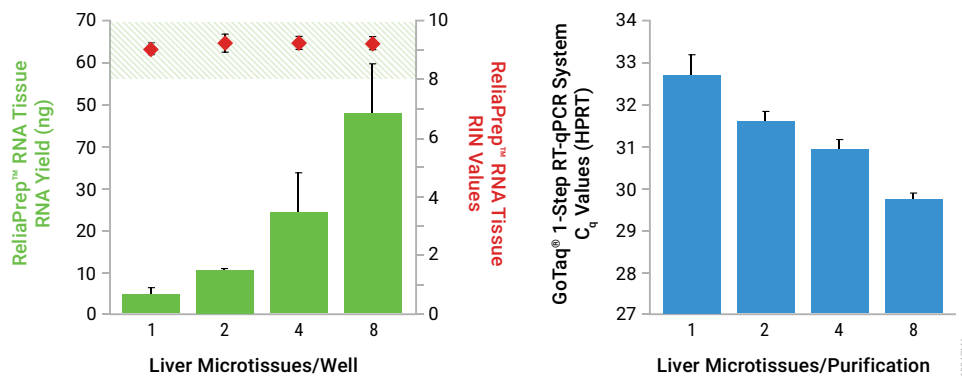


Figure 2. Liver microtissues ReliaPrep™ Tissue RNA extraction with RT-qPCR analysis. Total RNA was isolated from 1–8 of the 3D InSight™ Human Liver Microtissues (InSphero, ~200µm each) with the ReliaPrep™ RNA Tissue Miniprep System. Yields were determined with the QuantiFluor® RNA System and the Quantus™ Fluorometer. RNA integrity numbers (RIN) were determined using an Agilent Bioanalyzer and RNA 6000 Pico Kit. The isolated RNA was reverse transcribed and amplified with the BRYT Green™ dye-based GoTaq® 1-Step RT-qPCR System using primers to hypoxanthine guanine phosphoribosyl transferase (HPRT).

More ReliaPrep RNA Miniprep System Applications

Examples with Spheroid Cultures:

Murkherjee et al. (2) used a ReliaPrep™ RNA Miniprep System to isolate RNA from human liver microtissues (InSphero) treated with palmitic acid. The RT-qPCR analysis of palmitic acid-treated spheroids were consistent with NASH and differed from untreated control liver microtissue spheroids. Mannaerts et al. (3) examined the gene expression of mouse hepatic stellate cells over the course of 10 days in culture as a monolayer or as spheroids. Total RNA extracted with the ReliaPrep™ RNA Cell Miniprep System was converted to cDNA and quantification performed with the BRYT Green® Dye-based GoTaq® qPCR Master Mix.

Examples with Hydrogel Cultures:

(4) investigated gene expression of three transcripts from C2C12 myoblasts cultured on various hydrogel surfaces with dye-based RT-qPCR. Total RNA was extracted from the different hydrogel cultures with the ReliaPrep™ RNA Cell Miniprep System. Jeong et al. (5) worked with human embryonic and induced pluripotent stem cells processed on Matrigel® Matrix to form inner ear organoids with putative cochlear hair cells. RNA was extracted from the organoids with the ReliaPrep™ RNA Cell Miniprep System. The RNA was reverse transcribed with the GoScript™ Reverse Transcription System followed by BRYT Green® Dye-based qPCR with the GoTaq® qPCR Master Mix to analyze nine transcripts plus GAPDH for normalization.

OTHER RESOURCES

PC2

Wieczorek D., et al. Methods of RNA Quality Assessment. Promega Corporation.

References

- Schroeder, A. et al. (2006) The RIN: An RNA integrity number for assigning integrity values to RNA measurements. *BMC Mol. Biol.* 7, 3. PMID:16448564
- Mukherjee, S. et al. (2019) Development and validation of an in vitro 3D model of NASH with severe fibrotic phenotype. *Am. J. Transl. Res.* 11, 1531–1540. PMID: 30972180
- Mannaerts, I. et al. (2019) Unfolded protein response is an early, non-critical event during hepatic stellate cell activation. *Cell Death Dis.* 10, 98. PMID: 30718473
- Park, J. et al. (2019) Micropatterned conductive hydrogels as multifunctional muscle-mimicking biomaterials: Graphene-incorporated hydrogels directly patterned with femtosecond laser ablation. *Acta Biomater.* 97, 141–153. PMID: 31352108
- Jeong, M. et al. (2018) Generating inner ear organoids containing putative cochlear hair cells from human pluripotent stem cells. *Cell Death Dis.* 9, 922. PMID: 30206231

Maxwell® RSC Instrument and simplyRNA Kits

The Maxwell® RSC System combines Maxwell® RSC Instruments with modular nucleic acid extraction kits to the need of any laboratory. The small **Maxwell® RSC Instrument** (Figure 3) automates extraction of 1–16 samples at a time. The larger **Maxwell® RSC 48** (Figure 3) increases throughput to up to 48 samples at a time. Maxwell® RSC kits are available for variety of starting materials like blood, tissue, cells, FFPE tissue and buccal swabs to obtain highly pure DNA, RNA or miRNA.

The RSC instruments are magnetic particle movers, not liquid handlers. The cartridges contain lysis/nucleic acid binding solution, magnetic particles coated with a matrix to bind nucleic acid and wash solutions in separate wells. A plunger covers the magnetic bars, which move the magnetic particles from well to well and finally into the elution solution (Figure 4). Using prefilled reagent cartridges and preprogrammed methods, Maxwell® instruments deliver fast, reliable and consistent DNA and RNA purification, along with the flexibility to process the number of samples needed.

For expression analysis, three varieties of the Maxwell® RSC simplyRNA kits are available for total RNA from cells or tissues and miRNA from tissues. The **Maxwell® RSC miRNA Tissue Kit** was used to demonstrate extraction of miRNA from HCT116 cells cultured as spheroids or as hydrogel cultures for 4 days (Figure 5).

Messner *et al.* (6) used the **Maxwell® RSC simplyRNA Tissue kit** for transcriptomic analysis of multicellular human liver microtissues. RNA was isolated at various time points and was evaluated with Agilent TapeStation RNA Screen Tape and an Affymetrix array. Santoro *et al.* (7) used the simplyRNA Cells chemistry to isolate RNA from



Figure 3. Maxwell® RSC 48 and RSC Instruments. Both are controlled with a Microsoft® Surface Tablet.

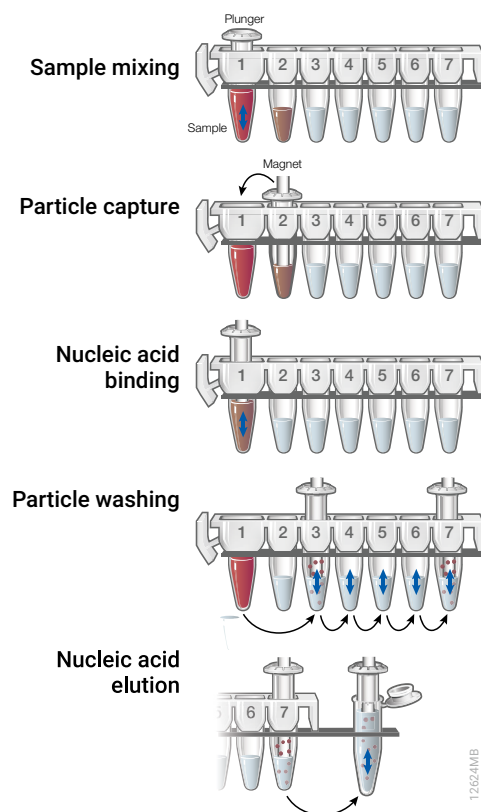


Figure 4. Overview of Maxwell® RSC Purification. The sample is placed into well 1 and mixed with the lysis/nucleic acid binding solution. The instrument retrieves the nucleic acid-binding matrix coated magnetic particles from well 2 and moves the particles to well 1 and mixes. The particles are moved through wells 3–7 with a series of capture and release washes. Pure nucleic acid is eluted into a 0.5ml microcentrifuge tube.

References

6. Messner, S. *et al.* (2018) Transcriptomic, proteomic and functional long-term characterization of multicellular three-dimensional human liver microtissues. *Appl. In Vitro Toxicol.* **4**, 1–12. DOI: 10.1089/aivt.2017.0022
7. Santoro, A. *et al.* (2019) p53 loss in breast cancer leads to myc activation, increased cell plasticity, and expression of a mitotic signature with prognostic value. *Cell Rep.* **26**, 624–638. PMID: 30650356

Need to Concentrate or Clean-Up an RNA Sample?

The ReliaPrep™ RNA Clean-Up and Concentration System can process a dilute sample capture and elute in only 15µl of water or TE buffer. For example, a 200µl RNA sample at 5ng/µl into a 50ng/µl can be processed solution in 15µl that is ready for conversion to cDNA. Recoveries typically exceed 75% with high purity.

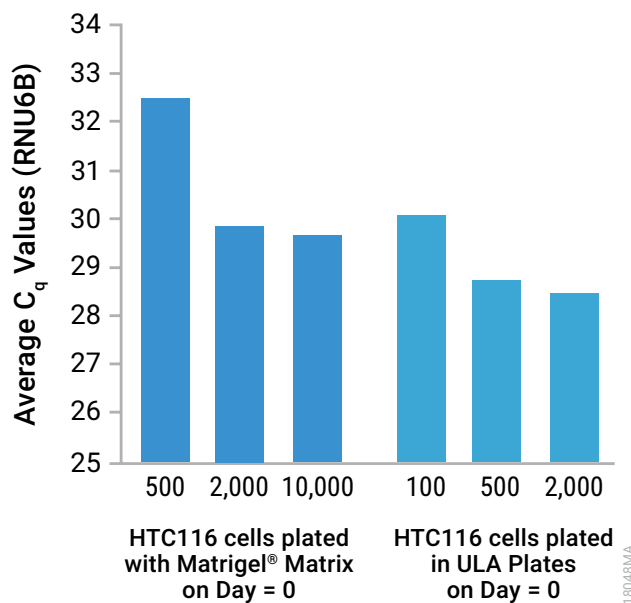


Figure 5. Analysis of Maxwell® RSC-isolated miRNA for spheroid and hydrogel cultures. Average C_q values from TaqMan® RT-qPCR with RNA (10ng) isolated from 3D microtissues with the Maxwell® RSC miRNA Tissue Kit (n=2). Target was the miRNA control gene RNU6B. The indicated number of cells were either plated in Matrigel® Matrix (Corning) or directly into an ULA plate (Corning) and cultured for 4 days. RNA was isolated with the Maxwell® RSC miRNA Tissue Kit and quantified with the QuantiFluor™ RNA System.

References

8. Martinez-Turrillas, R. *et al.* (2019) Generation of an induced pluripotent stem cell line (CIMAi001-A) from a compound heterozygous Primary Hyperoxaluria Type I (PH1) patient carrying p.G170R and p.R122* mutations in the AGXT gene. *Stem Cell Res.* **41**, 101626. PMID: 31715429
9. Chang, J. *et al.* (2018) Effect of migratory behaviors on human induced pluripotent stem cell colony formation on different extracellular matrix proteins. *Regen. Ther.* **10**, 27–35. PMID: 30525068

mammospheres and subsequently carried out cDNA synthesis with the ImProm-II™ Reverse Transcription System and dye-based qPCR. Martinez-Turrillas *et al.* (8) extracted RNA from patient-derived fibroblasts reprogrammed as iPS cells grown on Matrigel® matrix with the simplyRNA tissue kit chemistry and then performed two-step RT-qPCR. Chang *et al.* (9) examined iPS cell colony formation on different extracellular matrices. RNA was extracted with the simplyRNA tissue kit chemistry and adhesion molecule expression was analyzed by two-step, dye-based RT-qPCR.

Merging Gene Expression Analysis with Cell Health and Metabolism Assays

Analyzing how gene expression changes in response to treatment and correlating that gene expression to a change in cell health often requires use of parallel sets of wells. The variety of non-lytic live-cell kinetic and media-sampling cellular assays (Chapters 2 and 3) leave 3D cultures available for RNA extraction and analysis.

The presence of cell health assay reagents have been shown to not affect the yield or quality of extracted RNA (Figure 6). HEK 293 cells were grown as spheroids from increasing number of cells per well to generate spheroids of increasing size. Two sets of cells were cultured in the presence of the **RealTime-Glo™ MT Cell Viability Assay** and two other sets were cultured with media only. The luminescence was consistent with increasing spheroid size (Figure 6, Panel A). RNA was isolated from the RealTime-Glo™ MT wells and media-only wells with both ReliaPrep™ RNA Tissue Miniprep System (Figure 6, Panel B) and the Maxwell® 16 LEV simplyRNA Tissue Kit on a Maxwell® 16 Instrument (Figure 6, Panel C). The Maxwell® 16 Systems were the predecessors to the Maxwell® RSC Systems and the purification chemistries have not changed between the systems. The RNA yield varied little between the manual and automated method no matter if the cell

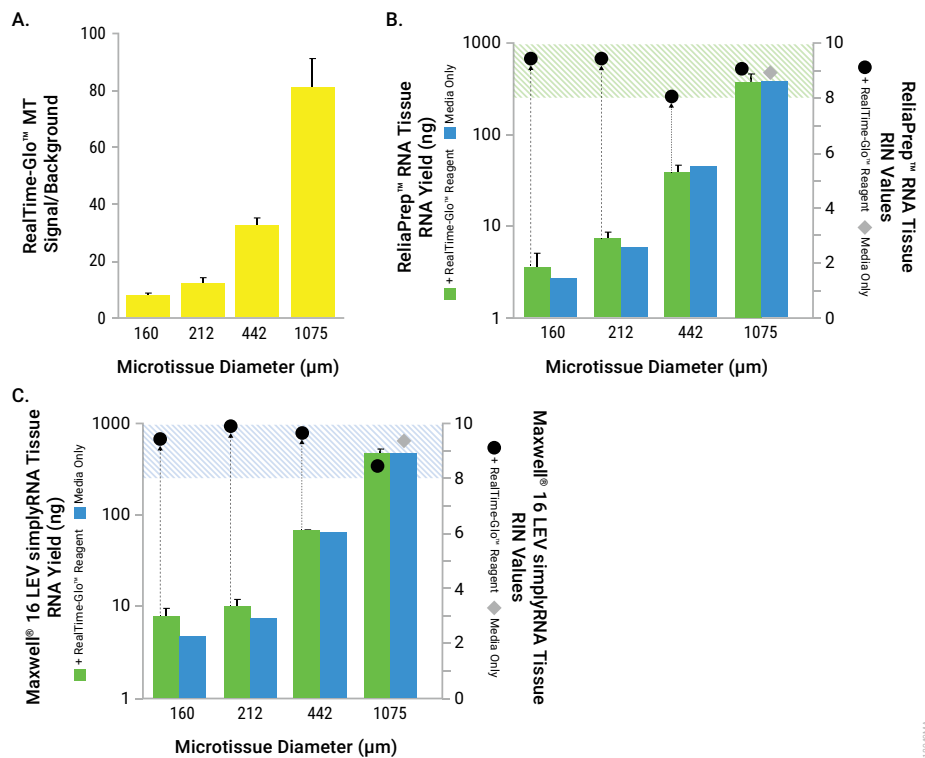


Figure 6. Comparison of RNA yield in the presence or absence of the RealTime-Glo™ MT Cell Viability Reagent. HEK293 microtissues were formed over 4 days with the GravityPLUS™ System (InSphero) and microtissues were collected into white-walled, clear bottom plates. RealTime-Glo™ MT Reagent or culture medium was added to wells, shaken for 10 minutes to mix and incubated at 37°C for 50 minutes. Luminescence was measured with a GloMax® Discover instrument (**Panel A**). Microtissues were transferred to 1.5ml microfuge tubes and processed with the ReliaPrep™ RNA Tissue Miniprep System (**Panel B**) or the Maxwell® 16 LEV simplyRNA Tissue Kit on a Maxwell® 16 Instrument (**Panel C**). RNA yields were determined with the QuantiFluor® RNA System using the Quantus® Fluorometer. RIN values were measured on an Agilent 2100 Bioanalyzer with the RNA 6000 Pico Kit.

health reagent was present and high RIN values were observed. The yields agreed with an earlier study by Hook and Bratz (**PC1**) that compared RNA yields from spheroid cultures by the same manual and automated methods without cell health assay reagents present.

As another example, miRNA expression was measured in HCT116 cells grown in monolayer, Matrigel® and spheroid culture and treated with 5-fluorouracil for 48 hours (**PC3**). Cell viability and cytotoxicity were measured with RealTime-Glo™ MT Cell Viability Assay and CellTox™ Green Cytotoxicity Assay. Apoptosis was tested in parallel with the Caspase-Glo™ 3/7 Assay. The treatment affected cell proliferation: the reading from the viability assay was about 20%

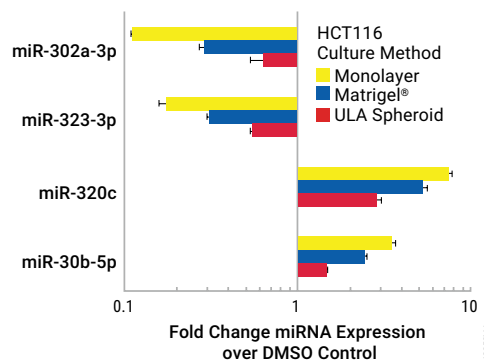


Figure 7. Cell culture format affects strength of miRNA response to 5-fluorouracil treatment. HCT116 Cells were grown in monolayer, Matrigel and as 3D spheroids (Corning ULA plates) then dosed with 30μM 5-Fluorouracil for 48hr. After determining cell viability (RealTime-Glo™ MT Cell Viability Assay) and cytotoxicity (CellTox™ Green Cytotoxicity Assay), RNA was extracted with the ReliaPrep™ miRNA Cell and Tissue Miniprep System and quantified using the QuantiFluor® RNA system. Four miRNA targets were amplified from 5ng of total RNA using TaqMan® assays and expression was normalized to RNU6B. Fold change compared to vehicle controls are shown (**PC3**).

OTHER RESOURCES

PC3

Hook, B., et al. Differential Expression of miRNA in 2D and 3D Human Colon Cancer Cell Cultures after Therapeutic Compound Treatment. Promega Corporation.

lower compared to untreated cultures but no cytotoxicity or apoptosis was apparent. These results were observed for all three of the tested culture types. RNA was extracted with the ReliaPrep™ miRNA Cell and Tissue System, quantified with QuantiFluor® RNA and analyzed by RT-qPCR for 4 miRNA transcripts. Figure 7 demonstrates that different culture methods respond similarly to the treatment but to different degrees. Monolayer cultures had the most extreme response while spheroid cultures gave a more modest response. Matrigel® cultures showed an intermediate response.

Downstream RNA Analysis

After RNA is extracted, the RNA analysis workflow is essentially the same no matter the source of the RNA. RNA needs to be protected, quantified and, typically, converted to cDNA for further analysis by RT-qPCR, microarrays or RNAseq. This section will illustrate how the Promega solutions for these steps work together and will relate examples from the literature demonstrating use of our reagents for RNA analysis.

RNase Protection

RNases are extremely stable and hard to eliminate. In 1981, Promega introduced the first in-reaction RNase inhibitor, the human placental ribonuclease inhibitor **RNasin® Ribonuclease Inhibitor**. At the time, most RNA analysis consisted of Northern blots with radioactively-labeled RNA probes. In vitro transcription reactions to make the probes from plasmid preps were extremely susceptible to carryover of RNases. Addition of the RNasin® Inhibitor to the reactions ensured full-length probes for blotting.

RNA analysis techniques have advanced significantly since that time, but exogenous RNases can continue to be a problem even with the most fastidious RNase-free lab environments (**PC4**). RNasin® Inhibitors have advanced to a human recombinant RNasin® Inhibitor and a more oxidation-resistant RNasin® Plus Inhibitor. These inhibitors meet the needs for an ideal inhibitor—rapid RNase inactivation, no addition of RNases and no interference with common applications (**PC5**). The GoTaq® RT-qPCR and GoScript™ Reverse Transcriptase Systems and Master Mixes include an RNasin® Inhibitor to protect the RNA under study.

In the early days of RNA analysis, Northern blots, RNase protection assays and other RNA analysis techniques required microgram quantities of RNA. Simple A_{260}/A_{280} readings were sufficiently accurate and sensitive enough for these applications. Techniques today not only require greater accuracy, but use much smaller quantities of RNA. Simple UV absorbance is not sufficient and cannot differentiate RNA from DNA. Quantitation methods using fluorescent RNA-binding dyes give more accurate quantitation of the RNA in the sample and are sufficiently sensitive to measure nanogram quantities of RNA.

The **QuantiFluor® RNA System** uses as little as 1 µl of RNA and can accurately measure concentrations as low as 0.5 ng/ml using 1 µl of a 100 µl sample. The data presented in Figures 5, 6 and 7 relied on the QuantiFluor® RNA System for measuring yields from the various purifications. The fluorescent measurements can be made on any fluorometer. The **Quantus™ Fluorometer** is a single-tube fluorometer specifically designed to work with the QuantiFluor® Systems (**AN217**). A Quantus™ Instrument is included with Maxwell® RSC

OTHER RESOURCES

PC4

Hendricksen, A., et al. RNase Contamination Happens; Recombinant RNasin® Inhibitor Can Safeguard Your Samples. Promega Corporation.

PC5

Hooper, K. RNasin® Ribonuclease Inhibitors: Superior Performance for All of Your RNA Analysis Needs. Promega Corporation.

Instrument and the quantitation data from the Quantus™ Instrument can be uploaded to the sample information reports within the Maxwell® RSC Instrument software. For more samples, a multimode plate reader with fluorescent capability (e.g., GloMax® Discover or Explorer) can be employed (AN250). The GloMax® Instruments have a preloaded QuantiFluor® RNA method and can even calculate the concentrations of your standards from a standard curve run on the same plate.

Conversion to cDNA

The advent of cDNA cloning was ushered in decades ago by the ability to make cDNA from RNA with reverse transcriptase enzymes. Many of these enzymes are still in use today, like **M-MLV Reverse Transcriptase** and **AMV Reverse Transcriptase**. Mutations to M-MLV Reverse Transcriptase, like elimination of the RNase H domain (e.g., **M-MLV Reverse Transcriptase, RNase H Minus**) or simply inactivating the RNase H domain (e.g., **M-MLV Reverse Transcriptase, RNase H Minus, Point Mutant**) were developed to convert longer stretches of RNA to cDNA for cDNA cloning. These enzymes and buffer formulation have remained essentially unchanged for decades and modern RNA analysis techniques were developed around these formulations.

The **ImProm-II™ Reverse Transcriptase** and **GoScript™ Reverse Transcriptase** were formulated for compatibility with RT-PCR and RT-qPCR, respectively. GoScript™ Reverse Transcriptase was co-developed with our GoTaq® dye-based and probe-based RT-qPCR systems and provides superior performance (PC7). The enzyme can operate in the presence of strong PCR inhibitors commonly encountered with RNA purification kits (Figure 8). GoScript™ Reverse Transcriptase is adept at transcribing RNAs from low to high copy number over a wide range of input RNA as demonstrated through 2-step RT-qPCR (Figure 9). GoScript™ Reverse Transcriptase is available in a kit with separate nucleotides, oligo(dT)¹⁵ primers, random hexamers and

OTHER RESOURCES

PC7

Ammerschläger, M., et al. Lining Up the Scripts: Reverse Transcriptase Comparison Study. Promega Corporation.

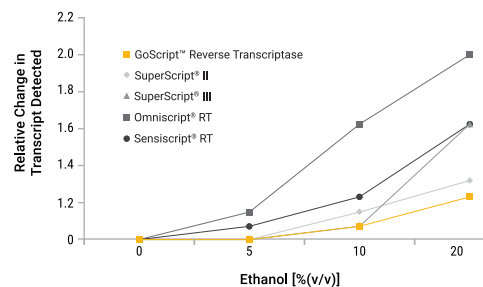
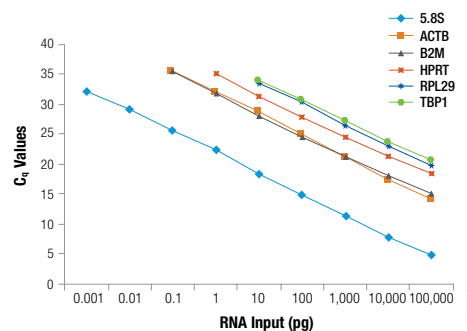


Figure 8. Sensitivity of reverse transcriptases to ethanol inhibition. An in vitro-transcribed RNA was reverse transcribed using oligo(dT) primer according to the manufacturer's instructions in the presence or absence of ethanol. cDNA was analyzed by qPCR using GoTaq® qPCR Master Mix. Changes in cycle threshold values in the absence and presence of ethanol were determined and converted to relative change in transcript level (n=3). Details can be found in (18)



Efficient cDNA Synthesis Over a Wide Range of Input RNA. Direct quantification of six different targets in human total RNA was carried out using GoTaq® 2-Step RT-qPCR System. Nine parallel large-scale GoScript™ RT reactions were performed, containing log-fold variations of input human reference total RNA (10ng/μl to 0.1fg/μl). 10μl fractions of each reverse transcription reaction product—representing 100ng to 1fg of input RNA—were sampled directly into triplicate GoTaq® qPCR reactions, without dilution, for six separate multiplex assays. Each assay was designed to be specific for a different RNA target with an anticipated, proportionally expression level: extremely high (5.8S rRNA), high (ACTB and B2M), moderate (HPRT) or low (RPL29 and TBP1). In each different model, the results demonstrate the desired ≈3.3 cycle change per Δlog input, but with different C_t's reflecting relative proportion within the total RNA sample.

rRNasin® Ribonuclease Inhibitor. GoScript™ RT Mixes, like those used in the GoTaq® 1-Step dye-based or probe-based RT-qPCR kits, are available premixed with either Oligo(dT)¹⁵ or random hexamers (PC8). The GoScript™ Reverse Transcription System has been cited for use in gene expression analysis. For example, the system has been cited for use with the BRYT Green® Dye-based GoTaq® qPCR System (10–13) as well as with other dye-based qPCR systems (14–20).

RT-qPCR Analysis

RT-qPCR is widely-used to analyze changes in gene expression at the RNA level. Two modes are used: 1-step or 2-step RT-qPCR. The 1-step method carries out reverse transcription and then qPCR in the same tube on the same sample. Reverse transcription is primed with the reverse primer used in the qPCR reaction. The 2-step method separates cDNA synthesis from the qPCR step. The cDNA reaction is primed with either oligo(dT), random hexamers, a mixture of the two or with gene-specific primers. The resulting cDNA is then split among different qPCR reactions each with different gene specific primers. While the 1-step method avoids contamination of sample between the reverse transcription and qPCR steps, the 2-step method allows the reverse transcript sample to be banked and used in additional experiments.

Dye-Based RT-qPCR: Two primary methods are used for qPCR quantitation: dye-based and probe-based qPCR. The most approachable is the dye-based quantitation method which relies on a DNA-binding dye intercalating between the bases of PCR products as they accumulate. These fluorescent dyes are designed to be weak fluorophores when free in solution but greatly increase fluorescent yield when intercalated between the hydrophobic bases of DNA. These dyes are not specific to any sequence and will bind to any DNA amplified in the PCR reaction.

SYBR® Green I was the first dye used in this application. Other, more modern dyes have appeared, like the BRYT Green® Dye designed for the GoTaq® qPCR System. The BRYT Green® Dye produces stronger fluorescence from a double-stranded template (Figure 10), which, in turn, produces a stronger signal in qPCR reactions (Figure 11). The GoTaq® qPCR

OTHER RESOURCES

PC8

Hook, B. & Lewis, S. Primer selection guide for use with GoScript® Reverse Transcription Mixes. Promega Corporation.

References

- Kumar, S.V. *et al.* (2019) Kidney micro-organoids in suspension culture as a scalable source of human pluripotent stem cell-derived kidney cells. *Development* **145**, 172361. PMID: 30846463
- Wei, J. *et al.* (2019) Gene manipulation in liver ductal organoids by optimized recombinant adeno-associated virus vectors. *J. Biol. Chem.* **294**, 14096–14104. PMID: 31366731
- Phipson, B. *et al.* (2019) Evaluation of variability in human kidney organoids. *Nat. Methods* **16**, 79–87. PMID: 30573816
- Wang, Z. *et al.* (2019) Generation of hepatic spheroids using human hepatocyte-derived liver progenitor-like cells for hepatotoxicity screening. *Theranostics* **9**, 6690–6705. PMID: 31588244
- Driehuis, E. *et al.* (2019) Patient-derived head and neck cancer organoids recapitulate EGFR expression levels of respective tissues and are responsive to EGFR-targeted photodynamic therapy. *J. Clin. Med.* **8**, 1880. PMID: 31694307
- Mullenders, J. *et al.* (2019) Mouse and human urothelial cancer organoids: A tool for bladder cancer research. *PNAS* **116**, 4567–4574. PMID: 30787188
- Sachs, N. *et al.* (2019) Long-term expanding human airway organoids for disease modeling. *EMBO J.* **38**, e100300. PMID: 30643021
- Pianezzi, E. *et al.* (2020) Role of somatic cell sources in the maturation degree of human induced pluripotent stem cell-derived cardiomyocytes. *Biochim. Biophys. Acta Mol. Cell Res.* **1867**, 118538. PMID: 31472168
- Fujiwara, C. *et al.* (2019) The significance of tumor cells-derived MFG-E8 in tumor growth of angiosarcoma. *J. Dermatol. Sci.* **96**, 18–25. PMID: 31447183
- Cui, N. *et al.* (2019) Doxorubicin-induced cardiotoxicity is maturation dependent due to the shift from topoisomerase IIα to IIβ in human stem cell derived cardiomyocytes. *J. Cell. Mol. Med.* **23**, 4627–4639. PMID: 31106979

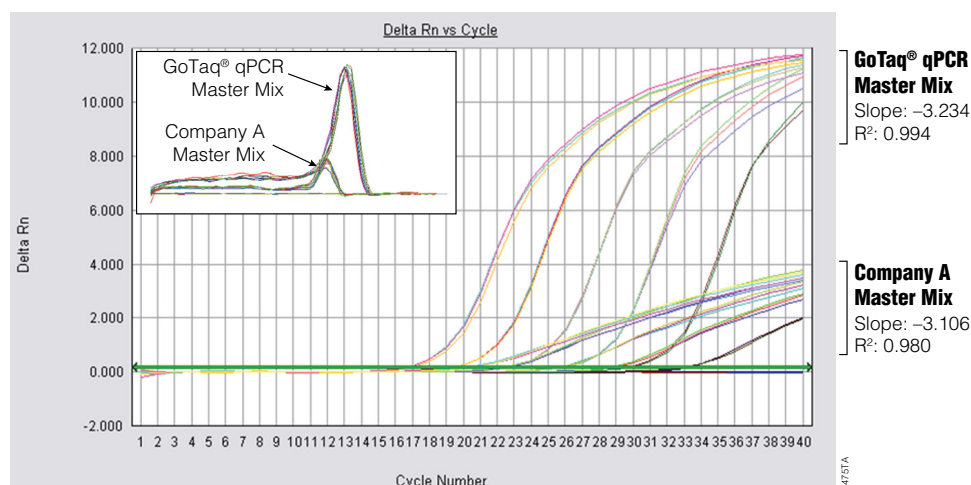


Figure 9. Performance comparison of GoTaq® qPCR Master Mix and Company A's master mix. GAPDH was amplified from ten-fold serial dilutions (0.01–100ng) of human genomic DNA. Inset shows comparison of dissociation profiles for both master mixes.

Master Mix can be read by any real-time amplification instrument that can read a SYBR® Green reaction using either standard or fast amplification protocols. If you are currently using a SYBR® Green-based qPCR Master Mix, Teter and Steffen (AN298) have guidelines for performance comparisons to a brighter dye-based system like GoTaq® qPCR Master Mix.

Two kits are available for the RT-qPCR with the BRYT Green® Dye: GoTaq® 1-Step and GoTaq® 2-Step RT-qPCR Systems. Both kits were designed with GoScript™ Reverse Transcriptase for cDNA synthesis. Figure 12 demonstrates the use of the GoTaq® 1-Step RT-qPCR System with RNA isolated from HCT116 spheroids using the ReliaPrep™ RNA Cell Miniprep System. Many examples cite the use of the GoScript™ Reverse Transcription System and GoTaq® qPCR System in the study of gene expression in 3D model systems (e.g., 5, 10–12, 21). Effectively, these are examples of the GoTaq® 2-Step RT-qPCR System. Jeong *et al.* (5) and Kamarudin *et al.* (21) used the ReliaPrep™ RNA Cell Miniprep System to isolate RNA prior to GoScript™ and GoTaq® qPCR reactions. There are also examples (e.g., 3, 22–25) where the GoTaq® qPCR Master Mix is used with other reverse transcriptases than the GoScript™ Systems for 2-step RT-qPCR.

Probe-Based RT-qPCR: Probe-based qPCR is target specific and relies on a third oligo that anneals to the PCR product. The third oligo—or probe—lies between the two primary PCR primers and contains both a fluorophore and a quencher molecule appended to bases in the oligonucleotide. The 5'→3' exonuclease activity of the amplification enzyme cleaves the bases of this probe releasing the fluorophore from the influence of the quencher. The gain of fluorescence as PCR products accumulate is the basis for probe-based quantification. Signals from different probe-based qPCR master mixes should vary little as the signal comes from the probe (Figure 13).

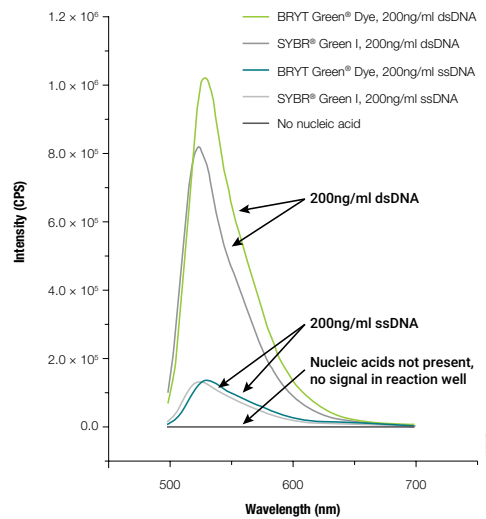


Figure 10. Fluorescence spectra of SYBR® Green I and the BRYT Green® Dye in the GoTaq® qPCR Master Mix. Fluorescence emission spectra were collected for both SYBR® Green I and Promega BRYT™ Green in the absence of dsDNA and in the presence of 50ng/μl or 200ng/μl dsDNA. Peak emission wavelength is 523nm for SYBR® Green I and 529nm for BRYT Green® Dye.

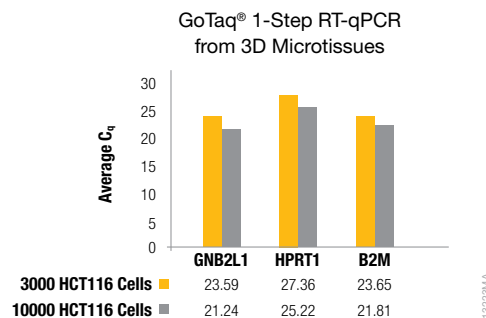


Figure 11. GoTaq® 1-Step RT-qPCR from 3D microtissues. HCT116 cells were seeded at two different densities on GravityPLUS™ hanging drop 96-well plates (InSphero) to form microtissues. Purified RNA was evaluated by looking at the gene expression levels of three genes (GNB2L1, HPRT1, and B2M) using the GoTaq® 1-Step RT-qPCR System. The GoTaq® System was able to detect all three genes from RNA purified from two different microtissue densities using the ReliaPrep™ RNA Cell MiniPrep System.

References

- Wrona, E.A. *et al.* (2019) Effects of polarized macrophages on the in vitro gene expression after co-culture of human pluripotent stem cell-derived cardiomyocytes. *J. Immunol. Regen. Med.* **4**, 100018. DOI: 10.1016/j.regen.2019/100018
- Kamarudin, T.A. *et al.* (2018) Differences in the activity of endogenous bone morphogenetic protein signaling impact on the ability of induced pluripotent stem cells to differentiate to corneal epithelial-like cells. *Stem Cells* **36**, 337–348. PMID: 29226476
- Diekmann, U. *et al.* (2019) Chemically defined and xenogeneic-free differentiation of human pluripotent stem cells into definitive endoderm in 3D culture. *Sci. Rep.* **9**, 996. PMID: 30700818
- Yabe, S.G. *et al.* (2019) Definitive endoderm differentiation is promoted in suspension cultured human iPS-derived spheroids more than in adherent cells. *Int. J. Dev. Biol.* **63**, 271–280. PMID: 31250910
- Fukuda, S. *et al.* (2019) The intraperitoneal space is more favorable than the subcutaneous one for transplanting alginate fiber containing iPS-derived islet-like cells. *Regen. Ther.* **11**, 65–72. PMID: 31193869
- Huang, W. *et al.* (2019) Regulatory networks in mechanotransduction reveal key genes in promoting cancer cell stemness and proliferation. *Oncogene* **38**, 6818–6834. PMID: 31406247

OTHER RESOURCES

PC9

Schmidt, B. & Nassif, N. Optimized Reagents for Probe-Based qPCR using the GoTaq® Probe qPCR and RT-qPCR Systems. Promega Corporation.

References

26. O'Sullivan, A. et al. (2019) Dimethylsulfoxide inhibits oligodendrocyte fate choice of adult neural stem and progenitor cells. *Front. Neurosci.* **13**, 1242. PMID: 31849577

27. Abu-Bonsrah, K.D. et al. (2018) Generation of adrenal chromaffin-like cells from human pluripotent stem cells. *Stem Cell Rep.* **10**, 134–150. PMID: 29233551

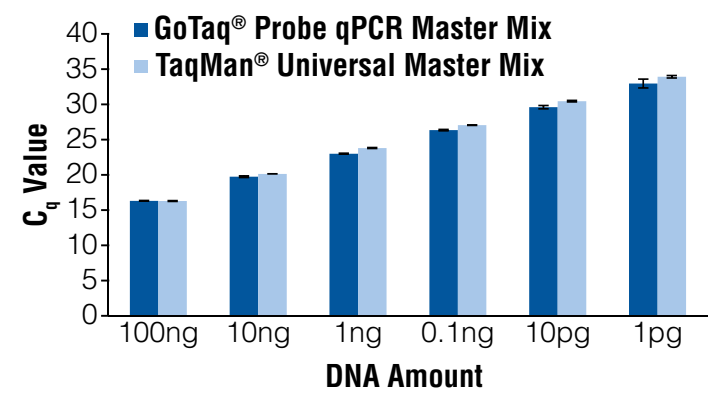


Figure 12. The GoTaq® Probe 2-Step RT-qPCR System performance was compared to that of the TaqMan® Universal Master Mix (Applied Biosystems) (PC9).

Two kits are available for probe-based RT-qPCR: **GoTaq® Probe 1-Step** and **GoTaq® Probe 2-Step RT-qPCR Systems**. As with the dye-based systems, both rely on GoScript™ Reverse Transcriptase for cDNA synthesis. Figure 14 demonstrates the use of the GoTaq® Probe 1-Step RT-qPCR System with RNA isolated from HCT116 spheroids using the ReliaPrep™ RNA Cell Miniprep System. The GoTaq® qPCR Master Mix has been used with other reverse transcriptases in the literature (e.g., 26, 27).

Transcriptional Reporter Assays

Measuring the effects of treatments on a specific target gene can become quite tedious if you are employing RT-qPCR. If transfection of your cells of interest is possible, a bioluminescent reporter gene often makes more sense. The process of measuring luciferase gene expression is far easier than isolating RNA, conversion to cDNA and

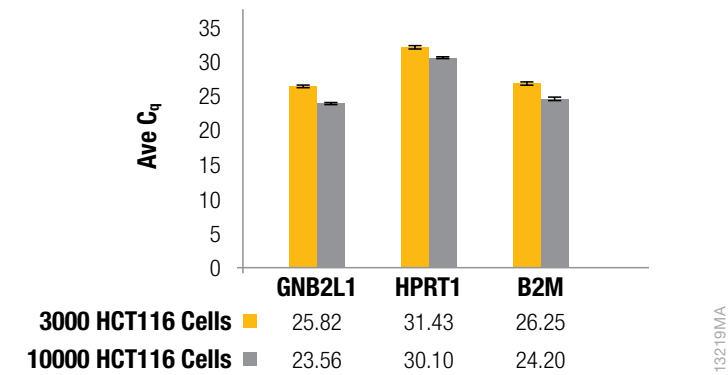


Figure 13. GoTaq® Probe 1-Step RT-qPCR amplification from 3D microtissue-derived RNA. HCT116 cells were seeded at two different densities on GravityPLUS™ hanging drop 96-well plates (InSphero) to form microtissues. Purified RNA was evaluated by looking at the gene expression levels of three genes (GNB2L1, HPRT1, and B2M) using the GoTaq® Probe 1-Step RT-qPCR System. The GoTaq® System was able to detect expression levels all three genes from RNA purified from two different microtissue densities using the ReliaPrep™ RNA Cell MiniPrep System.

amplification by qPCR even if you use a 1-Step RT-qPCR System. Once transfected, the process is mostly “add-mix-measure” (PC10, PC11).

A reporter assay replaces a gene of interest upstream of a promoter with a reporter like firefly or NanoLuc® Luciferase in the context of a plasmid. The reporter can be used to analyze changes in transcription for any target gene. Many researchers use reporters to indicate up or down regulation of a specific signaling pathway. Figure 15 demonstrates a signaling pathway indicator response of activation of the NF- κ B pathway to TNF α in stably transfected HEK 293 cells grown as spheroids. Figure 16 demonstrates how cells experience greater hypoxia as spheroid diameter increases through use of a reporter vector with a hypoxia response element.

Getting the reporter gene into the cells is the biggest challenge of this approach, especially if working with primary cells. Transfection is typically performed before the cells are cultured in 3D and transient expression. While stable transfection must be weighed depending upon how long the cells must be in 3D culture prior to testing.

An alternative method is to use the knock-in capabilities of CRISPR/Cas9. In Schwinn *et al.* (PC13), the bioluminescent 11aa peptide, called HiBiT, was inserted into either the N- or C-terminus of genes responding to an increase in HIF1 α stabilization due to an increase in hypoxia. The HiBiT tag and subsequent structural complementation by the LgBiT subunit to form an active NanoBiT® Luciferase was introduced earlier in the Cell Health Changes chapter. The method for knock-in of the small tag is straightforward and requires no cloning, just design work (PC14). The change in HiBiT-tagged endogenous protein levels indicates changes in gene expression just like a classic reporter assay. The HiBiT tag is quantified with a lytic reagent containing the LgBiT subunit with substrate for NanoBiT® Luciferase spontaneously formed from the HiBiT-LgBiT interaction.

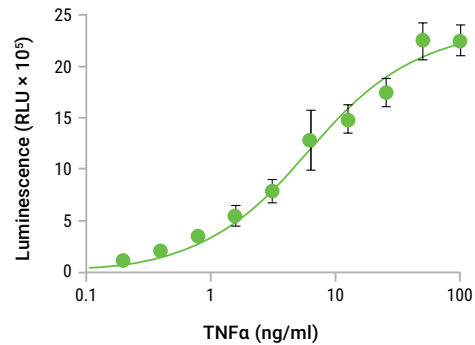


Figure 14. NF- κ B response in HEK293 microtissues to TNF α treatment. The GloResponse™ NF- κ B-RE-luc2P HEK293 cells were seeded in GravityPLUS™ 96-well plates (InSphero) and grown for 4 days then transferred to a white-walled, 96-well plate. The ~340 μ m microtissues were challenged with various concentrations of TNF α for 7 hours. ONE-Glo™ Luciferase Assay Reagent was added to wells, shaken for 10 minutes then allowed to sit at room temperature for 20 minutes prior to reading the luminescence on a GloMax® Instrument (PC12).

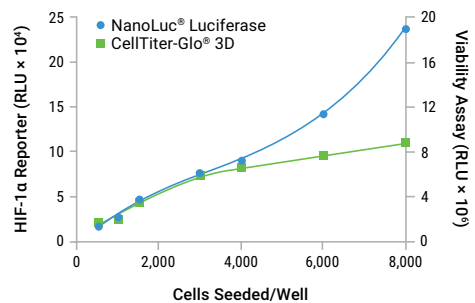


Figure 15. Hypoxia response increases with increasing spheroid diameter. HCT116 cells expressing NanoLuc luciferase from a HIF1 α -responsive promoter were cultured in InSphero GravityPLUS™ 3D Cell Culture system for 4 days to form ~200-700 μ m spheroids. One set of cells were measured for reporter activity with Nano-Glo® Reporter Assay System and the other set was measured for viability with the CellTiter-Glo® 3D Assay. After assay reagent addition, the plate was shaken for 10 minutes, and luminescence was recorded after a total 30 minutes incubation at room temperature.

OTHER RESOURCES

PC10

Reporter Genes and their Applications. Promega Corporation.

PC11

Understanding Luminescent Reporter Assay Design. Promega Corporation.

PC12

Schwinn, K. M., et al. CRISPR-Mediated Tagging of Endogenous Proteins with a Luminescent Peptide. ACS Chemical Biology. doi: 10.1021/acschembio.7b00549

PC13

Protocol for Adding HiBiT Tag to an Endogenous Gene Using CRISPR. Promega Corporation.

PC14

Protocol for Adding HiBiT Tag to an Endogenous Gene Using CRISPR. Promega Corporation.

Chapter 4

GENOME ANALYSIS IN 3D

Genomic DNA Extraction	46
Solution-Based gDNA Extraction	46
Spin Column-Based gDNA Extraction.....	47
Automated Magnetic Bead-Based gDNA Extraction	48
Genome Analysis.....	50
Whole Genome or Exome Sequencing.....	50
Genotyping	52
Methylation Analysis by Bisulfite Conversion.....	54
STR Profiling for Cell Authentication and Sample Tracking	55

Understanding the genetic basis for a disease can highlight the connection between genotype and phenotype, which may help to explain certain behaviors in a cell. Genetic alterations that cause disease can lie within an exon, intron, promoter, 5' UTR, 3' UTR and other genomic regions. Mutations within exons can affect protein function, making the protein dysfunctional, hyperfunctional or hypofunctional. Intron mutations can affect splicing and, ultimately, protein function. Mutations outside of these regions can be more difficult to classify, and could affect when a gene is turned on or off or to what degree gene transcription responds to stimuli. Identifying these mutations—or biomarkers—can inform disease research.

Determining these changes through genome analysis begins with genomic DNA (gDNA) isolation. Isolation of gDNA may be carried out with 3D cultured cells or with monolayer cells prior to being cultured in 3D. A important tool for identifying mutations is next generation sequencing (NGS). Researchers may opt for whole genome sequencing (WGS) to identify mutations anywhere in the genome or focus on the expressed genome with whole exome sequencing (WES). Investigating the presence of known mutations relies on PCR genotyping via Sanger sequencing or qPCR analysis. The role that methylation plays in the phenotype is explored through methods that can distinguish methylated cytosines from unmethylated cytosines. Finally, keeping track of the cell lines, especially primary human cell lines, relies on short tandem repeat (STR) analysis to generate a genome-specific fingerprint for cells. This chapter will explore tools available to assist with all these genome analysis tasks.

Genomic DNA Extraction

All methods of genome analysis require extraction of gDNA from the cells. The extracted gDNA can be used for genome analysis, exome analysis or genotyping. The choice of extraction method should meet the purity and quality requirements of the application. For example, you should consider if the analysis requires mostly intact gDNA or if fragmented gDNA will suffice.

Solution-Based gDNA Extraction

Long-read NGS systems (e.g., PacBio® and Oxford NanoPore® Instruments) work best with larger gDNA molecules. Obtaining the largest gDNA molecules possible requires different procedures than standard DNA extraction methods. The most important change is to avoid steps that cause unnecessary agitation of the gDNA, which can shear DNA strands and lead to lower molecular weight DNA. Vortexing, or even just dropping the sample tube, can cause shearing. Most researchers resort to solution-based salting out methods rather than spin column or magnetic particle-based purifications. All pipeting of samples containing the gDNA must be slow and use wide-bore pipette tips. Cutting off the end of a standard pipette tip to mimic a wide-bore tip is not recommended as the sharp edges generated by cutting can contribute to shearing of the gDNA even with slow pipeting.

The [Wizard® Genomic DNA Purification Kit](#) uses a gentle, solutions-based method to produce high molecular weight gDNA (Figure 1). Figure 2 demonstrates the increased size of gDNA produced with the Wizard® Genomic DNA Purification Kit prep in comparison to magnetic particle-based and spin column-based preps.

The Wizard® Genomic DNA Purification Kit is versatile and can be used for gDNA extraction from a wide variety of starting materials including blood, cultured cells and tissues. Recent citations that use the Wizard® Genomic DNA Purification Kit to extract gDNA from 3D cultures are available (1–5).

The **Wizard® Genomic HMW DNA Extraction Kit** is solutions-based gDNA extraction system designed with the needs of long-read NGS systems in mind. More information is available in [PC1](#).

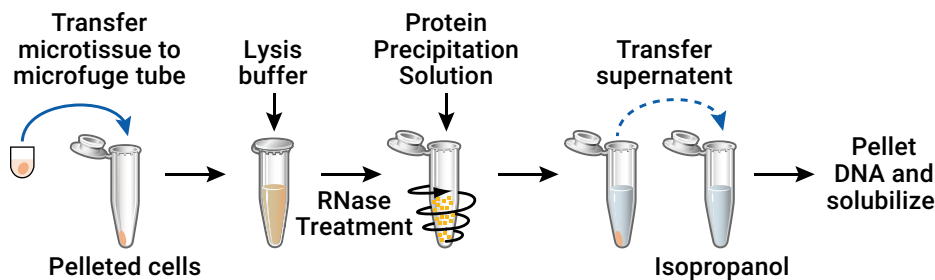


Figure 1. Overview of the Wizard® Genomic DNA Purification Kit procedure.

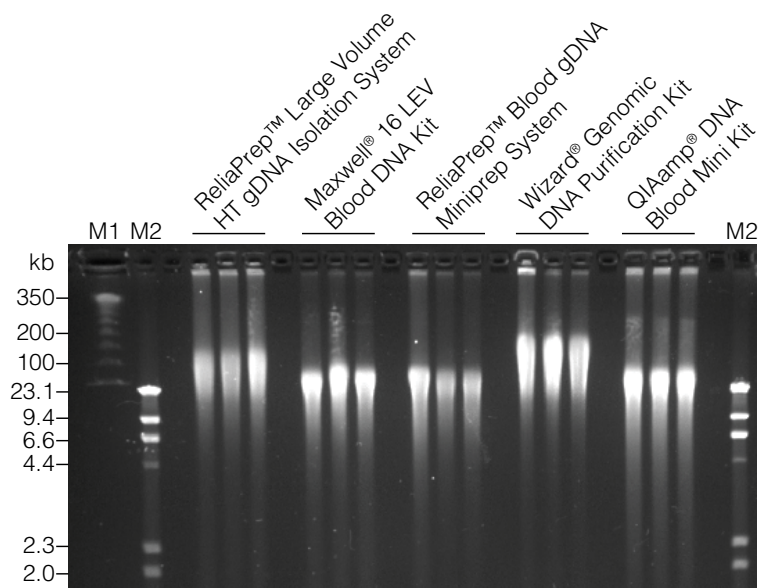


Figure 2. CHEF gel analysis of gDNA isolated with different gDNA kits. Each lane contains 5µg of gDNA isolated from whole blood with recommended protocols. M1 is a concatemer of lambda DNA (ProMega-Markers® Lambda Ladder) and M2 is Lambda/HindIII digest. Details are provided in reference ([PC2](#)). The ReliaPrep® RNA Miniprep and Maxwell® RSC Systems shown use magnetic bead-based purification. The QIAamp® Kit uses spin columns.

OTHER RESOURCES

PC1

Schagat, T., et al. Comparing Manual and Automated Genomic DNA Purification Methods for Genotyping Arrays. Promega Corporation.

PC2

Zegers, A., et al. Extraction of High Molecular Weight (HMW) Genomic DNA for Long-Read NGS Applications. Promega Corporation.

References

1. van der Graaf, L.M. et al. (2019) Generation of 5 induced pluripotent stem cell lines, LUMCi007-A and B and LUMCi008-A, B and C, from 2 patients with Huntington disease. *Stem Cell Res.* **39**, 101498. PMID: 31326748
2. Zhang, M. et al. (2019) Generation of a PARK2 homozygous knockout induced pluripotent stem cell line (GIBHi002-A-1) with two common isoforms abolished. *Stem Cell Res.* **41**, 101602. PMID: 31698191
3. Abdul, M.M. et al. (2019) Generation of an induced pluri-potent stem cell line (GIBHi003-A) from a Parkinson's disease patient with mutant PINK1 (p.I368N). *Stem Cell Res.* **41**, 101607. PMID: 31778937
4. Pianezzi, E. et al. (2020) Role of somatic cell sources in the maturation degree of human induced pluripotent stem cell-derived cardiomyocytes. *Biochim. Biophys. Acta Mol. Cell Res.* **1867**, 118538. PMID: 31472168
5. Selvaraj, B.T. et al. (2018) C9ORF72 repeat expansion causes vulnerability of motor neurons to Ca²⁺-permeable AMPA receptor-mediated excitotoxicity. *Nat. Commun.* **9**, 347. PMID: 29367641

Spin Column-Based gDNA Extraction

The speed and convenience of spin column-based gDNA extractions are appealing to anyone performing genome analysis. Amplification-based analysis methods do not require extremely high molecular weight gDNA. As such, spin column-based methods work well in these applications.

Though developed for extraction of gDNA from tissues, the **ReliaPrep™ gDNA Tissue Miniprep System** has found a place in many laboratories using 3D cell culture, especially organoid cultures (6–10). The ReliaPrep™ gDNA Tissue Miniprep System produces gDNA without the use of ethanol washes (a potential source of PCR inhibition) or precipitations (Figure 3).

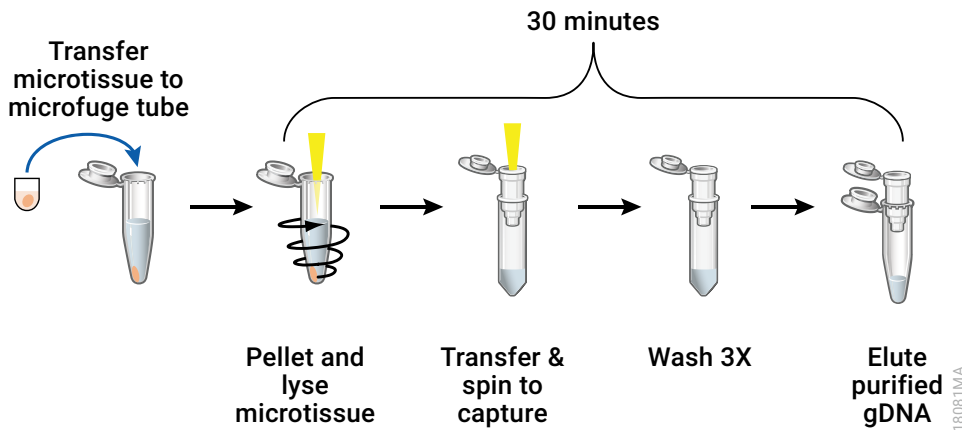


Figure 3. Overview of the ReliaPrep™ gDNA Tissue Miniprep System procedure.

Automated Magnetic Bead-Based gDNA Extraction

The Maxwell® RSC System combines Maxwell® RSC Instruments with modular nucleic acid extraction kits to fit any nucleic acid extraction need in the laboratory. The smaller Maxwell® RSC Instrument (Figure 4) automates extraction from 1 to 16 samples at a time. The larger Maxwell® RSC 48 (Figure 4) increases throughput up to 48 samples at a time. Maxwell® RSC kits are available to obtain highly pure DNA, RNA or miRNA from a variety of starting materials like blood, tissue, cells, FFPE tissue and buccal swabs. The RSC instruments are magnetic particle movers. The cartridges contain lysis/nucleic acid binding solution, magnetic particles coated with a matrix to bind nucleic acid and wash solutions in separate wells. A plunger covering the magnetic bars moves the magnetic particles from well to well and finally into the elution solution (Figure 5). Using prefilled reagent cartridges and preprogrammed methods, Maxwell instruments deliver fast, reliable and consistent DNA purification, along with the flexibility to process only the number of samples needed.

The **Maxwell® RSC Cultured Cells Kit** has been tested with HCT116 cells grown as spheroids and on Matrigel® Matrix (PC3). Different starting amounts of HCT116 cells were incubated in ULA plates (Corning) or in wells coated with Matrigel® Matrix. The cultures



Figure 4. Maxwell® RSC 48 and RSC Instruments. Both are controlled with a Microsoft® Surface Tablet.

OTHER RESOURCES

PC3

Welch, J. & Steffen, L. Purification of DNA from 3D cell cultures using the Maxwell® RSC Cultured Cells DNA Kit. Promega Corporation.

References

- Driehuis, E. *et al.* (2019) Pancreatic cancer organoids recapitulate disease and allow personalized drug screening. *PNAS* **116**, 26580–26590. PMID: 31818951
- Driehuis, E. *et al.* (2019) Oral mucosal organoids as a potential platform for personalized cancer therapy. *Cancer Discov.* **9**, 852–871. PMID: 31053628
- Schutgens, F. *et al.* (2019) Tubuloids derived from human adult kidney and urine for personalized disease modeling. *Nat. Biotechnol.* **37**, 303–313. PMID: 30833775
- Ishii, Y. *et al.* (2018) Activation of signal transduction and activator of transcription 3 signaling contributes to Helicobacter-associated gastric epithelial proliferation and inflammation. *Gastroenterol. Res. Pract.* **8**, 9050715. PMID: 29849601
- Drost, J. *et al.* (2016) Organoid culture systems for prostate epithelial and cancer tissues. *Nat. Protoc.* **11**, 347–358. PMID: 26797458

were grown for 4 days then gDNA was isolated with the RSC kit. DNA yields increase as the starting number of cells increase (Figure 6A). To test for amplification inhibitors, an equal volume of each purification was added to a DNA positive control and amplified. The eluates from the Maxwell® RSC Purification had no significant inhibition of PCR (Figure 6B).

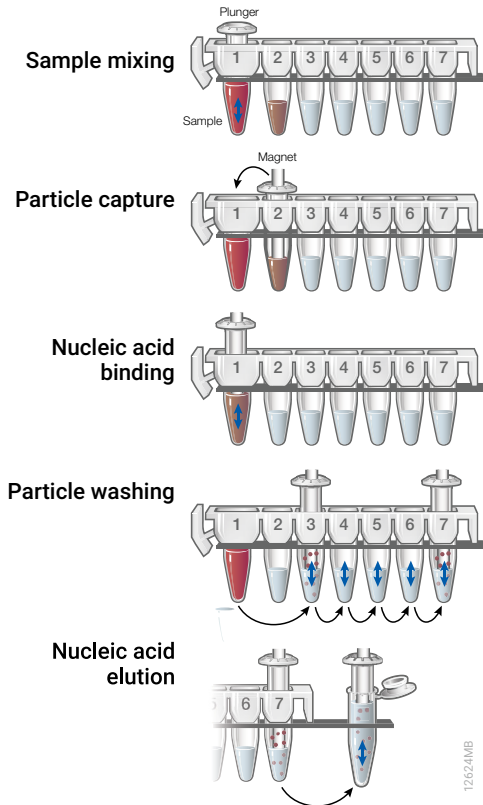


Figure 5. Overview of Maxwell® RSC Purification. The sample is placed into well 1 and mixed with the lysis/nucleic acid binding solution. The instrument retrieves the nucleic acid-binding matrix-coated magnetic particles from well 2 and moves the particles to well 1 and mixes. The particles are moved through wells 3–7 with a series of capture and release washes. Pure nucleic acid is eluted into a 0.5ml microcentrifuge tube.

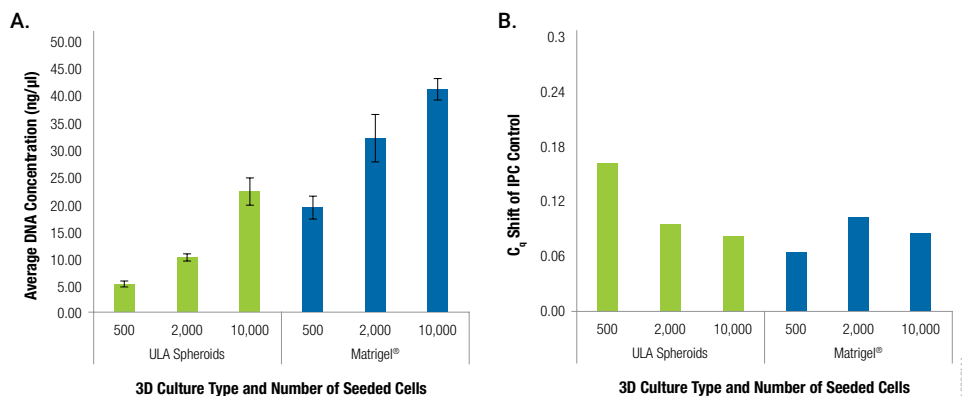


Figure 6. Yields of DNA from HCT116 cells grown on ULA Plates or Matrigel® Matrix with minimal carryover of inhibitors into amplifications. **Panel A:** Increasing numbers of HCT116 cells were cultured in ULA plates (Corning) or on Matrigel® Matrix for 4 days. Cellular DNA was isolated with the Maxwell® RSC Cultured Cells Kit on a Maxwell® RSC Instrument as described (PC3). DNA yields were measured with the QuantiFluor® ONE dsDNA System using a Quantus® Fluorometer. **Panel B:** Equal quantities of eluted DNA were mixed with a positive control PCR template (IPC), amplified and compared to a sample with no Maxwell® RSC-purified eluate. A deviation ≥ 0.3 C_q from the control sample is considered significant. None of the RSC-purified samples produced significant deviation from the control.

Genome Analysis

After gDNA extraction, the options for genome analysis are essentially the same no matter the source of the gDNA. The depth of genome analysis when studying cells in 3D culture depends upon how much is known about the cells of interest. Cell lines commonly available from vendors likely have well known genetic abnormalities which are represented in the phenotype. Patient-derived primary cells can be entirely unknown, and part of the research project to connect the genotype to the phenotype.

In general, three types of studies can be employed in the genome analysis: whole genome sequencing, whole exome sequencing and genotyping. The methylation status of the genome or specific genes can also provide important information. STR profiling is a type of genotyping that allows for positive identification of a cell line or cell line tracking throughout a study.

Whole Genome or Exome Sequencing

Whole genome sequencing (WGS) provides the most genetic information about the cells under study. WGS seeks to identify the sequence of every nucleotide in the entire genome by locating insertions, deletions, duplications and variants across the genome. Studies with commonly available cell lines are less likely to be subject to WGS, but work with primary patient-derived cells likely will include WGS.

Whole exome sequencing (WES) seeks to simplify analysis by focusing on just the expressed genome (exome) rather than the entirety of the genome. Analyzing the exons requires examination of only about 2% of the genome and, thus, is more rapid and cost effective than WGS. Both WGS and WES start with gDNA fragmentation, but WES adds a step to capture the coding sequences through either solution hybridization to oligos or array-based capture.

Short-read platforms, like the Illumina® MiSeq™ and HiSeq™, are commonly employed in WGS and WES studies (11, 12). The extracted DNA is fragmented, size-selected and then adapters are ligated to the ends. All NGS methods require accurate, consistent and sensitive nucleic acid quantification to ensure optimal results.

Long-read platforms like those offered by PacBio® (13) and Oxford NanoPore® (14) excel at WGS and are sometimes referred to as third-generation sequencing platforms. Reading larger regions of the genome allows quicker assembly of the full genome. Compared to the short 150–300bp reads of Illumina® Systems, analysis of larger fragments makes identification of translocations, deletions and repetitive regions easier.

QuantiFluor® ONE dsDNA Dye. The first step in preparing a genomic library from purified gDNA is to accurately quantitate how much DNA is in the sample. Depending upon the amount of starting material, microgram to nanogram quantities of nucleic acid may be present. Simple A_{260}/A_{280} measurements may not be sufficiently sensitive or accurate for quantitation (**PC4**). Quantitation using fluorescent DNA binding dyes gives more accurate quantitation of dsDNA in the sample and is sufficiently sensitive to measure nanogram quantities of dsDNA. The yield data presented in Figure 6A was measured with the QuantiFluor® ONE dsDNA dye read on a single-tube Quantus® Fluorometer.

OTHER RESOURCES

PC4

Clawson, L. M., et al. Genomic signatures of *Mannheimia haemolytica* that associate with the lungs of cattle with respiratory disease, an integrative conjugative element, and antibiotic resistance genes. *BMC Genomics*. doi: 10.1186/s12864-016-3316-8

References

11. Buermans, H.P.J. and den Dunnen, J.T. (2014) Next generation sequencing technology: Advances and applications. *Biochim. Biophys. Acta-Mol. Basis Dis.* **1842**, 1932–1941. PMID: 24995601
12. Jerzy K. Kulski (January 14th 2016). Next-Generation Sequencing — An Overview of the History, Tools, and "Omic" Applications, *Next Generation Sequencing - Advances, Applications and Challenges*, Jerzy K Kulski, IntechOpen, DOI: 10.5772/61964.
13. Rhoads, A. and Au, K.F. (2015) PacBio sequencing and its applications. *Genom. Proteom. Bioinform.* **13**, 278–289. PMID: 26542840
14. Jain, M., Olsen, H., Paten, B., and Akeson, M. (2016) The Oxford Nanopore MinION : Delivery of nanopore sequencing to the genomics community. *Genom. Biol.* **17**, 239. PMID: 27887629

ProNex® Size-Selective Purification System. Short read NGS methods, like Illumina®-based techniques, work best when DNA of a certain size is used. Prior to making libraries for the NGS reads, DNA must be randomly fragmented to generate DNA of the preferred size. Of course, DNA fragments are generated above and below this preferred range and should not be carried over into the steps in which adaptors are ligated. In early NGS workflows, size selection was performed on agarose gels with gel purification. Later, bead-based methods, like the AMPure® XP beads (Beckman Coulter), were employed that were quicker but not necessarily as accurate at eliminating fragments above the preferred range. Size selection can also benefit high molecular weight sequencing technologies by removing smaller fragments. PacBio® procedures recommend use of the ProNex® Size-Selective Purification System (15)

The ProNex® Size-Selective Purification System is a more precise rapid bead-based method for size selection (**PC5, PC6**). By varying the ProNex® chemistry:sample ratios, different size fragments can be purified as shown in Figure 7. To eliminate fragments above and below the desired range, a two-step size selection is performed. First, the ProNex® chemistry:sample ratio is chosen to bind fragments above the desired range (which are left attached to the magnetic beads). The supernatant is transferred to a new tube and the ProNex® chemistry:sample ratio is adjusted to capture the desired fragments and leave unwanted smaller fragments in the supernatant. The beads are then washed and eluted to yield DNA in the desired fragment size range.

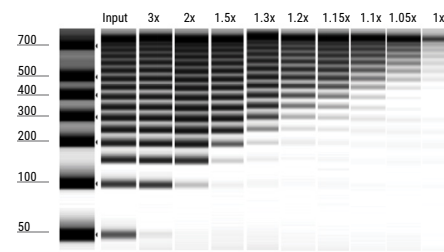


Figure 7. Size selection of DNA with varying ProNex® chemistry:sample ratios. The 50bp DNA Step Ladder (Cat. # G4521) was used as the source DNA.

The ProNex® Size-Selective Purification System can be used to remove reactants or amplification inhibitors from various stages of library preparation. The system gives a

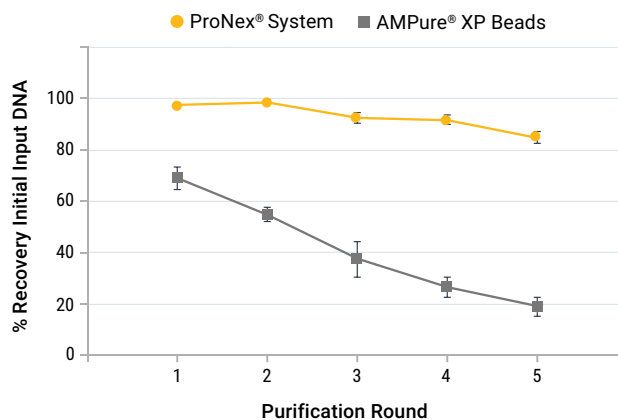


Figure 8. Serial buffer exchange/cleanup purification comparison between ProNex® Size-Selective Purification System and AMPure® XP beads. Five sequential cleanup rounds (AMPure® XP = 1.8X ratio, ProNex® = 3X ratio) were performed on a 200bp DNA step ladder. Ratios designed to retain all fragments. There are n=8 replicates per sample.

OTHER RESOURCES

PC5

Fernandes, N. L., et al. A Novel Highly Divergent Strain of Cell Fusing Agent Virus (CFAV) in Mosquitoes from the Brazilian Amazon Region. *Viruses*. doi: 10.3390/v10120666

PC6

Improved Chemistry for NGS Library Cleanup and Size Selection. Promega Corporation.

References

15. PacBio® Iso-Seq™ Express Template Preparation for Sequel® and Sequel II Systems Procedure & Checklist. [PacBio® Corporate Website](#).

high rate of DNA recovery with >80% of the starting DNA recovered after five successive rounds of purification (Figure 8).

ProNex® NGS Library Quant Kit. When performing Illumina®-based NGS, DNA fragments are tagged with adaptors to match the complementary DNA anchors within the flow cell. The adaptors can also contain unique barcodes for each library so more than one library can be added to maximize data generation from a single flow cell. Precise quantitation of each library is necessary to ensure maximum data collection. The ProNex® NGS Library Quant Kit was designed to specifically quantitate NGS libraries through dye-based qPCR measurement.

Each Illumina® library contains the P5 and P7 primers on opposite ends to match complementary capture sequences in the flow cell. The ProNex® NGS Library Quant Kit uses primers based on P5 and P7 to quantitate the libraries. A sample of the library is amplified by BRYT Green® Dye-based qPCR and compared to a standard curve generated from 0.02pM to 20pM of a ProNex® NGS Quant DNA Standard. Accurate quantitation leads to better cluster density in the flow cell (Figure 9).

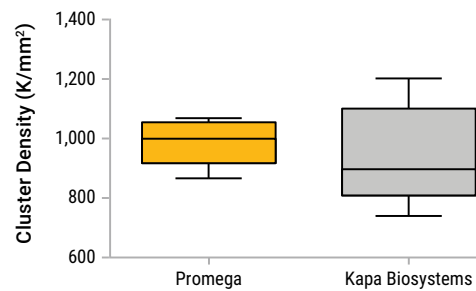


Figure 9. Comparison of cluster density between Illumina® library kit quantitation systems. Illumina® NGS libraries were quantified using either the ProNex® NGS Library Quant Kit or the KAPA Library Quantification Kit for Illumina® (Kapa BioSystems). The determined concentrations were used to normalize and pool libraries (n=10 pools) prior to sequencing on an Illumina® MiSeq instrument. Targeted cluster density was 1000K/mm². Cluster density was measured for all sequencing runs, showing significantly improved reproducibility when samples were quantified with the ProNex® System.

References

16. Engels, L. *et al.* (2019) Generation of a CFTR knock-in reporter cell line (MHHi006-A-1) from human induced pluripotent stem cell line. *Stem Cell Res.* **40**, 101542. PMID: 31473565
17. Turner, J.A. *et al.* (2019) BRAF fusions identified in melanomas have variable treatment responses and phenotypes. *Oncogene* **38**, 1296–1308. PMID: 30254212
18. Čančer, M. *et al.* (2019) Humanized stem cell models of pediatric medulloblastoma reveal an Oct4/mTOR axis that promotes malignancy. *Cell Stem Cell* **25**, 855–870. PMID: 31786016

Genotyping

Purified gDNA is often used for genotyping. Genotyping looks at differences between samples via inspection of specific genes rather than sequencing the entire genome. An example of genotyping would be the amplification of a known oncogene from various samples and sequencing the amplicons to determine if any of the samples carry known mutations associated with a disease phenotype. Genotyping typically starts with purified gDNA followed by PCR. The amplicon can be sequenced directly after clean-up in solution or after gel purification. Another option is to clone the amplicon of interest via PCR cloning prior to Sanger sequencing. This section will examine tools available to assist with genotyping. The genotyping protocol can be employed to clarify undefined or problematic regions encountered with WGS or WES.

PCR Amplification. The first step in genotyping is amplification of the desired sequence. Hot start amplification is typically employed due to the enhanced specificity of the reaction. However, a well-designed and optimized PCR reaction can use a standard polymerase like the **GoTaq® G2 Flexi DNA Polymerase** (16–18). Driehuis *et al.* (7) isolated gDNA with the ReliaPrep™ gDNA Tissue Miniprep System and amplified a portion of the KRAS gene with GoTaq® DNA Polymerase for Sanger sequencing to genotype patient-derived organoids. The PCR reaction components can be compiled individually entirely to precisely control the reaction conditions (e.g., **GoTaq® G2 Hot Start Polymerase**). In

contrast, using a master mix (enzyme, dNTPs, buffer, $MgCl_2$) allows for rapid reaction setup (e.g., [GoTaq® G2 Hot Start Master Mixes](#)). The GoTaq® G2 Hot Start Polymerase includes two reaction buffers, one green-colored and the other colorless. The green reaction buffer is especially useful if the next step involves gel electrophoresis. The reaction buffers allow direct loading into wells without needing to add sample loading buffer. The green color is composed of a: blue and yellow dye. The yellow dye will run to >50bp fragment and the blue will run to 3-5kbp (Figure 10). The GoTaq® G2 Hot Start Master Mixes are available in either the colorless or green varieties. If fidelity or length of amplification is a concern, the GoTaq® Long PCR Master Mix can be used. The long mix contains a mix of GoTaq® Hot Start Polymerase and a thermostable proofreading polymerase needed to achieve long amplicons.

PCR Clean-Up/Gel Purification.

The [ReliaPrep™ DNA Clean-Up and Concentration System](#)

can handle specificity instead. This spin column-based method can be used to purify fragments directly from a PCR reaction in less than 10 minutes. The eluate volume can be as low as 15µl to concentrate the sample. This system yields high quality DNA for applications like direct sequencing or subcloning.

For higher throughput applications, the [ProNex® Size Selective Purification System](#) can be employed to purify amplicons away from primers and reactants. The magnetic bead-based purification lends itself to automation with liquid handlers.

PCR Cloning. The [pGEM®-T Easy Vector System](#) has been used for decades to clone PCR products into a vector. Amplicons generated with *Taq* DNA polymerases like GoTaq® G2 Polymerase leave unpaired nucleotides at the 3' ends of amplicons, most commonly an A base. The pGEM®-T Easy Vector has unpaired T bases on the 3' ends of the vector linearized within the multi-cloning site to match the A base in the amplicon. The amplicon and the vector are mixed and rapidly ligated with the components of the LigaFast™ Rapid Ligation System and are ready for transformation into bacteria. Amplicons generated with a proof-reading polymerase are blunt ended but can be incubated post-amplification with a GoTaq® Polymerase with just dATP in the reaction ([PC7](#)). After ligation, the vectors are transformed into bacteria, then prepped for Sanger sequencing with a plasmid prep like the [PureYield™ Plasmid Miniprep System](#).

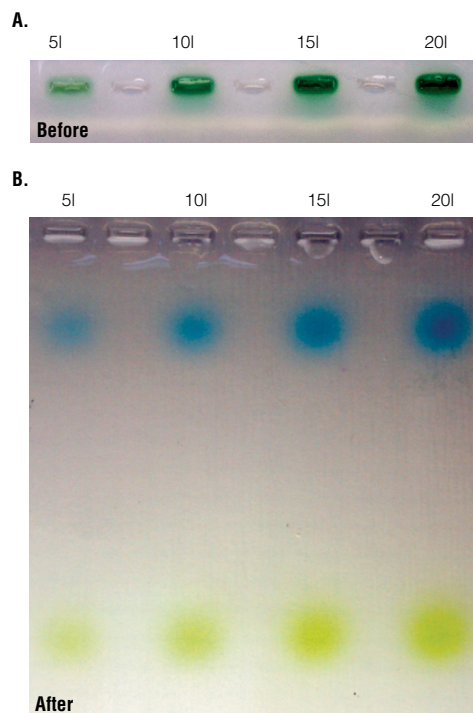


Figure 10. GoTaq® Green Buffer before and after agarose gel electrophoresis. Panel A. GoTaq® 5X Green (shown) and 5X Colorless Buffers contain a compound that increases sample density to help samples sink into the wells of a gel. **Panel B.** The 5X GoTaq® Green and Flexi Reaction Buffers contain blue and yellow dyes that migrate at the same rate as 3–5kb DNA fragments (blue) and ahead of primers (yellow) in a 1% agarose gel.

OTHER RESOURCES

PC7

Maciver, I. A Quick Method for A-Tailing PCR Products. Promega Corporation.

Sanger Sequencing. Sanger sequencing is accomplished through a synthesis reaction where a primer hybridized to the target is extended with a polymerase using four fluorescently modified non-extendable nucleotides of A, G, C and T in a mixture with all four unlabeled dNTPs. The mixture is loaded onto an instrument, like the [Spectrum Compact CE Instrument](#), that separates the reaction products through capillary electrophoresis. The reaction products pass by lasers that excite the dyes corresponding to A, G, C or T and the sequence of the DNA is determined. Sanger sequencing can read ~800bp from the primer (12). A sequencing kit like the [ProDye Terminator Sequencing System](#) provides all the required chemistry, including a proprietary thermostable DNA polymerase

qPCR Genotyping. Quantitative PCR can be applied to identify single nucleotide polymorphisms (SNPs). Often, probe-based qPCR, the [GoTaq® Probe qPCR Master Mix](#), is used to look at small changes where hybridization of the probe is dependent upon the presence or absence of a particular base. The reaction is performed on gDNA with two probes, each corresponding to a different base at the SNP location. The probes are also tagged with different fluorophores. The fluorophore that is released from the quencher indicates which base resides at the SNP. Dye-based qPCR systems, such as the GoTaq® qPCR Master Mix can be used if the SNP or insertion/deletion results in an amplification product that produces a different melt curve in comparison to a standard.

Methylation Analysis by Bisulfite Conversion

WGS and genotyping methodologies can be used to assess the methylation status of the genome or of specific genes. After extraction of gDNA, a portion of the gDNA is exposed to sodium bisulfite, which reacts with cytosine but not 5-methylcytosine. The bisulfite reaction deaminates the cytosine, converting it to uracil. The sequence of the bisulfite-converted DNA is compared with the unreacted DNA sequence to identify the 5-methylcytosines. Changes in methylation can lead to changes in gene expression without altering the actual DNA sequence.

The conversion is performed before analysis by NGS or PCR amplification of specific gene sequence. Another available technique is methylation-specific PCR (MSP). In MSP, primers are designed to span a potentially methylated region. One primer is designed as if all the cytosines are methylated that is, the cytosines (remain C's after bisulfite conversion) or all converted to uracils. Primers can also be designed for cases where partial conversion has occurred. Separate PCR reactions with each primer gives the methylation status based on which primer produces a product under stringent amplification conditions.

The [MethylEdge™ Bisulfite Conversion System](#) contains reagents for the bisulfite conversion and cleanup of the reaction with minimal fragmentation of the gDNA ([PC8](#), [PC9](#)). Lu *et al.* (19) analyzed the methylation status of specific genes in hair follicle mesenchymal stem cells by MSP. The gDNA was converted with the MethylEdge™ System. Part of the study also examined whether the cells could form spheroids. Kim *et al.* (20) studied bladder cancer using organoids and opted to bisulfite-treat gDNA with the MethylEdge™ System and then amplify a 2kb region around CpG-containing areas of the *Shh* gene sequence. The amplicon was cloned in the pGEM®-T Vector prior to Sanger sequencing.

OTHER RESOURCES

PC8

A New Edge in Bisulfite Conversion. Promega Corporation.

PC9

MethylEdge™ Bisulfite Conversion System. Promega Corporation.

References

19. Lu, Y. *et al.* (2019) OCT4 maintains self-renewal and reverses senescence in human hair follicle mesenchymal stem cells through the downregulation of p21 by DNA methyltransferases. *Stem Cell Res. Ther.* **10**, 28. PMID: 30646941
20. Kim, S. *et al.* (2019) Epigenetic regulation of mammalian Hedgehog signaling to the stroma determines the molecular subtype of bladder cancer. *eLife* **8**, e43024. PMID: 31036156

STR Profiling for Cell Authentication and Sample Tracking

Short Tandem Repeats (STRs) are repetitive sequence elements 3–7 base pairs in length and scattered throughout the human genome. By amplifying and analyzing these polymorphic loci and then comparing the resulting STR profile to that of a reference sample, the origin of biological samples such as cells or tissues can be identified and verified. The more loci that are amplified, the higher the statistical power of discrimination. For example, analyzing 15 STR loci yields a power of discrimination as high as 1 in 1.42×10^{18} , making it highly unlikely that two DNA profiles will match at random (PC10).

STR profiling should be a standard practice in any lab that works with different human cell lines to ensure correct cell lines are in use (PC10). Papers are often retracted because work was performed on an incorrectly identified cell line. Examples of authenticated cell lines can be found in the International Cell Line Authentication Committee web site (www.iclac.org). Cell line providers like the American Type Culture Collection (www.atcc.org) routinely STR profile new and existing cell lines and post the STR profile online.

Journals (e.g., *Nature*, *American Association for Cancer Research* and *Endocrine Society* publications) are aware of the issue of cell line identity, and many require or strongly encourage authentication of cell lines prior to publishing. NIH grant applications must include plans for cell line authentication within new funding applications. Resources for cell line authentication with links to journals and service providers are maintained at www.promega.com/CLA.

Working with primary human-derived cell lines offers a challenge as each line is unique to the donor and will not be found in databases of established cell lines. Researchers turn to STR profiling to create a unique fingerprint to positively identify a sample which can be used to keep track of dozens to hundreds of individual cell lines maintained in a lab. Different cell lines obtained from the same donor will have the same STR profile, so other methods must be used to differentiate these cells from one another.

STR profiling is essentially a genotyping workflow: gDNA extraction is followed by DNA quantitation, multiplex PCR, capillary electrophoresis for STR allele separation and sizing and, finally, data analysis. To match established cell lines to databases provided by cell line providers like ATCC, the **GenePrint® 10 System** amplifies all the loci in the databases. Researchers using 3D models have cited the use of the GenePrint® 10 System to perform cell line authentication on established cell lines (21–23). Some studies choose to use more loci to STR profile their cells for better discrimination. The **GenePrint® 24 System** provides 24 loci for cell line authentication. Gubert *et al.* (24) used the GenePrint® 24 System to profile four patient-derived iPS cell lines. GenePrint® Systems are pre-programmed for analysis on the Spectrum Compact CE System (AN359).

STR profiling is used extensively for forensic and paternity resolution of individuals. The PowerPlex® Systems kits were developed for these applications and have been employed for cell line authentication and sample tracking as well (25, 26). PowerPlex® System analysis is also pre-programmed into the Spectrum Compact CE System.

OTHER RESOURCES

PC10

Research Laboratory Applications of STR Technology. Promega Corporation.

References

21. Vande Voorde, J. *et al.* (2019) Improving the metabolic fidelity of cancer models with a physiological cell culture medium. *Sci. Adv.* **5**, eaau7314. PMID: 30613774
22. Romo-Morales, A. *et al.* (2019) Catalytic inhibition of KDM1A in Ewing sarcoma is insufficient as a therapeutic strategy. *Ped. Blood Cancer* **66**, e27888. PMID: 31207107
23. Martín-Pardillos, A. *et al.* (2019) The role of clonal communication and heterogeneity in breast cancer. *BMC Cancer* **19**, 666. PMID: 31277602
24. Gubert, F. *et al.* (2019) Generation of four patient-specific pluripotent induced stem cell lines from two Brazilian patients with amyotrophic lateral sclerosis and two healthy subjects. *Stem Cell Res.* **37**, 10144. PMID: 31077962
25. Balaban, S. *et al.* (2019) Extracellular fatty acids are the major contributor to lipid synthesis in prostate cancer. *Mol. Cancer Res.* **17**, 949–962. PMID: 30647103
26. Leung, D.T.H. *et al.* (2019) Combined PPAR γ activation and XIAP inhibition as a potential therapeutic strategy for ovarian granulosa cell tumors. *Mol. Cancer Ther.* **18**, 364–375. PMID: 30530769

Chapter 5

MEASURING ASSAYS WITH A PLATE READER

Bioluminescence Measurement 57

Fluorescence Measurement 59

Plate Choice Influences Sensitivity 62

Most of the cell health and metabolism assays presented in Chapters 1 and 2 rely on bioluminescence for measurement. Bioluminescence is a highly sensitive methodology for plate-based measurement of biological events. Figure 1 compares in vitro biochemical sensitivities of a bioluminescent and two fluorescent assays for caspase-3. The bioluminescent assay provides the greatest signal-to-noise ratio.

OTHER RESOURCES

PC1

Wood, V. K. The Bioluminescence Advantage. Promega Corporation.

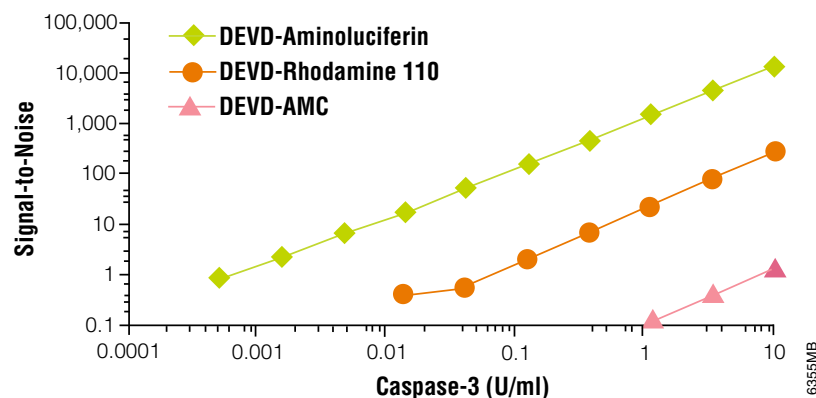


Figure 1. Comparison of sensitivities of different detection methods for assaying active caspase-3 in a biochemical assay. Various concentrations of caspase-3 were mixed with the Caspase-Glo® 3/7 Assay Reagent (DEVD-aminoluciferin; Green), Apo-ONE® Caspase-3/7 Assay Reagent (DEVD-Rhodamine 110; orange) or the Caspase™ 3/7 Assay Reagent (DEVD-AMC; pink). Measurements were made on a multimode GloMax® Instrument.

Bioluminescence can be 10- to 100-fold more sensitive than a fluorescent assay. The reason bioluminescence assays are so sensitive is due to the nature of the reaction. Bioluminescence depends on chemical energy released through the action of enzymes. Without the enzymes, the bioluminescent substrates produce very little light through a process called autoluminescence. Firefly luciferin has especially low autoluminescence since it requires a two-step process to generate light. Thus, the background luminescence is extremely low or non-existent. Reactions with coelenterazine produce more light since the reactions involve only a single step. Care must be taken in reagent design to limit coelenterazine autoluminescence. Fluorescence, in contrast, is dependent upon light energy. The excitation energy needed usually exceeds the emission produced and contributes to background absorbance. The excitation and emission spectras can overlap so some of the excitation light is detected in the emission channel. Another contributor to background absorbance is any profluorescent compound that is biologically converted to the fluorescent compound. A more detailed discussion is provided in [PC1](#).

Bioluminescence Measurement

Sensitivity is the key attribute of bioluminescent reactions due to the low background luminescence, but a key limiting factor to the sensitivity is how well the luminometer isolates one well from another. Luminescence should only be measured from one well with no contribution from adjacent wells. Instruments usually achieve this by using plate or well masking to focus the detector on a single well as demonstrated in Figure 2.

The plate-reading GloMax® Instruments use physical masks to block adjacent wells and minimize the distance from the plate to the detector. For the **GloMax® Navigator Microplate Luminometer**, which is a dedicated 96-well luminometer, the plate mask (with 96 holes) snaps over the entire plate (Figure 3). For the **GloMax® Discover Microplate Reader** and **GloMax® Explorer Multimode Microplate Reader**, the mask has one hole and covers a broad area since these instruments can measure luminescence from 6-, 12-, 24-, 48-, 96- and 384-well plates. The preinstalled mask is used to measure the 6–96-well plates, while another with a smaller aperture is used with 384-well plates. The smaller 384-well aperture is needed to isolate the smaller wells from one another.

An experiment was designed to measure how effectively different instruments isolate one well from another (**PC2**). A bright luminescent signal was placed in a well of a 96-well, white-walled plate bordered by four wells containing only water (Figure 4). Luminescence was measured in the bright well and the surrounding water wells. The measurement in the water wells is interpreted as well-to-well cross talk. It should be noted that the same plate was read in each instrument. The results are presented in Table 1. Table 1 demonstrates an important point when working with multiple luminometers: relative light units (RLUs) should never be directly compared between instruments. There is no universal standard to which RLUs are calibrated. Each instrument has its own algorithms and, thus, each will report a different number for the same sample (**PC3**).

How well an instrument isolates one well for measurement, which includes well-to-well cross talk, contributes to the sensitivity of an instrument. Figure 5 demonstrates how different instruments vary in the limit of quantitation.

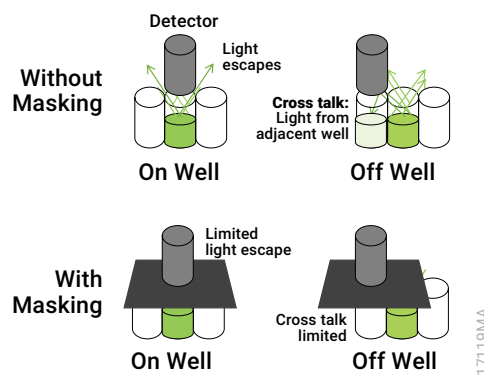


Figure 2. The concept of the plate mask to increase sensitivity. Without a plate mask, light can bounce around and either be missed by the detector or contribute light to an adjacent well, increasing the apparent signal. Plate masks isolate the well being measured from adjacent wells, limiting light escape and well-to-well cross talk.

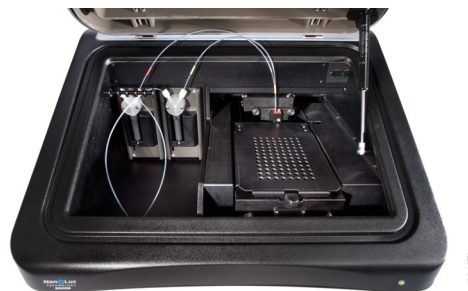


Figure 3. Interior of the GloMax® Navigator Microplate Luminometer. Plate mask is just right of center with a grid pattern matching a 96-well plate.

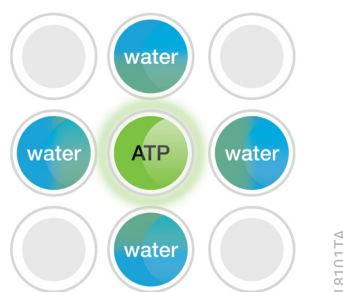


Figure 4. Concept of the cross talk experiment. A bright luminescent signal was initiated in the center well (ATP & Kinase-Glo® Reagent). Luminescence was measured in that well and in the surrounding wells containing water. Details are available in reference **PC2**.

OTHER RESOURCES

PC2

Wieczorek, D., et al. How Sensitivity and Crosstalk Affect Your Bioluminescent Assay Results. Promega Corporation.

PC3

Just What is an RLU (Relative Light Unit)? Promega Corporation.

Instrument	Blank RLU	Avg. ATP RLU	Avg. Water RLU	Cross Talk (Water/ATP)	Cross Talk increase over GloMax® Discover
GloMax® Discover	333	3.05×10^7	3.33×10^3	1.09×10^{-4}	1.00X
Infinite® M1000 PRO	19.3	8.69×10^6	1.37×10^3	1.58×10^{-4}	1.45X
Mithras LB 940	29.2	1.05×10^7	1.86×10^3	1.76×10^{-4}	1.61X
Infinite® M200	7.18	6.85×10^6	2.10×10^3	3.06×10^{-4}	2.81X
CLARIOstar	43.5	9.37×10^6	7.29×10^3	7.78×10^{-4}	7.14X
POLARstar Optima	43.5	1.64×10^5	1.85×10^2	1.13×10^{-3}	10.37X
Varioskan Flash	57.9	3.32×10^7	3.80×10^4	1.14×10^{-3}	10.46X
PERAstar	15.8	1.79×10^6	6.54×10^3	3.65×10^{-3}	33.49X

Table 1. Detection instrument comparison for cross talk between wells. High luminescent wells containing 100µl of a 100µM ATP solution plus 100µl of Kinase-Glo® Max Reagent were plated on a standard 96-well opaque white plate next to water-only wells (200µl Nuclease-Free Water). Signal in the water-only wells was measured after room temperature incubation for 10 minutes to achieve steady-state luminescence (luminescent half-life ~5 hours). A blank plate containing only 200µl of water/well was prepared to determine background. The background and experimental plates were read in the different microplate readers with 0.5 second integration times per well. The average background was determined for each instrument and this average was subtracted from the water-only and ATP/Kinase-Glo® Max wells. The average water-only RLUs were determined and the average ATP/Kinase-Glo® Max RLUs determined. The average water-only RLUs were divided by the average ATP/Kinase-Glo® Max RLUs to calculate the cross talk value. Details are in reference [PC2](#).

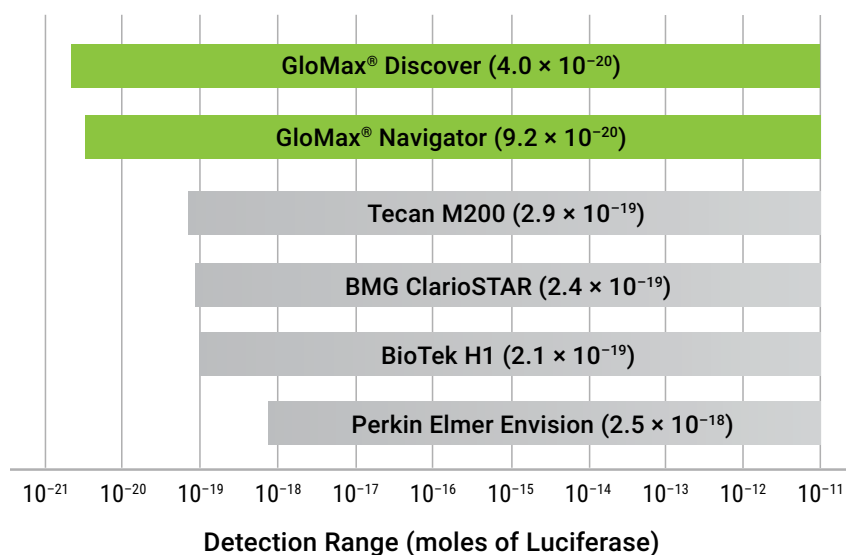


Figure 5. Sensitivity of various instruments to light generated by luciferase and Bio-Glo™ Assay Reagent. Numbers refer to limit of quantitation measured for each instrument in moles of QuantiLum® Recombinant Luciferase ([PC2](#)).

Fluorescence Measurement

The CellTox™ Green Cytotoxicity assay described in Chapter 1 uses a dye that becomes highly fluorescent when bound to DNA as a means of monitoring dead cells no matter when the cytotoxic event occurred. The QuantiFluor® Dye Assays for quantifying nucleic acids (Chapters 3 and 4) operate on the same principle, with different dyes discriminating between double-stranded DNA and RNA, and can also be read with a plate-reading

fluorometer if higher throughput is needed. There are many fluorescent assays for monolayer cell cultures and several instruments that can be used to read them. As with luminescent assays, sensitivity is extremely important.

Although monochromator-based instruments will detect the assays, our Research and Development scientists recommend the use of filter-based instruments due to the greater sensitivity over monochromator instruments. Filter-based instruments direct more excitation energy to the fluorophore and capture more emission energy when compared to the narrow input and output of a monochromator-based system (Figure 6). If two fluorophores are measured in the same sample, filter-based systems change measurement modes faster than monochromators.

References

1. Jones, E., Michael, S. and Sittampalam, G.S. (2012) Basics of Assay Equipment and Instrumentation for High Throughput Screening. In: *Assay Guidance Manual*, Eli Lilly & Company and the National Center for Advancing Translational Sciences, Bethesda, MD. PMID: 22553880

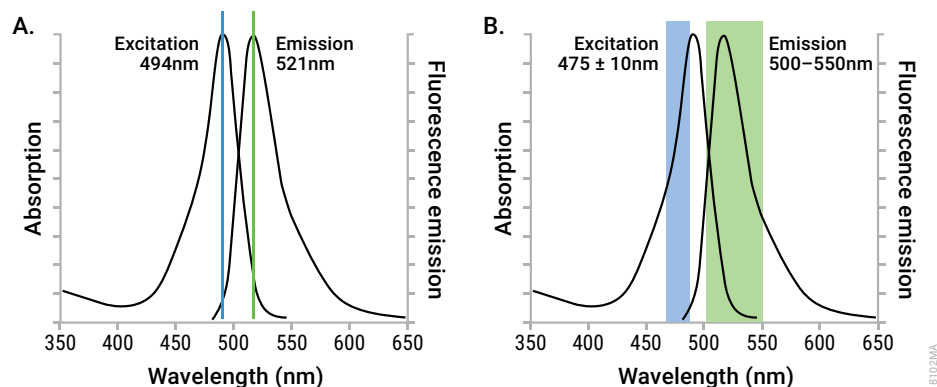


Figure 6. Comparison of spectral coverage of fluorescein with monochromator-based and filter-based fluorometers. Filter-based instrument excitation/emission windows based on the GloMax® Discover Microplate Reader.

Monochromators use a white light source (e.g., xenon lamp) and diffraction grating to separate the light into a spectrum. A device with a narrow slit is positioned in the spectrum to direct light to the sample. The emission is captured through a similar device. Monochromators are extremely flexible and can be used to measure most fluorophores. These instruments can perform a spectral scan to characterize an unknown fluorophore or spectral shifts. However, sensitivity suffers due to the reduction of signal caused by significant light loss in the diffraction gratings. Filter-based, detection-based instruments use optical filters of a specific wavelength and bandwidth in both the excitation and emission light paths. The use of optical filters instead of diffraction gratings effectively separate excitation and emission wavelengths with a minimal loss of signal, providing greater sensitivity than monochromators. These instruments cannot perform spectral scans and may require users to maintain a variety of filter sets or use instruments with a variety of excitation/emission filters pre-installed (1).

Most filter-based instruments use a white light source and filter the required excitation wavelengths. The GloMax® Discover and Explorer Systems utilize a set of wavelength-matched light emitting diodes as the excitation source. The LEDs emit a specific

wavelength that is further refined by excitation filters to an intense, specific excitation window. The light is directed to the top of the sample and fluorescent emission is measured through a somewhat broader emission filter placed next to the detector (Figure 7). GloMax® Instruments maintain a short excitation/emission path to limit light loss over a distance. The use of the dichroic beam splitter and the emission filter ahead of the detector also ensures that extraneous light coming from the excitation LED does not contribute to the emission signal. Figure 8 demonstrates the difference in sensitivity of a hybrid instrument using a xenon lamp to provide both filter-based and monochromator-based detection modes in comparison to the GloMax® Discover.

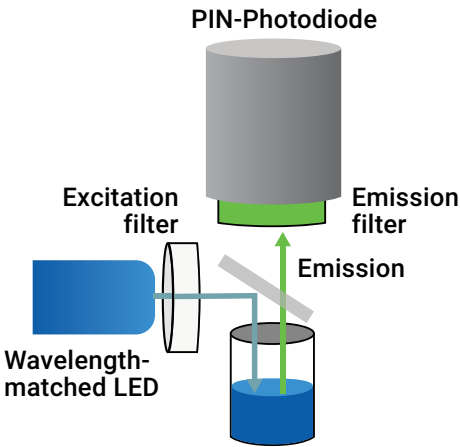


Figure 7. Diagram of the filter-based fluorescent detection system in the GloMax® Discover and Explorer Instruments.

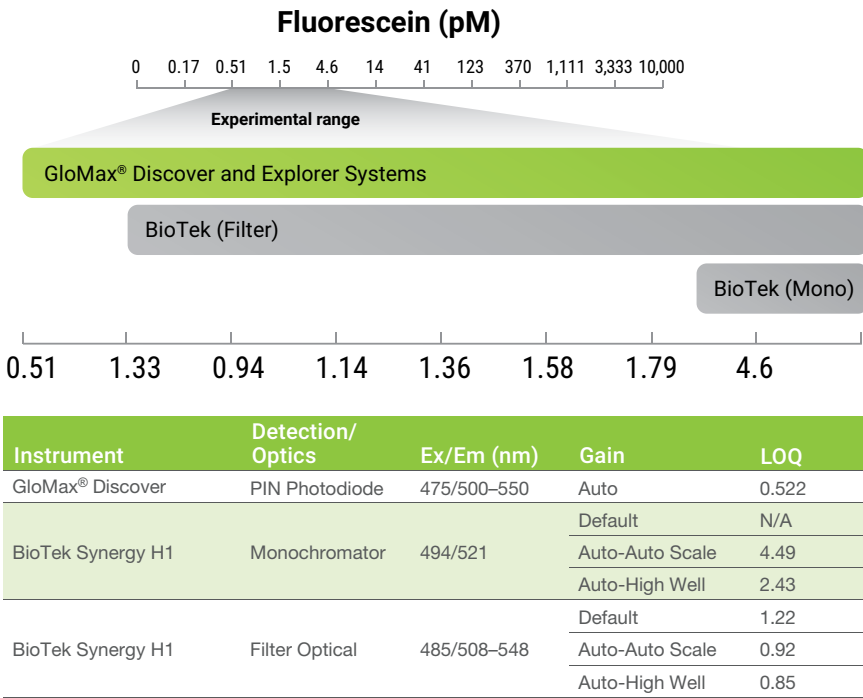


Figure 8. Comparison of GloMax® Discover and BioTek Synergy H1 in monochromator or filter mode limit of quantitation. Indicated range of fluorescein concentrations were tested with the automatic gain setting of the GloMax® Discover and three selections of gain setting on the BioTek instrument. N/A indicates that the instrument saturated at top three data points. Limit of quantitation (LOQ) calculated as 10X standard deviation of background divided by the slope. Test performed by Promega Scientific Application Services.

Plate Choice Influences Sensitivity

One of the most common missteps researchers make when beginning to use bioluminescence is choosing the wrong plates. Often, the error is the choice of a standard clear, colorless plastic plate, like you would use to culture cells or perform a colorimetric ELISA assay. However, clear, colorless plates offer little resistance to light signals bleeding through to adjacent wells.

Opaque-walled 96- or 384-well tissue culture plates are available in white or black with either solid bottoms or clear bottoms ([PC4](#)). The clear bottom plates offer the advantage of allowing cells to be examined by microscopy during the experiment. The primary difference between white and black plates is their reflective properties:

- For luminescent assays, white plates reflect light and will maximize light output signal.
- For fluorescent assays, black plates absorb light and reduce background and cross talk.

For multiplexed luminescent and fluorescent assays, using a white plate will support maximum light output signal for the luminescent portion of the assay, but may result in higher cross talk and background for the fluorescent portion of the assay. Using a black plate in a multiplex assay will reduce fluorescent signal cross talk and background but will reduce the luminescence signal (expect to lose about one order of magnitude in luminescent signal using a black plate).

3D cell culture offers some challenges with regard to plates. The most popular method to produce microspheroid cultures uses ULA plates. These plates tend to have a U- or V-shaped bottom that is clear for viewing the culture. Clear U- or V-bottom plates are not ideal for measuring luminescent assays if the cells are to be lysed for assay (e.g., ONE-Glo™ Luciferase Assay or CellTiter-Glo® 3D Cell Viability Assay). Our research and development scientists experienced best results when developing the CellTiter-Glo® 3D Cell Viability Assay by growing and treating microspheroid cells in ULA plates. At end of the incubation, the CellTiter-Glo® 3D Assay Reagent was added directly to the ULA plates for lysis. For measurement, the reactions were transferred to a white luminometer plate. White-walled 96- or 384-well ULA plates are available, and researchers report better performance for culturing spheroids followed by measuring luminescent assays directly in the plate compared to black-walled plates.

Eight Considerations for Getting the Best Data from Your Luminescent Assays ([PC5](#))*

1. Use the Right Plates

We recommend using white, opaque-walled assay plates because they reflect light, maximizing the output signal for luminescence assays. However, if you are multiplexing a luminescence assay with a fluorescence assay, a white-walled plate can result in higher cross talk and background fluorescence. Different brands of white-walled plates will have varying degrees of auto-luminescence and cross talk.

Using a black-walled plate in a multiplex assay will reduce fluorescent signal crosstalk and background but will also reduce the luminescence signal (by about 1 order of magnitude).

* Considerations 1–7 apply to fluorescent assays as well. Consideration 8 only applies to luminescent assays.

OTHER RESOURCES

[PC4](#)

Why You Don't Need to Select a Wavelength for a Luciferase Assay. Promega Corporation.

[PC5](#)

Eight Considerations for Getting the Best Data from Your Luminescent Assays. Promega Corporation.

If your luminescence signal is too strong in a white-walled plate, you may want to switch to using a black-walled plate as they absorb some of the light of the reaction.

2. Avoid Bubbles

Bubbles in assay solutions cause light scattering and can result in erroneous signals when read on a luminometer.

3. Mix Your Samples Well

Poor mixing can result in aggregation, precipitation, variations in reaction rates and well-to-well concentration differences. Avoid creating droplets of reagent on the upper surfaces of the wells, because these can increase the likelihood of cross talk.

4. Use Uniform Assay Volumes

Small differences in assay volume can cause large differences in signal. Use at least the minimum volume recommended by the instrument manufacturer.

5. Ensure Consistent Temperature

Luminescence assays are typically temperature-dependent due to their enzymatic nature. While fluorescent assays may be incubated at room temperature or 37°C, luminescence assays should be incubated at the same temperature that the plate reader is set to.

6. Time Reagent Incubation Carefully

The timing of reagent incubation for luminescent assays can be important. Reading the samples too soon may negatively impact the signal-to-noise ratio, sensitivity or dynamic range. Incubating too long may decrease the detection range by saturating the assay or detector with too much signal.

7. Don't Compare Raw Signal Across Instruments

Instruments calculate RLUs by different methods, so it is important that you don't compare the raw values across instruments, even if they are the same model. All instruments will have some level of background due to various factors, including the phosphorescence of plastics, differences in reagents and electronic "noise".

The dynamic range and sensitivity of an instrument is a key factor when measuring the extremes of very high or very low signal, and a sensitive instrument will have a clear distinction between the blank noise and the sample signal. We recommend comparing a positive control with a high signal to a background control in order to get a better understanding of the readings to expect for your instrument and experimental conditions.

8. No Wavelength Necessary

Don't worry about selecting a wavelength for your assay—in most cases it isn't necessary. Luminescence is a by-product of an enzymatic reaction, not light exciting fluorophores in the sample. This means that there is no need to filter out any light coming from a luciferase assay as you would with a fluorescence assay. More detail are available in [PC4](#).

OTHER RESOURCES

PC6

Luminometer and Microplate Reader Selection Guide. Promega Corporation.

Instrument	Luminescence	Fluorescence	Vis Absorbance	UV Absorbance	BRET/FRET
GloMax® Discover Model GM3000	✓	✓	✓	✓	✓
GloMax® Explorer Model GM3500	✓	✓	✓	optional	optional
GloMax® Explorer Model GM3510	✓	✓	optional	optional	optional
GloMax® Navigator Model GM2000	✓				

Table 2. Comparison of plate-reading GloMax® Instruments. A checkmark (✓) indicates that the module is preinstalled on that model of GloMax® Instrument. Adding optional modules to a GloMax® Explorer Instrument will require installation at an authorized GloMax® Service Center. A more detailed comparison is available ([PC6](#)).

